



# LEXNET Low EMF Exposure Future Networks

# D3.3 Exposure Index assessment v2

Contractual delivery date: M24
Actual delivery date: M26

#### **Document Information**

Version	V4.0	Dissemination level	PUBLIC
Editor	Günter Verm	eeren (iMinds)	
Other authors	Thierry Sarre Shoaib Muh (Satimo), Julien Stépha Luis F. Díez, Mladen Kop Jelena Milink	David Plets, Wout Joseph, Luc Martebourse, Joe Wiart (Orange), ammad Anwar, Sylvie Le Gall, an, Yoann Corre (Siradel), Laura Rodríguez de Lope, Ramón privica, Aleksandar Nešković, Martebouric, Stevan Nikšić (TKS) a, Michal Mackowiak, Luis M. Corre	Yann Toutain Agüero (UC) lilica Popović,

#### PROPRIETARY RIGHTS STATEMENT

This document contains information, which is proprietary to the LEXNET Consortium. Neither this document nor the information contained herein shall be used, duplicated or communicated by any means to any third party, in whole or in parts, except with prior written consent of the LEXNET consortium.



Abstract	LEXNET aims at assessing the realistic exposure of a population in an area induced by wireless network communications by taking into account the uplink (UL) exposure besides the downlink (DL) exposure. Electromagnetic field exposure data will be available from EMF measurements with dosimeters, narrowband and broadband measurement systems, 3D EMF simulations (e.g. based on ray tracing methods) and receive and transmit data obtained from the user's mobile device and base stations / access points.  This deliverable updates D3.3 updates D3.1 and describes thoroughly the method to assess the Exposure Index and provides an overview of the EMF data available for assessing the EI.
Key words	Exposure index, exposure metric, electromagnetic fields

## **Project Information**

Grant Agreement n°	318273
Dates	1 <sup>st</sup> November 2012 – 31th October 2015

### Document approval

Name	Position in project	Organisation	Date	Visa
Joe Wiart	Coordinator	France Telecom	23/12/2014	OK

### **Document history**

Version	Date	Modifications	Authors
V1.0	10/11/2014	Input from all partners. Draft version for partner review before submission of early version to EC.	All
V2.0	17/11/2014	Revised draft version of D3.3. This early version will be submitted to the EC.	All
V3.0	11/12/2014	Version for internal review.	All
V4.0	23/12/2014	Final version submitted to EC	All



# **Table of Contents**

<u>1</u>	INTRODUCTION	7
<u>2</u>	EXPOSURE INDEX ASSESSMENT METHODOLOGY	8
2.1	ASSESSMENT AND CONVERSION OF <b>PTX</b> AND <b>S</b> INC	
2.2	INTERPOLATION, EXTRAPOLATION AND COMBINING DOWNLINK EXPOSURE METRICS	13
2.3	EXPOSURE INDEX UNCERTAINTY ASSESSMENT	
<u>3</u>	EXPOSURE DATA	16
3.1	MEASUREMENT DATA	16
3.2	NETWORK DATA	28
3.3	SIMULATION DATA	35
3.4	LIFE SEGMENTATION DATA	43
3.5	ICT USAGE DATA	45
3.6	SAR DATABASE	46
<u>4</u>	EXTRAPOLATION MODELS	48
4.1	ESTIMATION OF EMF ON GROUND LEVEL FROM LAMP POST DOSIMETERS	48
4.2	ESTIMATION OF EMF FROM SINGLE-POLARIZED MEASUREMENTS	49
5 SENSOR NETV	SIMULATION-GUIDED DESIGN AND EXPLOITATION OF THE WIRE	<u>LESS</u> 53
<u>6</u>	DISCUSSION AND CONCLUSIONS	58
<u>7</u>	REFERENCES	<u> 59</u>
APPENDIX A	DEDICATED SIMPLIFIED LOW-COST UL/DL MEASUREMENT EQUIP	
	BY SATIMO	
APPENDIX B	HUMAN BODY IMPACT ON UL MEASUREMENTS	
APPENDIX C STUDY	MONO-AXIAL VS. ISOTROPIC MEASUREMENT RESULTS FROM A DOSIM 66	<u>ETER</u>
APPENDIX D	EXAMPLES OF MEASUREMENT RESULTS OBTAINED FROM NETV	
APPENDIX E	EXAMPLE OF ANALYTICAL APPROACH TO EI UNCERTAINTY EVALUATION	
APPENDIX F	CALIBRATION OF THE JDSU DRIVE TEST	
APPENDIX G	SMARTPHONE VS A DOSIMETER FOR DL POWER MEASUREMENTS	
APPENDIX H	UL DUTY CYCLE MEASUREMENTS USING A DOSIMETER.	
APPENDIX I	EXTRAPOLATION OF E-FIELD MEASUREMENTS FROM 6M TO 1.5M	
APPENDIX J	ESTIMATION OF EMF FROM PERSONAL AND FIXED POINT DOSIMETERS	
APPENDIX K	INTERNAL REVIEW	115



# **Executive Summary**

LEXNET aims at assessing the realistic exposure of a population in an area induced by wireless network communications by taking into account the uplink (UL) exposure besides the downlink (DL) exposure. Electromagnetic field exposure data will be available from EMF measurements with dosimeters, narrowband and broadband measurement systems, 3D EMF simulations (e.g. based on ray tracing methods) and receive and transmit data obtained from the user's mobile device and base stations / access points. This deliverable updates D3.3 updates D3.1 and describes thoroughly the method to assess the Exposure Index (EI) using detailed flow charts and provides an overview of the EMF data available for assessing the EI. The EI assessment has four main steps: (1) the assessment of the exposure data; (2) the conversion of the exposure data into quantities used in the El formulation; (3) interpolation, extrapolation and combination of the downlink exposure data; and (4) the calculation of the EI using the formulation as well as uncertainty assessment. The data for EI assessment can be obtained from electromagnetic field (EMF) simulations, (EMF) measurements, sensor in the wireless communication network, and time use surveys. As the EI quantifies the combined exposure from downlink and uplink, it is mandatory that at least one data set for downlink and for uplink is taken into account.

Version 4.0 Dissemination level: PUBLIC



# List of Acronyms

ANFR French National Radio Frequency Agency

BCCH Broadcast Control Channel

BS Base station

CDR Call Detail Record

CDF Cumulative Distribution Function

CPICH Common Pilot CHannel

DCS Digital Cellular Service

DL Down-link

El Exposure Index

GBSC Geometrically Based Statistical Channel
GSM Global System for Mobile communications

HETUS Harmonised European Time Use Survey

ICT Information and Communication Technologies

IMSI International Mobile Subscriber Identity

LTE Long Term Evolution

LOS Line of Sight

MIMO Multiple-Input Multiple-Output

MSISDN Mobile Station International Subscriber Directory Number

NLOS Non Line of Sight

QoS Quality of Service

RAT Radio Access Technology
RNC Radio Network Controller
RSCP Received Signal Code Power
RSRQ Received Signal Received Quality
RSSI Received Signal Strength Indication

Rx Receiver

SAR Specific Absorption Rate SAS Customer Analytics System

Version 4.0

Dissemination level: PUBLIC

# Document ID: D3.3 Exposure Index Assessment v2 FP7 Contract n°318273



SINR Signal to Interference plus Noise Ratio

TO\_F Torso front Tx Transmitter

UE User equipment

UL Up-link

UMTS Universal Mobile Telecommunication System

UTD Uniform Theory of Diffraction

WA\_B Waist back
WA\_F Waist front
WA\_L Waist left
WA\_R Waist right

WSN Wireless Sensor Network

Version 4.0



#### 1 Introduction

The objective of the LEXNET project is to reduce the realistic exposure induced by (future) wireless communication networks averaged over the entire population in a selected area. To quantify this exposure, the LEXNET consortium has defined in D2.4 [1] a new exposure metric called the Exposure Index (EI) and updated this metric in D2.6 [2]. The EI depends on, amongst others, the usage, posture, life segmentation data, network deployment and management.

This deliverable D3.3 updates deliverable D3.1 "Exposure Index Assessment v1", which provided a general overview of the exposure data available and the methodology for assessing the EI. This deliverable goes beyond D3.1 as it details the description of the available exposure assessment tools, includes life segmentation data and presents methods to extrapolate exposure metrics if no direct assessment of the exposure metric is possible. Furthermore, this deliverable describes the method to assess the EI and visualises this in detailed flow charts.

Section 2 describes the EI assessment methodology and how the exposure data are combined to obtain the EI. Section 3 provides an overview of the data available for EI assessment. Section 4 discusses the extrapolation of EMF on the ground from the lamp post dosimeters, which are at a typical height of 6 m and the estimation of the EMF from a single-polarized incident field measurement. Section 5 shows how a wireless sensor network can be designed and exploited using a numerical tool. Section 6 concludes this deliverable. Additional information on the exposure index assessment methodology and data can be found in appendices Appendix A – Appendix J.



### 2 EXPOSURE INDEX ASSESSMENT METHODOLOGY

The EI aggregates downlink (DL) and uplink (UL) exposure data to assess the total exposure over a population in an area. Experimental setups as well as numerical tools can be applied for assessing both downlink and uplink exposure. Some quantities can be immediately used in the EI formulation, others first need conversion before they can be used as an input in the EI formulation.

Assume that we neglect the uplink exposure by mobile devices from other users – which can be regarded as a downlink exposure –, then the EI becomes:

$$EI^{SAR} = \frac{1}{T} \sum_{t,p,e,r,c,l,pos}^{N_{T},N_{p},N_{E},N_{R},N_{C},N_{L},N_{pos}} f_{t,p,e,r,l,c,pos} \left[ \sum_{u}^{N_{U}} (d^{UL} \bar{P}_{TX}) + d^{DL} \bar{S}_{inc} \right] \left[ \frac{W}{kg} \right]$$
(1)

with N denoting an amount, t period within the considered time frame T, p population category, e environment, r Radio Access Technologies (RATs), c cell type, I user load profile, pos posture, u usage of the device,  $\overline{P}_{\rm TX}$  average transmitted power by the mobile device,  $\overline{S}_{\rm inc}$  average incident power density,  $d^{UL}$  the uplink dose and  $d^{DL}$  the downlink dose, and f is the fraction of the population p with user load profile I in posture pos connected to RAT r for a cell type c in environment e during the time period t. The fraction f can be obtained from life segmentation data and Information and Communication Technologies (ICT) usage data.

Figure 1 shows the general flow chart for Exposure Index assessment. Four main steps can be distinguished: the assessment of the exposure data; the conversion of the exposure data into quantities used in the EI formulation [2]; interpolation, extrapolation and combination of the downlink exposure data; and calculation of the EI using the formulation as well as uncertainty assessment.

The EI has six input variables: T, SAR,  $\overline{S}_{\rm inc}$ ,  $\overline{P}_{TX}$ , TD, and f. For the calculation of the EI, reference SAR data are calculated once and taken into account in  $d^{UL}$  and  $d^{DL}$ . Most of the time this will probably also be the case for life segmentation data, which will be mainly obtained from the literature, and for ICT usage data, obtained through measurements of Key Performance Indicators (KPIs) by sensors inside the network.  $\overline{P}_{TX}$  and  $\overline{S}_{\rm inc}$  are obtained from simulations, measurements and network data. The measurement and network data often requires a conversion or translation into an input exposure metric of the EI equation. For instance, when the dosimeter is worn on the body shadowing by and coupling with the body must be taken into account.

Before we can calculate the EI, the DL data might require some post-processing, i.e., extrapolation, interpolation and combining data from different data sets. The flow of DL, UL and temporal data is visualised by the different colours of the connectors in the flow chart.

For the calculation of the Exposure Index, we distinguish three cases (see Figure 1): (1) only the DL and UL exposures from a single operator are taken into account which is of interest to network operators for reducing the El of their own network; (2) the exposure in DL from all operators and in UL only from a single operator is taken into account which is of interest from a user perspective; (3) the exposure from all operators in DL as well as UL are taken into account which is of interest from a regulator perspective.



Uncertainty assessment is an important aspect when calculating the EI. An exposure metric can be assessed with different tools or measurement devices, all with their particular uncertainty. Hence, the EI assessment also requires a methodology to properly assess the uncertainty.

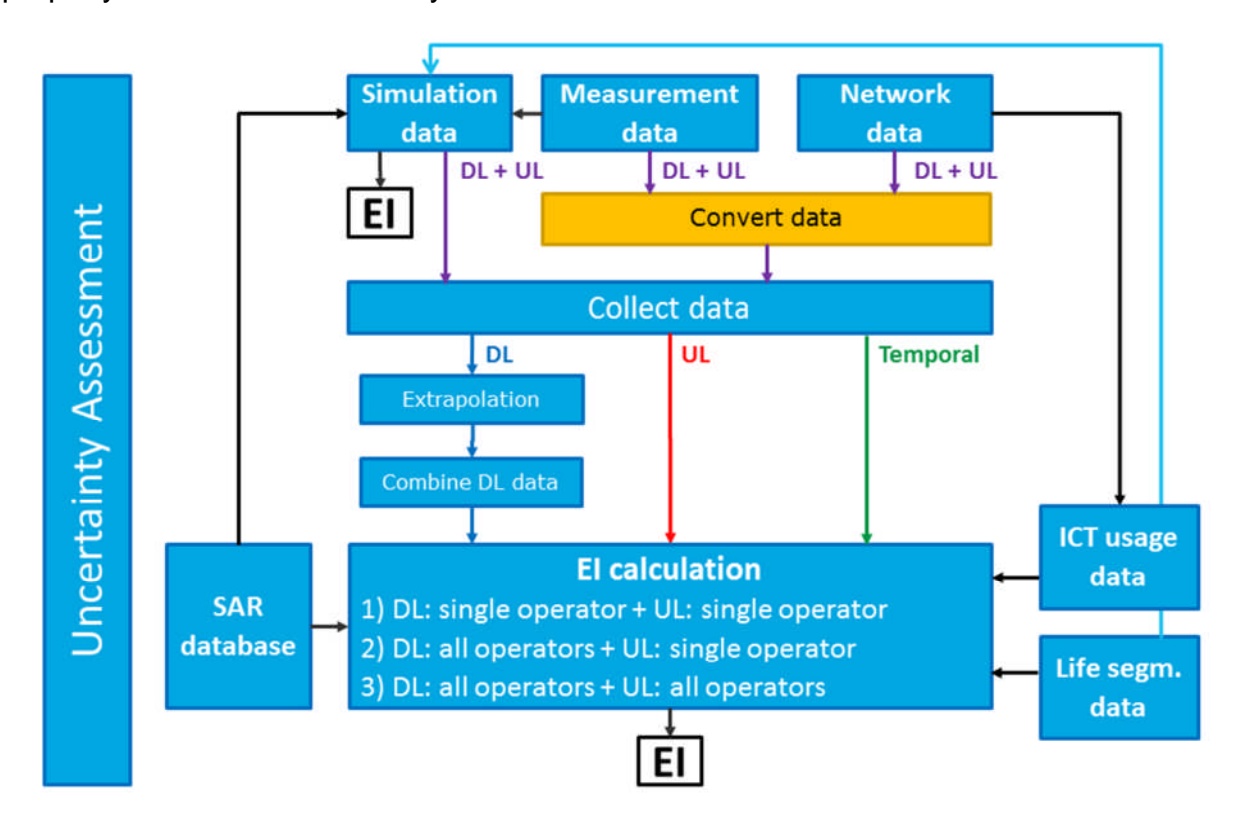


Figure 1: General flow chart for calculating the Exposure Index.

## 2.1 Assessment and conversion of $\overline{P}_{TX}$ and $\overline{S}_{inc}$

As detailed in Section 3,  $\overline{P}_{TX}$  and  $\overline{S}_{inc}$  can be assessed by various means, whether experimentally or numerically. The quantities returned by the various exposure assessment methodologies are, for DL exposure, the incident electric field or incident power density, total electric field, Received Signal Strength Indication (RSSI) or power density, single polarized electric fields, and for UL exposure, transmitted power, RSSI, duty-cycle, bitrates, DL and UL throughputs, etc.

Some of these metrics can be directly used in the EI formulation, others need conversion, for instance, to de-embed the influence of the body or to estimate the incident power density from a device's RSSI. But even if a metric does not need conversion, interpolation or extrapolation (for instance: estimation of the electric-field levels at ground level from dosimeters attached to lamp post) can be applied to improve the characterization of the assessed metric.

#### 2.1.1 Simulation data

The flow chart in Figure 1 shows that simulation tools allow the direct calculation of the EI. Within the LEXNET project there are simulation tools focusing at cellular networks (see Section 3.3.1), and indoor networks (see Section 3.3.2). Besides the direct calculation of the EI, the simulation tools can also provide DL and UL metrics.

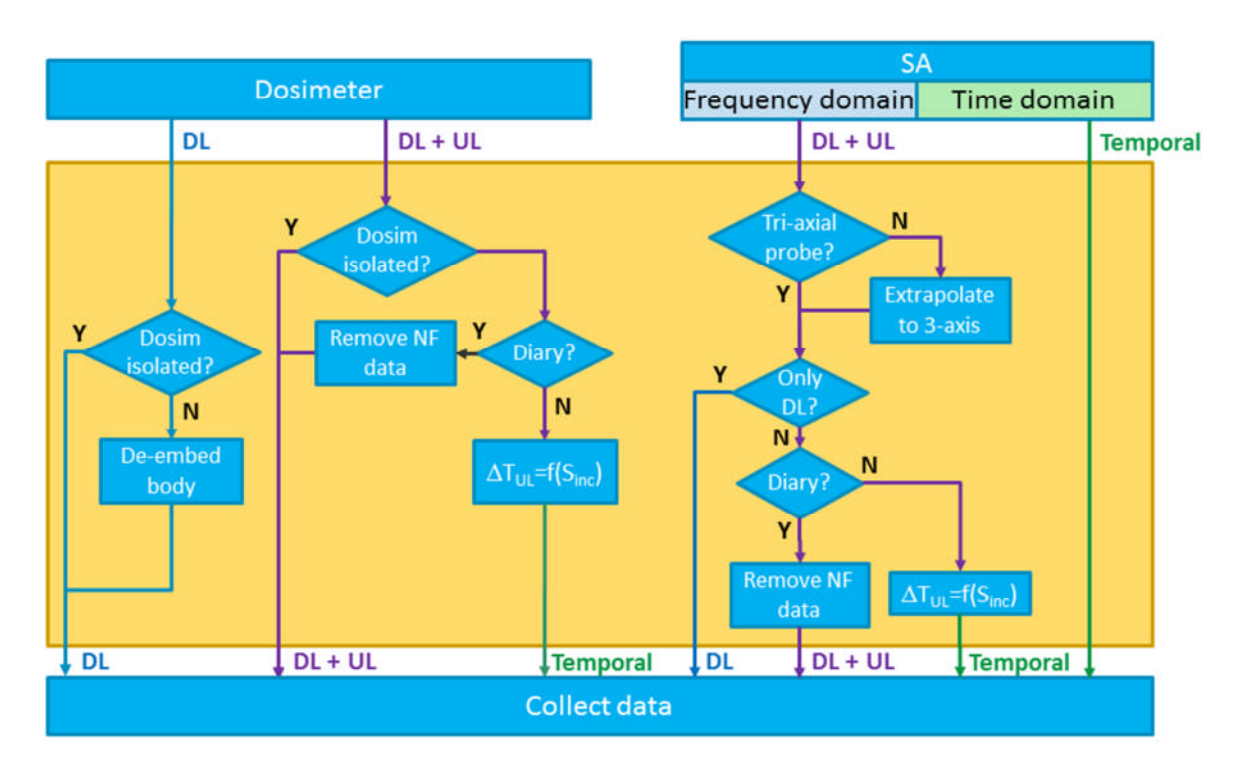


In this way, simulation data can be combined with experimental data for the assessment of the EI over a population in an area within a time frame T.

#### 2.1.2 Measurement data

 $\overline{P}_{TX}$  and  $\overline{S}_{inc}$  can be measured using dosimeters, spectrum analyser setup with triaxial or mono-axial probe, trace mobile, and low-complexity dosimeter deployed within a sensor network (see Section 3.1). The flow charts for the measurement data are shown in Figure 2 and visualise the conversion of the measured quantities into input quantities for the El calculation. Each measurement type has its own branch explaining the conversion of the measured metrics into a metric which can be applied in the El formulation.

In addition, broadband measurements do not provide data that can be directly used in the El calculation, but these measurements might be valuable in case of co-kriging (Section 2.2.1) as low-fidelity data which can be assessed easily and fast.



(a)



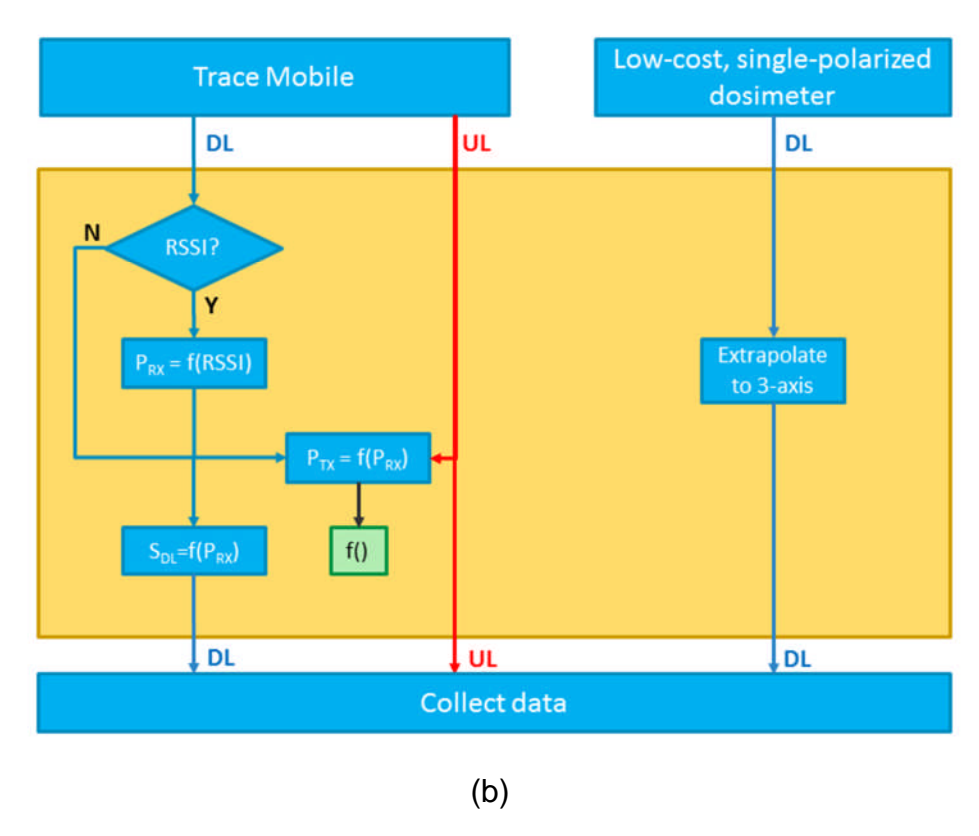


Figure 2: Flow chart of the measurement data: (a) dosimeter and spectrum analyser setup and (b) trace mobile and low-cost, single polarized dosimeter.

#### 2.1.2.1 Dosimeters

The flow chart for the dosimeters is shown in Figure 2(a). Dosimeters are designed to assess the personal exposure in terms of electric field or power density. Typically, these devices are worn on the body (e.g., on the belt), but they can also be used under isolated conditions. In case that the dosimeter is worn on the body, it is important to de-embed the influence of the body on the measured values (see Section 3.1.4.1).

Dosimeters can be categorized according to their frequency selectivity, which can be RAT-selective or operator-selective (see Section 3.1.4).

A dosimeter measures the exposure for different wireless communication frequency bands at the same time. Depending on the radio access technology, dosimeters provide separate DL and UL exposure data (in case of frequency division duplexing) or combined DL and UL exposure data (in case of time division duplexing, e.g., Wi-Fi). If UL signals are present in the same frequency band as the DL signals (for example, Wi-Fi, DECT) and usage of personal devices is not written down in a diary, then, only temporal information can be obtained, because it is impossible to differentiate UL and DL signals in the same frequency band. Moreover, when dosimeters are worn by a person, they are not suitable for assessing the UL exposure of the device operated by this person as the position of the dosimeters with respect to the mobile device is unknown and shadowing of the human body increases the variability of the uplink exposure measured by the dosimeter. Measuring the incident field level for these communication technologies is only



possible if one assures that there are no uplink signals present in close proximity of the dosimeter.

#### 2.1.2.2 Spectrum analyser setup

The flow chart for the spectrum analyser setup is shown in Figure 2(a). A spectrum analyser setup can measure in the frequency domain as well as in the time domain. The time domain measurement is mainly used for assessing duty cycles or time durations of the exposure. In the frequency domain, the spectrum analyser setup is the most flexible setup in terms of frequency selectivity, but can only be used for assessing downlink exposure. If only a single polarization is measured, then extrapolation to three axes can be applied to estimate the total incident field (see section 4.2).

If the spectrum analyser is not isolated, i.e., close to a transmitting device (e.g., laptop), then a diary can be used to remove the signals from this close device.

#### **2.1.2.3** *Trace mobile*

The flow chart for the trace mobile is shown in Figure 2(b). A trace mobile is the only suitable measurement tool to measure the uplink exposure. A trace mobile also measures the received power in terms of RSSI. Although these devices are not the most suitable for measuring downlink signals, studies have shown that the incident power density can be assessed in case of a proper calibration [3]. But, of course, the uncertainty will be larger than dedicated measurement equipment for assessing incident power density, such as a dosimeter or spectrum analyser setup. In addition, the trace mobile allows investigating the duality between DL and UL signal.

#### 2.1.2.4 Low-cost, single-polarised dosimeter within a sensor network

The flow chart for the low-complexity dosimeter is shown in Figure 2(b). The low-cost, single polarized dosimeter is designed to be used within a sensor network. For instance in the SmartSantander test bed (Section 3.1.3), these dosimeters will be deployed to assess the exposure over a specific area. The typical conversions of the measured data for usage in the EI formulation are: extrapolation of the single-polarized fields to the total (i.e., three-axis) incident fields, and the extrapolation from the height where the dosimeter is deployed to the height where the exposure levels are evaluated in the EI formulation (see Section 4.2).

#### 2.1.3 Network data

DL, UL and temporal data for the El calculation can be obtained from the transmitted power of base station antenna, received power or RSSI at a mobile device and throughput.

The methodology for EI assessment requires mapping data from different sources which is described in more detail in Section 3.2, after introducing the available sources of data and the methodology data are obtained.

Version 4.0



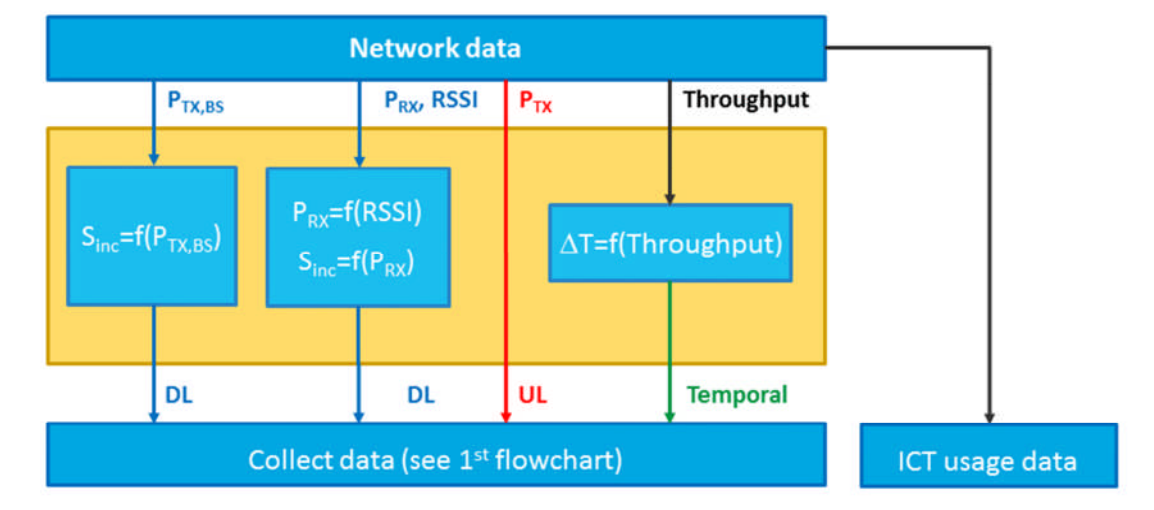


Figure 3: Flow chart for the network data.

# 2.2 <u>Interpolation, extrapolation and combining downlink exposure</u> metrics

After converting data to the input variables of the EI formulation, DL data might require some post processing (interpolation, extrapolation and combining downlink exposure data obtained by different tools) before calculating the EI. For example, extrapolation of DL data to another from 6 m to 1 m (see Section 4.1), estimation from indoor exposure levels from outdoor exposure levels (see Section 5) and extrapolation from single axis measurement to three axes (see Section 4.2).

#### 2.2.1 Combining downlink exposure data: Co-kriging interpolation

As shown in Figure 1, an additional step might be required before calculating the El using the formula defined in D2.6 [2], namely combining the exposure data obtained from different sources (e.g., combining DL exposure data from measurement and simulation). In this case, the co-kriging technique allows assessing the exposure based on the combined data from used measurement or simulation tools.

#### **2.2.1.1** *What is co-kriging?*

Kriging was originally proposed by Krige in 1951 [4], and further explored by various researchers [5–7]. Because of its distinct advantages over other interpolation techniques (e.g., *splines*, *inverse distance weighting*, etc.) when dealing with spatially correlated variables, it is popular in several research disciplines [8], including environmental RF-EMF exposure [9–12]. Additionally, the Kriging interpolation technique can be combined with additional information other than just the collected data, resulting in different formulations of Kriging [5], [6], one of which is *co-Kriging*. Using co-Kriging, the interpolation model is constructed with data of different "fidelities" (e.g., in case of data obtained using different measurement devices, the fidelity will depend on the measurement accuracy). The mathematical breakdown of the co-Kriging technique can be found in [6] and [13].

#### 2.2.1.2 Example of co-kriging used in RF-EMF exposure assessment

A recent study by Aerts et al. [14] demonstrated the validity of combining RF-EMF measurement data from different measurement devices by means of co-Kriging



interpolation. In this study, a set of 31 high-fidelity (HF) spectrum analyser measurements and a set of 50 low-fidelity (LF) exposimeter measurements were used to construct four types of models: (1) a Kriging model built with 30 HF measurements (called "HF K"); (2) a Kriging model built with 50 LF measurements (called "LF K"); (3) a Kriging model built with 30 HF and 20 LF data points (called "HF+LF K"); and (4) a co-Kriging model built with 30 HF and 20 LF points (same points as for "HF+LF K") (called "HF+LF coK").

The results (correlation parameters and error metrics) of a validation with the HF data (leave-one-out cross-validation for the three models including HF data) are shown in Table 1; from which it is clear that, while combining LF and HF data with no regard to their respective fidelity might even result in a worse model than using simply the HF data (compare "HF + LF K" to "HF K" in Table 1), using co-kriging results in a better-performing model than any of the other types.

Table 1: Correlation parameters and error metrics of the four types of models. κ, sens(itivity), and spec(ificity) were calculated using tertiles as cut-offs. RMSE = root mean square error.

Model	#	Spearman	R2	K	sens	spec	RMSE
	points	(-)	(-)	(-)	(-)	(-)	(V/m)
HF K	30	0.58	0.23	0.32	0.64	0.80	0.061
LF K	50	0.55	0.07	0.32	0.64	0.80	0.067
HF + LF K	50	0.45	0.10	0.23	0.55	0.75	0.066
HF + LF coK	50	0.64	0.41	0.42	0.73	0.85	0.054

#### 2.3 Exposure Index uncertainty assessment

When reporting the result of a measurement of a physical quantity, it is obligatory that some quantitative indication of the quality of the result be given so that those who use it can assess its reliability [15]. Without such an indication, measurement results cannot be compared, either among themselves or with reference values given in a specification or a standard. Uncertainty of measurement is a parameter, associated with the result of the measurement, that characterizes the dispersion of the values that could reasonably be attributed to the measurand.

The Exposure Index is the output of an analytical model expressed by the Equation (1) with a number of uncertain input variables [2]. To propagate the uncertainty associated to the input variables in the model, the first step consists in characterizing the distribution of input variables. Second step is determination of the uncertainty of (overall) El result, based on the uncertainty of input variables, what is referred to as the propagation of distributions (uncertainties).

Each uncertain variable input will be described by a statistical distribution [2]. The uncertainties of the life segmentation data will be analysed and modelled using computable functions such as Gamma, Gaussian or uniform distributions. Uncertainties on the time use structure on an average day, the usage segmentation and the average durations of usage will be also characterized.



Tx and Rx powers are estimated using specific configurations, environments and usages. The downlink power absorbed by the user and the uplink power emitted by the device (and so partially absorbed by the user) depend on these configurations, environments and usages. Their statistical distributions have to be characterized in order to be incorporated in the total EI statistical uncertainty.

The uplink exposure characterization requires a precise modeling of the power emitted by the device. Usually, this exposure will depend on two parameters: the position of the personal device relative to the user body and the variation in spatial distribution of the antenna gain due to the induced coupling effects. The impact of the positioning of the wireless device has been investigated by varying the position of personal device with respect to the body. Results have shown that the whole-body SAR is not very sensitive to the device position.

To investigate the impact of the antenna gain on the variability of the emitted power, we have used a statistical model of propagation channel [16].

The downlink exposure is very sensitive to the electromagnetic environment [17], [18]. Many physical obstacles (such as tunnels and buildings, or even the user) between the transmitter and receiver can affect the characteristics of the ambient electric field. This latter depends on many parameters such as the number of wave components (due to the diffractions undergone by the original wave radio), the fluctuations of the wave amplitude, its phases and arrival angles. In the literature, several studies focused on the modeling of the electromagnetic environment in realistic conditions, by giving the statistics distributions of all of these parameters [17], [19].

For the second step (propagation of uncertainties) various approaches are available:

- the GUM (Guide to the expression of Uncertainty in Measurement [15]) uncertainty framework generally approximate;
- analytic methods exact;
- a Monte Carlo method (MCM) providing a solution with a numerical accuracy that can be controlled.

An example of an analytical approach to EI uncertainty evaluation based on certain assumptions is given in Appendix E.



#### 3 EXPOSURE DATA

We remark that not all the assessment tools and data are available to all stakeholders (i.e., general public, regulatory bodies and network operators). Table 2 lists the data which are available to the different stakeholders. The level of accessibility is indicated by colours: red indicates data that are not accessible, orange designates medium accessibility indicating that the data might require the support of experts, and green means that the data are accessible. Measurement data are available to all stakeholders if the measurement equipment is publicly available. However, the operation of some measurement devices requires expert support. Simulation data are also available to all stakeholders if input parameters (location of base station antennas or access points, transmitted powers, etc.) are publicly available. Network data are typically available to the operator only.

Table 2: Data available to different stakeholders.

Type of data	Regulator	Operator	Public
Measurement data			
Dosimeter		•	•
SA	•	•	_
Trace Mobile		•	•
Low-cost dosimeter within WSN	•	•	•
Network data	•	•	•
Simulation data, e.g.,			
Exposure- / Propagation tools (e.g., WHIPP tool, VolcanoLab)	•	•	•
Life segmentation data			•
ICT usage data	•	•	•
SAR data			
FDTD / FEM-MoM	•	•	•

### 3.1 Measurement data

Figure 4 gives an overview of the measurement equipment available for assessing UL and DL exposure metrics. The downlink exposure can be measured with a spectrum analyser (combined with tri-axial probe) and dosimeters, whereas a drive test measurement assesses the UL transmitted power of a mobile device.



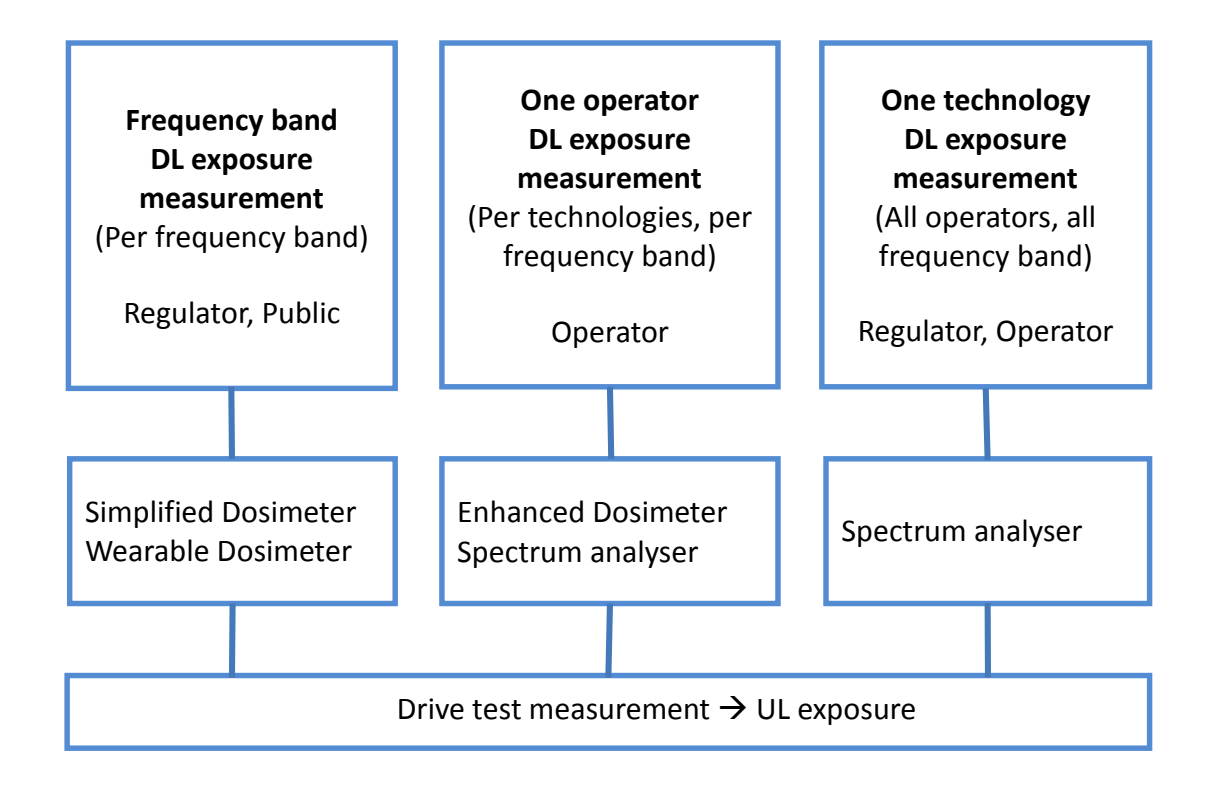


Figure 4: Measurement equipment for assessing DL and UL exposure metrics.

The measurement tools can also be categorized depending on their frequency selectivity as shown in Table 3. We distinguish four types of frequency selectivity: single frequency-selective, carrier-selective, RAT-selective and Operator-selective. The measurement setup with spectrum analyser and tri-axial probe is the most flexible one as it allows all frequency-selective measurements of the DL exposure. Besides the spectrum analyser setup, dosimeters can also be used for RAT-selective and operator-selective measurements. Currently, three types of dosimeters are available: simplified dosimeter and wearable dosimeter, which are both RAT-selective, and the enhanced dosimeter which is RAT- and operator-selective. Finally, in the UL, the drive test tool is of the carrier-selective type.

Table 3: Frequency-selectivity of the measurements tools for assessing downlink and uplink exposure.

Frequency selectivity	Measurement type
Single frequency	Spectrum analyser setup
Carrier	Spectrum analyser setup,
	Drive test
RAT	Spectrum analyser setup,
	Simplified dosimeter (single polarized),
	Wearable dosimeter,
	Enhanced dosimeter
Operator	Spectrum analyser setup
	Enhanced dosimeter



#### 3.1.1 Drive test



Figure 5: Drive test measurement tool

Drive test measurement tools are modified mobile phones that are able to log all the communication events that are involved in a mobile communication, i.e., voice call and/or data transfer. There are two types of drive tests:

- Mobile phones connected to a computer that collects the data.
- Android smartphones on which a drive test application has been installed that runs in the background. The collected data are recorded in the memory of the smartphone.

The advantage of the second type is that the drive test application is not a constraint to the real usage of the phone.

The data collected that can be used to assess the LEXNET EI are the type of RAT, the cell ID the mobile is connected on, the power received  $(P_{RX})$  and the power emitted  $(P_{TX})$  by the phone during a communication, the GPS position, and the data throughput in the case of data transfer.

In the following paragraphs are presented two measurements campaign, one for voice calls and one for data transfer.

#### 3.1.1.1 Example of drive test measurement for voice call:

A drive test measurement campaign was done in Santander jointed with dosimeter measurements.

During this campaign, two JDSU FTA drive test system installed on Samsung S4 smartphones were used. The two mobiles were connected to one operator network, and a voice call was established between them. One of the phones was forced to connect to the 2G network, the other one was forced to connect to the 3G network. They were hand held along the measurement path.

In all the cases we recorded the position, the  $P_{RX}$ , the  $P_{TX}$ , the RAT, Common Pilot Channel (CPICH) in 4G or Broadcast Control Channel (BCCH) in 3G which can give the frequencies, and cell ID.



In Figure 6 below the uplink transmit power  $(P_{TX})$  of the mobile for a 3G voice call is represented on the map.

Similar mapping was obtained for the 3G  $P_{RX}$  values and for  $P_{RX}/P_{TX}$  in the case of 2G communication.



Figure 6: Example of 3G Tx measurements in Santander downtown area

#### 3.1.1.2 Example of Drive test measurement for data:

Drivetest can also be used to assess the exposure in the case of data usage as HTTP browsing, File Transfert Protocol (FTP), or User Datagram Protocol (UDP). By getting the values of throughput for each type of protocole we can determine the duration that is needed to upload the data and by this way assess the exposure.

In Figure 7 and Figure 8 are shown the results of an FTP upload measurement operated in a car in Paris. A scenario was created in the drivetest in order to repeat a number of times the uploading of a file during movement.

Among the information collected are presented bellow the mean throughput for each sending of the file an the transmif power  $(P_{TX})$  of the mobile.





Figure 7: Mean throughput during FTP upload



Figure 8: Transmit power ( $P_{TX}$ ) during FTP upload

The drive test solutions presented above are quite expensive and are dedicated for professional use. In LEXNET, a low-cost solution has been developed which permits us to carry out UL and DL measurements along with other network parameters (cell-ID, SINR, RSRQ, etc.) and throughput measurements. It consists of a multi-standard modem terminal and external antennas connected to a PC and a GPS device. The initial work progress on this device has been presented in [20] (Section 3.4.4). Some further results can be found in the 7Appendix A.

#### 3.1.1.3 Use of the tool in the EI assessment.

The drive test tool can be used to:

- Measure the transmit power  $(P_{TX})$  in an area, for one RAT, one operator, for one type of usage at a time.
- Measure the received power  $(P_{RX})$  in an area for one RAT, one carrier, one operator and for one usage at a time. Some precautions have to be taken to assess the DL exposure. Because of the non-isotropy of the mobile phone antenna a measurement method proposed in [3] has to be followed in order to get averaged values and to calibrate the tool.
- The metrics of this tool for the received power and transmit power is dBm
- The uncertainty due to the tool is inferior to 1dB (see calibration in 7Appendix F).



#### 3.1.2 Spectrum analysis

#### 3.1.2.1 Presentation of the tool.

This type of measurement can be achieved with a system containing

- A 3-axis electric-field probe which captures the 3 spatial components of the electromagnetic field at the measurement point.
- A spectrum analyzer connected to the probe via a switch to analyse the 3 axis of the probe,
- Software which drives the measurements, integrates the spectrum and saves the electric-field strength (E) in V/m.

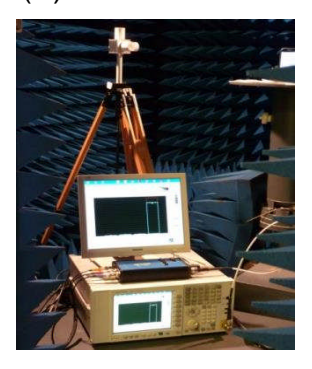


Figure 9: Spectrum analysis measurement system

With this measurement system it is possible to have a precise separation of the frequencies, of the RAT and of the operator bandwidth. As shown in Figure 10 a spectrum analysis of the 900 MHz DL band done in downtown Santander it is possible to separate the emissions coming from 2G and 3G and from each operator present in the frequency band.

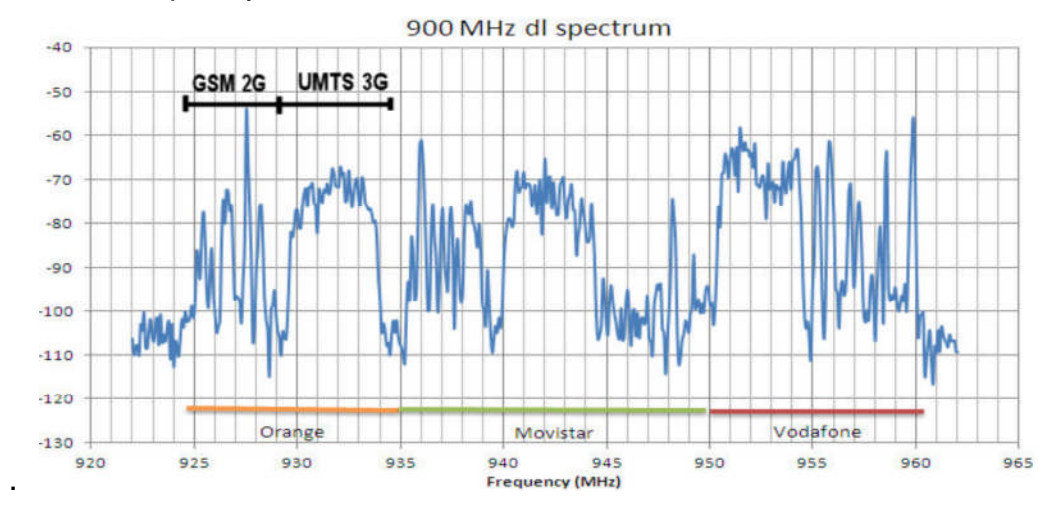
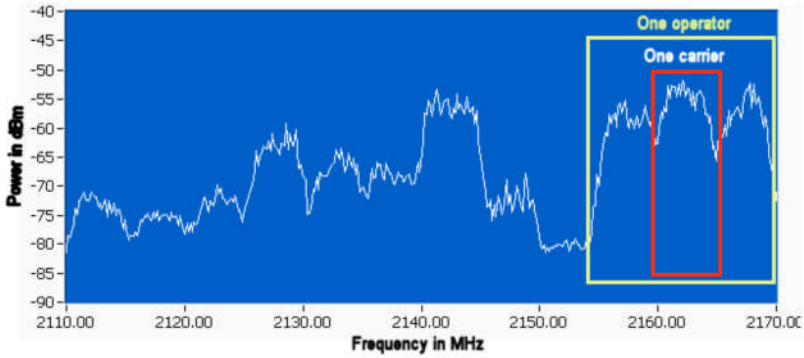


Figure 10: GSM and UMTS in the 900MHz frequency band

In Figure 11 and Figure 12 the different values of the DL exposure are shown that can be extracted from a spectrum analysis are shown. In this example the results of the measurements for the whole 3G 2100 MHz bandwidth are presented, for one operator and for one carrier.

Dissemination level: PUBLIC





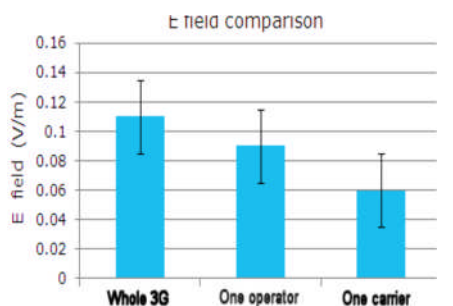


Figure 12: Exposure values for the separate bandwidths

Figure 11: One operator bandwidth and one carrier in a 3G spectrum in the 2100 MHz frequency band

#### 3.1.2.2 Use of the tool in the EI assessment.

The main use of spectrum analysis measurement tool in the assessment of the EI is the measurement of DL exposure.

With a spectrum analyser setup, we can measure:

- A whole frequency band, as for example 900 MHz band.
- A whole RAT, all operators combined, divided over different frequency band.
   As an example the DL exposure due to 3G carriers in the 2100 MHz and in the 900 MHz frequency bands are added to assess the global 3G exposure.
- The one operator exposure for one RAT in different frequency band or for all RAT combined.

The metrics of this measurement is the electric-field in V/m.

#### 3.1.3 Sensor network [UC]

Unlike other measurement tools (for instance, a spectrum analyser), the use of the simplified dosimeter has been envisaged so as not to work in isolation. These devices will be massively deployed, originating a sensor network, in order to characterize the EMF exposure of a relatively large area within long time periods, taking periodic measurements in short time intervals. In this sense, the network of deployed dosimeters will shape a new measurement tool per se.

This measurement methodology will allow public stakeholders and regulators to overcome the lack of real network data, providing them with an efficient tool to characterize the EMF exposure in a large scenario (for example a city) with a low-cost solution. Moreover, it will also provide real-time measurements within long time periods.

As has been previously discussed, the simplified dosimeters have been designed to measure just the downlink exposure; besides, they will be deployed using the city furniture (such as lampposts, and walls). As a consequence, they cannot provide meaningful information regarding the uplink induced exposure. Provided that the El considers both uplink and downlink contributions, the measurements gathered with



the simplified dosimeters need to be complemented either with data provided by other tools (for example wearable dosimeters, spectrum analysers or drive-test tools) or by means of extrapolation techniques based on off-line simulation studies. The EI assessment methodology has been thoroughly described in Section 2.

In order to cover an area as broad as possible, while keeping a reasonable measurement accuracy, the selection of the simplified dosimeters locations will be based on thorough simulation (carried out within WP6) and analytical studies. These simulations are carried out over the Volcano platform [21] and consider the base stations locations, the types of buildings within the target area and the way the dosimeters will be deployed (i.e. whether they will be placed at walls or lampposts).

In the LEXNET project, the deployment of simplified dosimeters will be integrated in a smart city testbed [22], which facilitates the data acquisition and handling procedures. A detailed description of the testbed architecture and functional overview can be found in [20].

By using this kind of framework, public stakeholders and regulators, even the end users, might be able to remotely access the data by means of web services. By subscribing to the EMF measurements, it would be possible for a user to register the data, building historical records to further characterize the EI within the overall area. Additionally, the flexibility offered by the platform will allow focusing on particular zones, by subscribing to a subset of dosimeters; this last feature might be of especial interest for regulators.

#### 3.1.4 Portable dosimeters

If one relies only on the measurement data coming from the fixed dosimeters described above, it will introduce errors due to the impact of spatial fading endured by the fixed measurement devices. In addition, the fixed dosimeters will be placed at a certain height (lamp-post, or building wall) hence the electric-field strength measured by them would not represent the exposure at the human body level (considering an adult at about 1.5m for example).

To overcome the issues identified above, portable dosimeters can be used to gather DL exposure data at different points in space. This data will remove the spatial fading effect as encountered in the fixed point measurements. A detailed study regarding the existing dosimeters and the LEXNET portable dosimeter can be found in [23].

The portable dosimeters are intended to be deployed in the LEXNET validation test benches and to gather DL exposure data over a given period of time. This would result in a large amount of data from different locations representing the real DL exposure during a given day. For example we can have statistical data for one or several subjects (each having this dosimeter with them) during their daily activities in different scenarios (home, work place, outside activities, etc.). This can serve as a data base for the EI estimation and for calibration of network simulations.

The use of portable dosimeters poses a problem of human body effect. When a person is wearing the dosimeter, the measurement can be affected depending on the relative positions of the dosimeter and the body with respect to the radiating source (BTS, Access point, mobile device etc.). This aspect has been studied in detail and correction schemes have been proposed ([23], chapter 4).

One can also argue that a smart device (smart phone or tablet) can be used to estimate the DL exposure and as most of the users are equipped with these devices,

Version 4.0 Dissemination level: PUBLIC



one can gather this data instead of using a dedicated device (dosimeter). This aspect has also been studied in LEXNET. A comparison of Wi-Fi exposure measurements carried out from a tablet and a dosimeter in a controlled environment ([20]) has shown that the tablet provides unreliable results (large variations) and that they are dependent on the orientation of the tablet. A similar study has been carried out comparing real signals for different standards (2G, 3G, and LTE) measured by a smart phone (Samsung Galaxy S4) and an EMESPY 200 dosimeter. The objective was to compare the isotropy of the mobile device and the EME SPY dosimeter with real signals generated by an emulator with controlled power transmission. The comparison is shown in Figure 13.

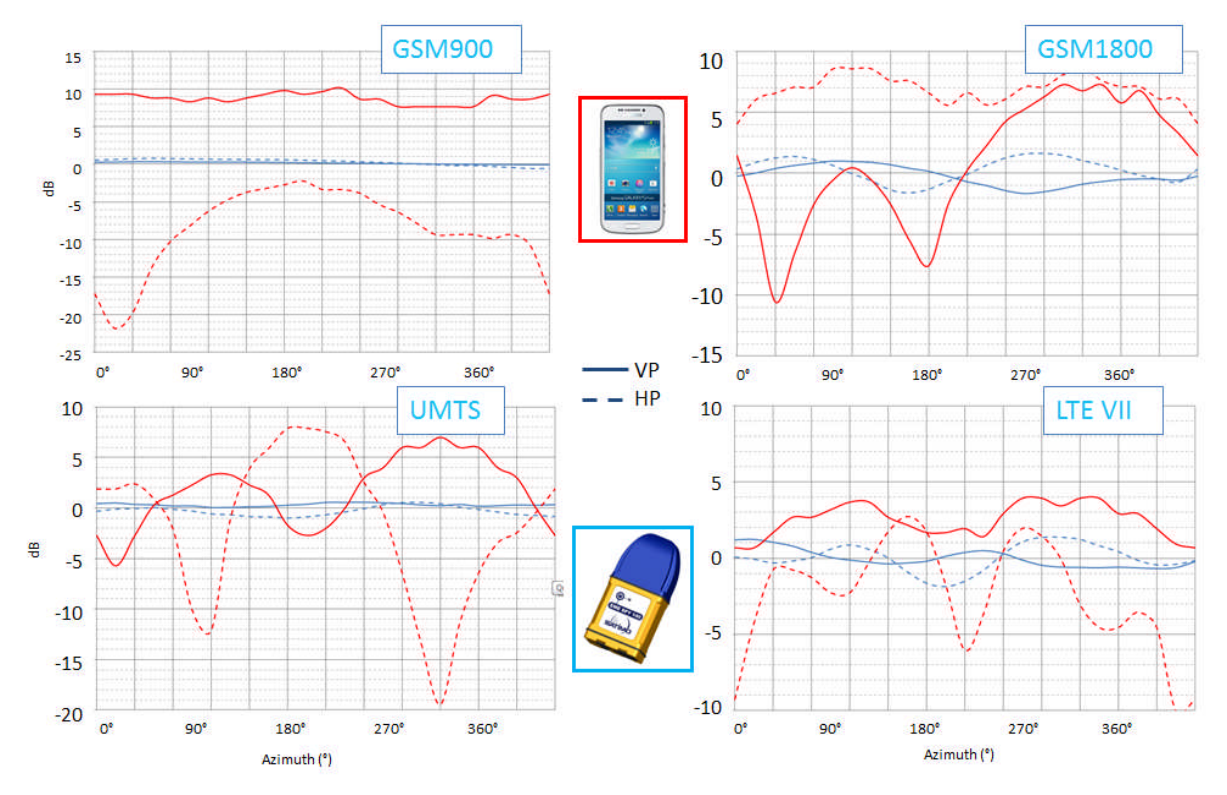


Figure 13: Isotropy plots in the azimuth plane for the smartphone (red curves) and the EMESPY 200 dosimeter (blue curves) for the vertical polarization (filled line) and horizontal polarization (dashed line) incident field.

The results clearly show that the isotropy of the mobile phone is poor and if one uses this device for DL power measurements; variations up to 30 dB can be expected. These variations will be higher when the device is hand-held. The measurement setup and detailed results are shown in 7Appendix G. Considering the above results, one cannot rely on the measurement data from the smart devices for the evaluation of the EI.

The portable dosimeters are also able to measure the UL exposure with good precision in an isolated state. However, if the dosimeter is worn by a person, the UL exposure measurements are not reliable, as they depend on the relative positions of the mobile device and the dosimeter on the body. The above statement has been confirmed using a simple experiment shown in Appendix B The use of the dosimeter to measure the UL power (or E-field) in the case of Wi-Fi has been studied in 7Appendix H. As the Wi-Fi uses the same frequency for the UL and DL signals which are distinguished using time domain duplexing, the dosimeter can be used to extract



the UL or the DL signals by placing it either close to the access point or the mobile device. The results confirm that we can easily extract the Duty cycle and average power emitted from the mobile device or the access point. The same results can be applied to DECT standard where the UL and DL signals are separated in the time domain.

#### 3.1.4.1 Estimation of EMF from personal and fixed point dosimeters

An important task is to develop a methodology to assess the exposure data obtained from personal and fixed point dosimeters. Obviously, due to body shadowing, the exposure data obtained from personal dosimeter will be different depending on the on-body placement. Moreover, the temporal variation and correlation between exposure data obtained from personal and fixed point dosimeters should be analysed. Accordingly, this section summarises the results of a study aiming to assess the impact of the body shadowing on the wearable dosimeter EMF measurements. The details of the study are given in 7Appendix J. This study served as a basis for an example of calculation of the exposure index in deliverable D2.6 [2].

When modelling the radio link between the dosimeter located on the body and the base station, one considers the influence of the body (*i.e.*, body coupling, [24], and body movements, [25]), and accounts for the propagation environment using a geometrically based statistical channel (GBSC) model (*i.e.*, multipath propagation). The simulated scenarios consider a reference isotropic dosimeter on the head of the user (simulating the real body exposure), together with five wearable dosimeters, as depicted in Figure 14.

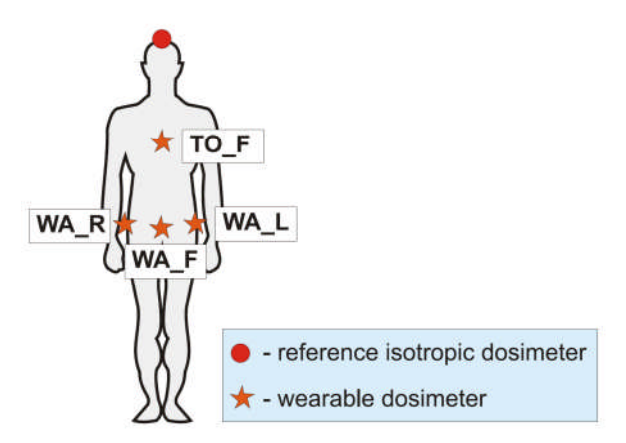


Figure 14. Placement of wearable dosimeters on the body.

A multipath macro cell street environment has been considered, containing a 3-sector base station antenna in the middle of the street. As shown in Figure 15, the user is moving on a straight line or in a loop movement (random motion).

Version 4.0 Dissemination level: PUBLIC



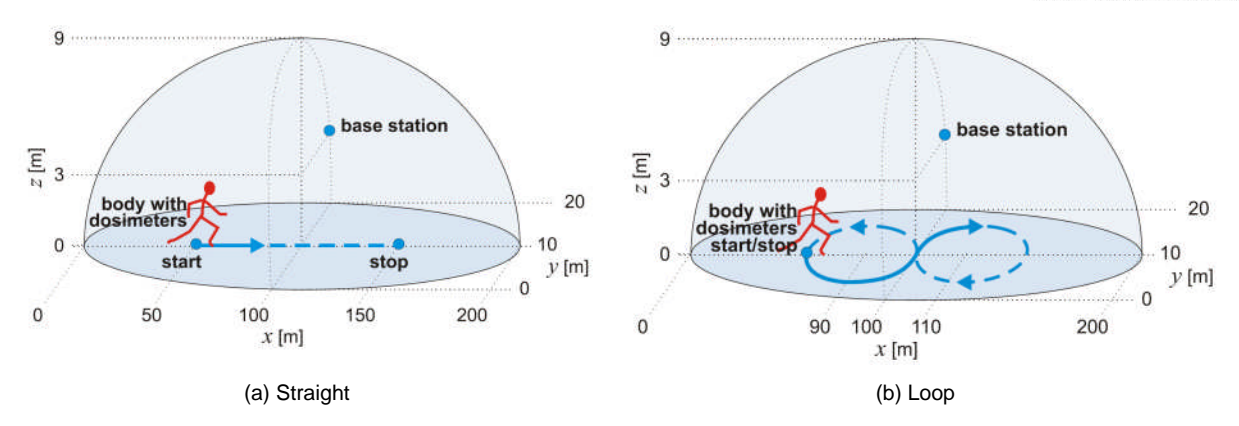


Figure 15. Scenarios.

Figure 16 exemplifies the average Rx power density obtained from the isotropic reference probe and the dosimeters located at WA\_L and WA\_R. The received power density at WA\_L dosimeter is very similar to the one gathered at the isotropic probe, which mainly comes from the similar Line-Of-Sight (LOS) propagation conditions. As expected, the power received in WA\_R dosimeter is much lower, due to the body shadowing.

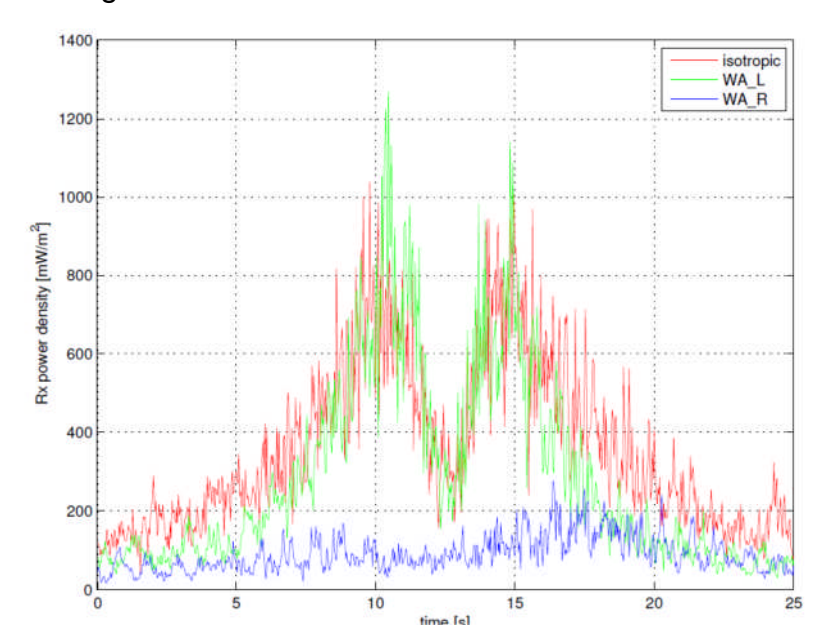


Figure 16. Rx power density for straight scenario at 2600 MHz.

The ratio, RRR, between the Rx power densities obtained from the different on-body dosimeters and the reference isotropic probe is calculated as:

$$R = \frac{S_{Rx[W/m^2]}^{dosim}}{S_{Rx[W/m^2]}^{isotr}}$$
(1)

Table 4 provides the values of  $\underline{\mathbb{R}}$  for the two analysed scenarios. These ratios provide a measure of the body shadowing in the dosimeters measurements, in a multipath environment.



Table 4. Ratio between the Rx power densities obtained from the on-body dosimeters and the reference isotropic probe.

	R		
	Straight	Loop	
WA_L	0.79	0.49	
WA_R	0.25	0.49	
WA_F	0.51	0.25	
WA_B	0.82	0.80	
TO_F	0.51	0.27	

Concerning the straight scenario, the ratio of the Rx power densities gathered by the different dosimeters to the reference dosimeter ranges in [0.25, 0.82]. These ratios can be used as a measure of the body shadowing effect, which is really severe in non LOS conditions. In this scenario, the use of a wearable dosimeter in the right side of the body displays a Rx power density reading about 4 times lower than the real one.

In this case of loop movement, the ratio of the Rx power densities gathered by the different dosimeters to the reference dosimeter is more balanced. Two dosimeters worn in the right and left sides of the body will display a similar Rx power density reading. Concerning front and back locations, the readings can be much different, because there is not the same symmetry (*i.e.*, the user is inclined to the front, and the back dosimeter always displays higher Rx power densities).

#### **3.1.5 Summary**

To conclude, the measurement tools available for the EI assessment (developed in the LEXNET project or already existing tools) are summarized in Table 5 with their capabilities. These tools will be employed in the WP6 demonstration test benches for EI evaluation.

Table 5: Summary of measurement tools selected for LEXNET EI assessment

Measurement tool	Use in LEXNET	Availability	Output	Limitations	
Simplified Fixed dosimeters	Santander smart city deployment for DL exposure measurements. Coupling to simulations and other measurement data.	Low-cost dedicated sensor designed under the LEXNET project. Deployment to start in Mo 24.	Continuous DL E- field.	Suffers from spatial fading. Does not represent the exposure at user level. Cannot measure UL exposure.	
Portable dosimeter	Calibration of simulations and measurements from fixed dosimeters.	EME SPY 200 dosimeter available.	Geo-localized DL / UL exposure data for a particular user over a given time	Impact of human body on measurements. Incorrect estimation	

Version 4.0 Dissemination level: PUBLIC



	Measurement of user exposure from DL		frame (one day). Can also measure UL exposure.	of UL exposure. Cannot differentiate between different service providers.
LEXNET wearable dosimeter	Same as for 'Portable dosimeter".	Expected in final year of project.	Geo-localized DL / UL exposure data. Can measure the exposure from a particular service provider. Takes into account the impact of human body impact.	Incorrect evaluation of the UL exposure
Trace mobile	Evaluation of DL / UL exposure using drive test.	Limited availability.	Service provider specific DL / UL exposure data. Other network parameters available.	Not user specific. Exposure data for specific conditions only. Expensive to deploy in terms of material and human cost.
LEXNET Low- cost UL/DL power measurement equipment	Same as for "Trace mobile".	Development in LEXNET project. Prototype available for testing.	Service provider specific DL / UL exposure data. Other network parameters available. Low cost. Can be deployed over a large scale.	Not user specific. Data for specific conditions only. Prototype version and needs further detailed evaluation.
Spectrum measurements	DL measurements for one RAT or one service provider.	Professional use.	DL measurements, power or E-field	Expensive to deploy and cover a given area.

### 3.2 Network data

Another approach to assess the EI assumes that it is possible to obtain data directly from the network. Namely, operators can use the live networks' measurements, as well as statistical and raw data from the network (e.g. usage data, cell statistics) stored in various databases (operation and support systems, call data records, customer analytics system, probes on network interfaces).

For network operation and management, there are different measurements available that can be used to assess the EI. Some of these measurements are taken on regular basis, while for other measurements special reports need to be triggered. Some of the measurements are done by network elements, while others are performed by probes, sensors, robots (e.g. UE apps - User equipment applications, drive test), thus the measurements may be gathered from them. The quantities that may be used to assess the EI include UL Tx power (per UE, per cell), DL Rx power (per UE, RSSI, RSCP, base station transmission power, etc.). Using network measurements and obtaining network statistics, the goal is to determine values of the parameters required for the calculation of the EI, i.e.:

 Distribution and average transmit power values on the UL: per technology; per velocity, per network load;



- Distribution and average DL power level: per technology; per velocity, per network load;
- Duration of exposure, call/session duration;
- Service utilization (UL/DL per type of traffic (elastic vs. non elastic)/ per time/ per area, per device, per age, per user type, per device type, ...);
- Population profile: e.g., genre, age, working day, user subscription profile;
- Inventory of the network (e.g. location of base station/type of technology/ transmit power/) type of area (urban/rural/sub urban).

Measurements in network reports (e.g. UE Tx power) on a cell (area) level are done on statistical basis, which is thoroughly described in [26]. Different technologies use different methodologies for network reporting, implying different uncertainties, which is also described in detail.

The main disadvantage of these reports is that the power samples are taken when the transmitter is actually transmitting, thus the periods of silence in between (needed for time-averaging) need to be measured with external equipment (field measurement equipment), in order to obtain the activity (duty) factor. This factor depends on the application and technology used, load conditions (let us limit ourselves just to high/low load traffic hours), radio conditions, mobility, and thus requires many measurements to be performed under different conditions. Yet, these measurements are on per-user basis and again, statistical in nature, bringing in uncertainties. The same user using the same application over the same technology, and even, suppose theoretically (as it always changes), with the same network load, and even being static, will have different signal appearance on the radio interface in different time due to ever-changing radio conditions.

Keeping in mind that it is not possible to obtain all the necessary data (for the calculation of the EI) only from network measurements, other sources should be used. Sources of data for assessing the EI are (Figure 6):

- 1. Network management system
- 2. Customer analytics system
- 3. Other databases and measurement systems
- 4. Field measurements
- 5. Census

Version 4.0
Dissemination level: PUBLIC



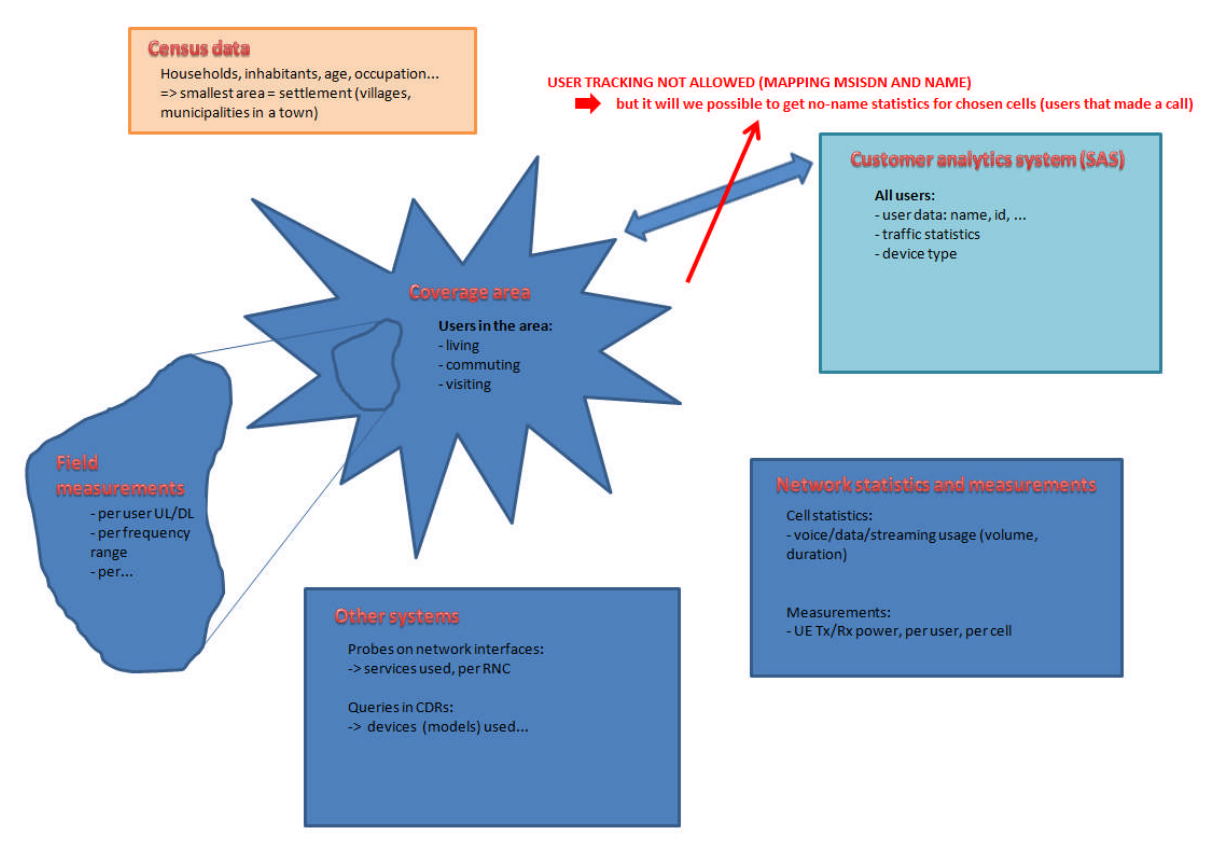


Figure 17: Sources of data

Considering the EI definition tree [1], [2] components of the EI that can be assessed with network measurements are:

- 1) Type of area: urban, suburban, rural;
- 2) Time: low hours, rush hours (related to traffic load);
- 3) Networks with regards to RATs and network layers;
- 4) Usages: voice/data, average duration of the call, etc.

Components of the EI that may be retrieved from other systems, and need to be linked to network measurements:

- User profile: data on registered users (only over the age of 18) can be extracted from SAS – Customer Analytics System, e.g., age, address, employment, residential/business, voice/data (subscription), UE (phone/dongle/tablet), weekday and weekend traffic data (incoming/outgoing calls, duration, SMS, MMS, #of data sessions, duration, traffic), etc.);
- 2) Usage data: type of UE used (mobile/tablet/laptop), type of service used, posture (hand/lap).

## Document ID: D3.3 Exposure Index Assessment v2 FP7 Contract n°318273



Data on customers and their habits concerning traffic, found in SAS, might be linked to a certain area (and measurements performed in that area/cells) in two ways:

- By International Mobile Subscriber Identity (IMSI) / Mobile Station International Subscriber Directory Number (MSISDN): exact population found in an area in a given moment.

However, MSISDNs of UEs that made an active call in a cell may be found in Call Detail Records (CDRs) and queried in the SAS database, which would mean tracking of a user, and this is forbidden by the Law on the protection of personal data and the Consumer Protection Act;

- By address: only customers (private/business) registered to the address.

This would involve exploring all addresses in an area and linking them to SAS data. Not only would it be quite a work (less automation), but it would not give exact information on people exposed to EMF in an area, as home address means a person is probably not there during the day, and sometimes firms are registered to one address, but working on the other, etc.

This would also be "static" linking, i.e., data on calls is stored in a database and later linked to statistic data from SAS, i.e., a subset formed based on MSISDNs involved in active connections in that area (cell) in some time period. This also means that we cannot get the number of (our) users in the area (cell) that did not establish an active connection in the period that data is required for.

As an example, in TKS network measurements can be triggered on per cell basis, but the list of IMSIs attached to that cell cannot be obtained. Only measurements per user (IMSI) or a list of users may be obtained (tracking a user for troubleshooting), but this involves usage of multiple cells. Some companies offer solutions for real-time measurements that could provide a list of users in cell (to be explored). Even in the future, this would require processing of enormous amounts of data, or using (at least for usage data) predefined "average/usual/approximate" values.

For instance, TKS had some analysis of usage in a part of the network - more precise; all used UE models are listed with the corresponding number of MSISDNs using them and volume of transferred data. Data was gathered from CDRs and it took 2 months for processing. We could get some statistical data for an area, for exact MSISDNs, but without MSISDNs stated in the final table. This means we would have required data for an area, but no customers could be identified. Three areas were chosen, to decrease the amount of data, and all cells covering them (2G, 3G, outdoor, indoor). For the same site, coverage areas of 2G and 3G BTSs are not the same, meaning that attention should be paid to the fact that statistics for MSISDNs



taken for a 2G cell at 900 MHz "cover" a wider area than 2G at 1800, or 3G at 2100, i.e., the area is not exactly defined this way.

TKS also disposes of fixed data on type of service used for an RNC, obtained by probing.

Components of the EI that cannot be determined from network are:

1) Population: children/retirees

This information may be estimated through the census info (general percentages) for the area applied to the connections (network measurements) in the area.

SIM cards registered to business users are mapped to working people group. For SIM cards registered to private customers, we cannot know if the card is in fact used by a child or by grandparents.

2) Location: outdoor/home (only signal level may be determined; data on general home/office/outdoor location (% of time of usage) may be used, if available)

Properties of an area are:

- 1) population: number of people living, commuting, shopping
  - census data: number of people living
- 2) subscribers:
  - percentage of the population
  - subscribers using the service may be seen through network measurements on per cell basis
  - subscribers that made an active call in a cell may be seen through CDRs (billing system)

Depending on the technology, for the same site, selected cells cover different areas, implying that the "area" is not "firmly" defined.

#### Since:

- the exposure of a user consists of its background exposure, and own exposure when active, and that
- the exposure when active, particularly exposure in the UL (but depending on the relative position to the site), dominates over the background exposure, and that
- a user uses technologies sequentially, i.e. cannot use GSM and WCDMA at the same time, and that

Version 4.0 Dissemination level: PUBLIC



- exposure of a population in an area is the sum of exposures from all technologies and all operators, for non-users and users, and that
- it is expected that GSM exposure dominates over 3G and 4G exposure, and that UL exposure dominates (for the majority of people in the cell) over DL exposure.

The overall exposure of a population in an area is dominated by GSM UL induced exposure, meaning that the "area" in cases of large coverage differences between technologies, might be linked to GSM cell coverage area, Figure 18. In [26], it is shown that for the same service, in hours with high or low traffic load, GSM tehnology induces higher UL Tx power profiles than 3G, as expected due to power control algorithms. If we presume that for a type of service (voice, data) the UE is held in the same manner towards the body, we can deduce that GSM UL induces higher exposure than UMTS/HSPA UL.

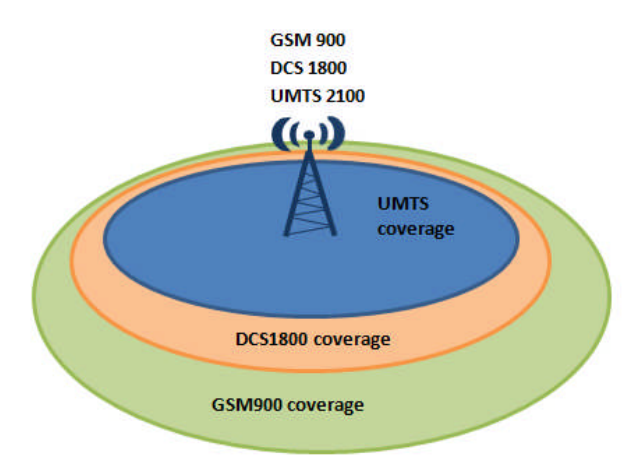


Figure 18: Coverage areas for different networks.

Getting data (network measurements etc.) for the exact (firmly defined) area is not possible since:

- the area can be only defined geographically,
- the position of a user is not known, the distance from the site may be extracted, only his address is known, if he is a post-paid residential customer,
- thus, network data from different serving cells in an area, whose borders
  do not exactly follow the borders of the subject area, cannot be linked to
  the exact subject area using some geographical query, we may only speak
  of loose borders (corresponding to a particular cell of a particular
  technology),
- people move, thus any geographical query not using current position is not valid.



Furthermore, the number of users in an area cannot be determined exactly – even the number of users in a cell (only users that made an active call, including visitors/roamers, through CDRs; due to radio conditions even if not moving, the same user may switch 2G/3G repeatedly, so the same person will appear in both 2G and 3G cells call statistics).

The analysis of cell statistics for different types of cells is provided in 7Appendix D. The main conclusion arising from these measurements is that the data should be analyzed and El assessed for a specific cell, not per type of area – although urban/suburban/rural cells have different characteristics, the limits between these types are loose. Further, even the two urban cells show different characteristics – while in the strictly business area the traffic drops during weekends, in the business/shopping area the traffic volume has rather same daily variations for all week days.

The data that can be obtained from the network and auxiliary means (drive-test and field measurements), to be combined together, is summarized in the Table 6.

Table 6: Data that can be obtained from different sources for evaluating EI in a real network

Source	Cell statistics	Network reports	Drive-test measurements	Call data records (CDRs)	Customer analytics system (SAS)	Automatic Device Configuration platform	Probes on network interfaces	Field measurements (frequency-selective equipment)
Data	- network KPIs - traffic load etc.	<ul> <li>measurements of UE Tx/Rx power per user, per cell</li> </ul>	measurements of UE Tx/Rx powers	IMEIs) that made an active call in	<ul> <li>per MSISDNs, usage data (avg. Call duration, avg. No. of calls, avg. Session duration, avg. Data volume, profile data</li> </ul>	UE type and model	- all exchanged message	<ul> <li>duty factor measurements (per applications, technologies)</li> <li>overall DL power from all operators, DL power from the own operator, UL power from surrounding users</li> </ul>
Purpose	classes of services used (voice, data, interactive) etc.	mapping it with user data is under question     UL; indicator of exposure level only if mapped with UE type and application	thus intended for single-user exposure assessment based on UE type, applications used, time of day (traffic load), type of cell	active call, as an input for other systems	- with CDR data on active calls in a cell: typical usage profile for a specific area	- pressumption on posture, position of the UE relative to the body based on the type of UE (phone, smartphone, laptop, tablet) and service (voice/data)	applications, protocols used etc.	time averaging of power samples recorded in network reports/drive-test measurements     - assessment of the background exposure profile

The data discussed so far is data that can be obtained from different network resources and drive-test and field measurements. Missing data with respect to the EI definition are the normalized SAR values, that can only be obtained from external sources (institutions that deal with SAR measurements).

Further, the main problem in the EI assessment in a live network is mapping data from different sources, which are statistical and extracted using different methodologies. The time-averaging of power samples over an area implies averaging over all connected users in the area - this is not possible, as explained, since we have data on powers from network reports only for a sample of users/call durations in a cell (depending on technology, see [26]), statistical subscriber (usage) data (customer analytics system) for a defined period only for users that made an active call in a cell, and data on applications used from probes on core network interfaces for an RNC or eNB. Advanced software tools that are emerging in the market could map radio signalling data (RNC, eNB) with user plane data (probes), giving us the linked information on users (IMSIs) and applications used. Yet, correlating actual recorded power samples (from network reports, differing per technology and service, see [23]) in a cell with duty factors determined by field measurements for different applications and technologies (and also load conditions, velocity...) remains the problem. In power profiles extracted for a cell (see [26]), we can not determine whether the UE was emitting with high power because it was far from the base station or because it was close and using a demanding application. The duty factor is



crucial for time-averaging, and the aforesaid implies that we can currently only make a mapping between average power level on a cell basis with the duty factor calculated by weighting duty factors of different applications used with the percentages of the time of usage vs. total time. This is not the same as weighting power samples with exact duty factor for the application used and time of usage (per user), and then averaging over a cell, as defined by EI, but is the only possible with the current network resources.

The introduction of new optimization tools with geolocation could help obtain more precise data for EI assessment. These tools are being developed in the late years with the growing complexity of the network including the deployment of small cells, offering customer-oriented near-realtime analytics and network optimization. They collect and analyse the Layer 3 messages from the Network Management Systems for different technologies and equipment vendors, use patented algorithms to extract position of users up to a 50 m precision, and analyse network key performance indicators along will call data. These tools may even replace drive-test measurements, and represent a powerful means for collecting data necessary for EI assessment. Such a big-data analysis of customer-oriented data (per cell, per IMSI), with some modifications, would definitely help in EI assessment and would decrease the present uncertainties. Mapping power measurements with usage data (applications used i.e. duty factors) would require some additional tool-development effort, and the other option would be to have agents on UEs collecting data on applications used and corresponding power levels in time.

#### 3.3 Simulation data

Simulation can be a valuable alternative to El measurements in some occasions:

- Exposure assessment in the pre-deployment stages, where the network design and parameter of future base stations (or access points) are decided;
- Consideration of exposure constraints or objectives in the optimization of existing but capacity- or coverage-limited networks;
- Complement to limited measurement data, i.e. for extrapolation from a measured samples to exposure maps.

Both sub-sections below present how the El can be implemented into the simulation of respectively cellular networks and indoor networks.

#### 3.3.1 Simulation-based EI assessment methodology for cellular network

The methodology proposed in this section aims at simulating the exposure metrics required for EI computation (DL field strength and UL transmit power) into a cellular network, based on radio-planning like techniques. The general flowchart of this methodology is given in Figure 19. This simulation-based assessment may be used to characterize either the exposure during the pre-deployment network design phase or the exposure induced by an already deployed network. It may also be integrated into the network optimization process, to evaluate the impact of tested network modifications (topology, radio parameters, network configuration) on the exposure.

The main bricks are (1) the scenario definition from input data (map data, network properties, users), (2) the computation of propagation losses for any kind of radio link, the cell selection and the link performance evaluation based on advanced Version 4.0

Dissemination level: PUBLIC



simulation engines, and (3) the display and reporting of simulation outputs. They are respectively further detailed in the next three subsections. The last subsection focuses on the different benefits that are expected from a joint usage of simulations based from this methodology and measurements.

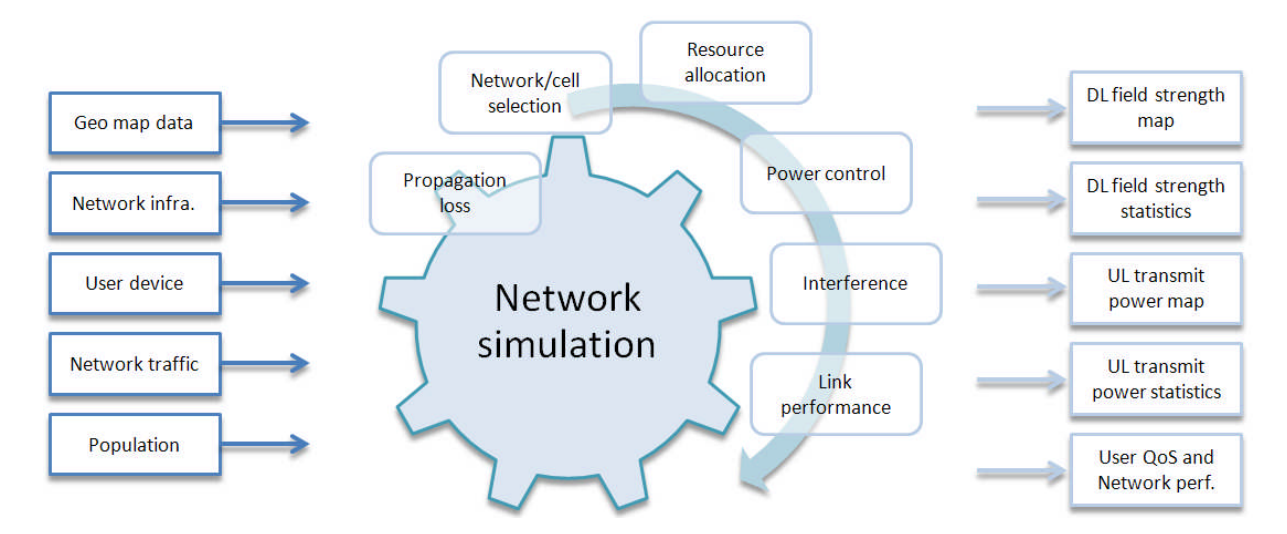


Figure 19: Simulation-based methodology for a cellular network.

#### 3.3.1.1 Inputs

The first input is the representation of the environment obtained by means of digital **geographical map data**. This commonly includes the terrain elevation, clutter type (building, vegetation, etc.) and clutter height above ground. This data is produced either from satellite pictures (low-resolution data) or from airplane stereographic pictures (high-resolution data).

Usual recommendations from radio-planning are as follows:

- Rural: 20 50 meter resolution with statistical clutter description;
- Urban: ≤ 5 meter resolution with fine clutter description (distinction between buildings, streets, etc.) and 1 meter precision on clutter height;
- 3D vectors may also be used for finer geographical data precision and multipath propagation predictions.

The multi-RAT **network infrastructure** is defined by a set of base stations that are each described by their 3D location, antenna radiation pattern, azimuth, down-tilt, frequency band, technology, maximum DL transmit power, UL sensitivity, MIMO (Multiple Input Multiple Output) configuration, etc. Indoor stations (e.g. Femtocells, Home eNodeB) may be also integrated in the simulation, if they are supported by the propagation models and if their access mode (open / closed / shared) is known and supported by the simulation tool.

In case of an already-deployed network, the information is obtained from the network operator database or from the regulator database. The accuracy of this data, in particular the coordinates of urban base stations, may be a concern when predicting DL EMF exposure maps; however the impact of network infrastructure inaccuracies is expected to be lower on the EI, as the EI results from an average over the whole study area.



The **user device** is characterized by the antenna gain, DL sensitivity, UL maximum transmit power but also technology-specific parameters like supported MIMO modes. Typical user device properties are obtained from literature, device provider or laboratory measurements. It is recommended to make conservative assumptions when no precise information is available.

The **network traffic** may be defined in two different ways:

- 1. The network activity and interference levels are set directly as an input.
- 2. The network activity and interference levels are predicted during the simulation, derived from user traffic, network and resource management.

In the first computation mode, the traffic-dependent cell metrics, i.e. the average DL cell load (percentage of the maximum total power that is actually transmitted) and UL co-channel interference level, are set for each time period. Depending on available information, the values of those metrics are defined either at RAT level (same value for all cells), layer level (distinction between macro and smaller cells) or cell level. Statistics on cell loads are derived either from global network traffic (at national or regional scale) or from local network monitoring. The local network monitoring offers the highest possible accuracy and allows deriving average per-cell values.

In the second computation mode, the network traffic is defined by two components: (a) user profiles and (b) spatial distribution according to the time period. Each user profile is characterized by a specific network usage: average voice call duration (e.g. over a day), average DL/UL data amount and, when relevant, some subscription properties (e.g. 3G or 4G subscriber). A traffic map for each user profile and time period gives the user spatial distribution e.g. defined as users density per unit area. Those maps are derived either from global network traffic (at national or regional scale) or local network monitoring, possibly crossed with geographical information (i.e. distinction between rural, residential, commercial, industrial, urban, dense urban and hotspot areas).

The traffic information is used during the simulation process to compute DL cell loads and to evaluate the interference levels; its impact on final QoS (Quality of Service) and EMF results is significant, in particular when traffic is high.

The ratio between indoor and outdoor users densities is another key parameter. As the link performance, thus the impact on cell loads and interferences, is significantly different in those two environments, the balance between indoor and outdoor users strongly affects the average network performance. Getting a fine estimate of the indoor-outdoor ratio at the scale of a macro cellular network is complicated. That is why typical figures from literature are most likely to be used.

The last input is a **population map** that describes the population density in the study area for different time periods. The maps may be derived from census data (high precision) or macroscopic area definition (dense urban / light urban / industrial / etc.). They could also be normalized by public authorities in the perspective of EI-based exposure regulation. The population information is used at the end of the simulation process to compute DL exposure statistics. In absence of population map, a uniform spatial distribution of the population can be assumed.



### 3.3.1.2 Simulation engines

The simulation process given in Figure 19 is an extension of usual radio-planning methodologies. Indeed, the EI depends on the average DL network load, average UL interference levels and maximum UL throughputs, which are common metrics in network coverage simulation.

Prediction of the **propagation** is the first block in the simulation. Site-specific (or deterministic) propagation models are used that take advantage of the precise terrain representation to compute physical propagation mechanisms (reflection, diffraction, transmission or scattering). The predicted path-loss includes the well-known distance and frequency free-space dependencies, but also a deterministic shadowing component.

Propagation around macro-cell base stations is usually well approached by vertical-plane models. They calculate the diffraction losses due to the obstacles met in the vertical profile between both radio stations. In particular, the multiple knife-edge techniques (Deygout, Epstein-Peterson or other related methods [27]) offer good accuracy with low-computational effort. Comparisons to drive-test measurements show error standard deviations between 5 and 8 dB even in dense urban environments. These figures are empirically set, based on previous studies and acquired know-how.

Ray-based models (ray-tracing or ray-launching) build geometrical ray trajectories and make use of the UTD (Uniform Theory of Diffraction) asymptotic expansion of Maxwell equations to compute reflections and diffractions on buildings. The prediction of multi-paths allows those models to address any type of urban propagation configuration, including street canyoning, and makes them specifically appropriate for small-cells. The ray-launching is a time-efficient implementation that permits some commercial models to compute large propagation grids (few kilometers) in only tens of second (on usual computers) for an error standard deviation between 5 and 9 dB, even in complex small-cell situations.

Indoor penetration is mandatory to predict the path loss from outdoor base stations to inside the buildings. This may be done either by the addition of an average indoor penetration loss (typically in the range of 10 - 20 dB depending on the frequency band and environment) or by the prediction of multi-path indoor-to-outdoor propagation. The latter method generates more realistic indoor variations, with typically a lower path-loss close to the facade than further inside.

In system DL/UL simulations, the path loss (dB) is the sum of four components:

- The propagation loss between the base-station and mobile-station antenna;
- The base-station antenna gain, which depends on the antenna radiation pattern and propagation direction(s);
- An average body loss;
- The user device antenna gain.

Body losses and mobile-station antenna patterns computed in LEXNET, from different frequency bands and several types of equipment and posture may be furthermore considered.



In the calculation of the DL field strength exposure, the path loss must only include the propagation loss and the base station antenna gain: no user device or body obstruction is considered.

The **network/RAT** and **cell selection** for each user is based on the best-server identification. Specific network and user attachment rules (e.g. offloading, access modes or interference mitigation mechanisms) can be implemented.

The **resources allocation** consists in the distribution of DL/UL cell resources to each user according to its service requirements (voice or data traffic), and based on the link performance (peak throughput). Specific network management rules can be implemented in the simulator to reproduce the behavior of scheduling algorithm that runs in the equipment.

The **power control** mechanisms regulate the transmit power on allocated resources. It is essentially used on the UL to reduce power consumption of the user device and to limit or control the co-channel interference. The selection of the transmit power depends on the channel properties (including attenuation and noise) and interference levels.

The co-channel **interference** strongly impacts the link performance in high-traffic systems, leading to degraded link performance and thus increased resource allocation. According to the aforementioned computation modes, the DL/UL interference levels are:

- 1. Either directly given as an input:
  - UL interference level (or noise rise) at the base station;
  - DL base station cell load, which is used to compute the DL interference level at any location in the study area.
- 2. Or computed from the user traffic and resource allocation.

Finally, the DL/UL **link performance** is computed from lookup tables with the Signal-to-Interference-plus-Noise Ratio (SINR) as input.

Note the computation of respectively the DL and UL metrics relies on two separated calculation chains, with common blocks (path-loss, cell selection) but also specific processing blocks (co-channel interference, power control, resource allocation, link budget). The DL and UL metrics, and in particular the DL and UL exposure-related outputs, are correlated because they both depend on the path-loss. Nevertheless the relationship between those metrics cannot be represented by a simple analytical formula, as it also depends on the prediction of local interference levels, on the interference management techniques and on the network topology (e.g. heterogeneous link budgets in HetNets).

### 3.3.1.3 **Outputs**

This simulation provides the following outputs:

• **DL field strength map:** A map per frequency band and time period gives the average DL field strength (V/m) in each pixel. This field strength is the sum of DL contributions generated at the pixel by all neighboring base stations.



- **DL** field strength statistics: Statistics per frequency band, time period and environment (indoor or outdoor) are built from the aggregation of all DL field strength values over the map, with a probability per pixel that is proportional to the population density in the pixel. The average of those DL field strength statistics (V/m) are expected inputs to the EI computation.
- **UL transmit power/energy map:** The definition varies according to voice or data services:
  - Voice: a map per frequency band, time period and user device gives the average UL transmit power (W or dBm) in each pixel.
  - Data: a map per frequency band, time period, user device and type of service gives the average UL transmit energy per data unit (J/Mb) in each pixel.
- UL transmit power/energy statistics: Statistics per frequency band, time
  period, environment, user profile, user device and type of service are built from
  the aggregation of all UL transmit power/energy values over the map, with a
  probability per pixel that is proportional to the user profile density in the pixel.
  The average value of those statistics gives the expected inputs to the El
  computation:
  - Voice: average transmit power (W or dBm)
  - Data: average transmit energy per data unit (J/Mb).

The same simulation process that gives the exposure metrics also provides **user QoS** (service coverage, peak throughput) **and network performance** (capacity) results. Having all those metrics together at the end of a same simulation might facilitate the introduction of EI-based exposure constraints into the network optimization process.

### 3.3.1.4 Joint use of measurements and simulations

In a general way, the simulation and the measurement can mutually benefit each other. On the one hand, the simulation may be refined thanks to a calibration of the model parameters. On the other hand, the simulation permits the measurement to be extrapolated from discrete local data to larger coverage maps.

Table 7 summarizes the different benefits that are expected from a joint usage of measurements and simulations. Some of them will be demonstrated at the end of the project as part of WP6 results.

Dissemination level: PUBLIC



Table 7: Benefits of a joint use of measurements and simulations.

### Network monitoring

Monitoring measurements allow the **identification of several time periods to be implemented in the simulation**.

Monitoring measurements provide **precise and reliable inputs to the simulation** (after averaging over each period of time):

- Cell DL traffic load
- Cell UL interference level

Monitoring data could also help in the calibration of UL throughput and UL transmit power prediction models.

Monitoring data alone is sufficient to derive the El. However the simulation, based on inputs deduced from the monitoring, can provide complementary exposure maps.

WSN measurements allow for the identification of **several time periods** to be implemented in the simulation.

The relative variations in the DL exposure from one period of time to another that are captured by the WSN measurements can be used to adjust the DL user traffic or DL cell load variations in the simulation.

### Wireless Sensor Network (WSN)

WSN measurements are valuable inputs for **evaluation of the DL exposure prediction accuracy**.

WSN measurements alone are sufficient to derive statistics on the outdoor DL exposure. And the DL exposure inside the buildings can be deduced from simple extrapolation models. However the simulation, adjusted with WSN information on time variations, can generate **DL and UL exposure metrics over the whole area, including outdoor and indoor environments**. Also the simulation provides **exposure maps**.

Drive-test measurements allow for the **calibration and evaluation of the prediction models** involved in the simulation, from a comparison between geolocalized averaged measurements and predictions.

### SCANNER drive-test:

• Calibration and evaluation of the **propagation model**, if base station properties are known with high precision.

### TRACE mobile drive-test:

### **Drive-test**

- Calibration and evaluation of the UL transmit power prediction (e.g. adjustment of the average relationship between the path-loss and the UL transmit power).
- Calibration and evaluation of the UL throughput prediction (e.g. adjustment of the average relationship between the UL received power and the UL throughput).

Drive-test measurements also allow getting some **information on network configuration:** active cells, some DL/UL settings (e.g. thanks to SIB/MIB decoding), etc.

The combination of simulations and measurements will be demonstrated in Santander as part of the WP6 activity; and will be reported in the final WP6 deliverable. The analysis of WSN measurements will permit an adjustment of the daily cell load variations used as an input to the simulation. And the adjusted simulation will, at the end, complement the measured exposure statistics with predicted exposure maps and an extrapolation to inside the buildings. Some Trace mobile measurements are planned as well in Santander downtown; they might be exploited to calibrate the UL transmit power prediction for a specific operator and



RAT (e.g. the Orange LTE in frequency band 2.6 GHz). The simulation will then be able to refine its estimate of the UL exposure component and extend the measurement-based statistics with predictions over the whole Santander downtown, at different time periods.

### 3.3.2 Indoor EMF maps

The WiCa Heuristic Indoor Propagation Prediction (WHIPP) tool [28] is a heuristic network predictor and planner, developed and validated for indoor environments, and suitable for WiFi, Zigbee, and/or 3G/4G. It takes into account the effect of the environment on the wireless propagation channel and its calculations are based on the establishment of the dominant path between transmitter and receiver, i.e., the path along which the signal encounters the lowest obstruction.

Besides throughput and path loss predictions of a given wireless network configuration, the tool also enables a quick automatic network design, where user-defined coverage requirements in the different rooms of the building are achieved with the smallest number of access points. Finally, the tool allows the reduction of the number of access points in over dimensioned networks without affecting the coverage. The used algorithms can serve as a basis for future developments and extensions.

The tool has been extended with an exposure index calculation module. Other exposure metrics, such as incident electric field distribution or incident power density and SAR values. Figure 20 shows an example of the whole-body SAR distribution induced by the access points of a Wi-Fi network for a typical and exposure-minimised topology.

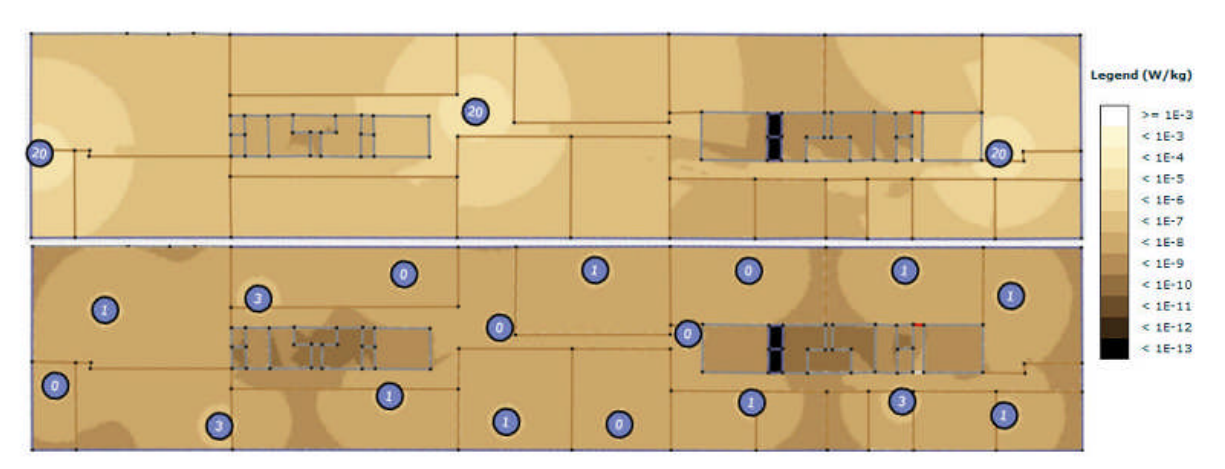


Figure 20: Whole-body SAR induced by Wi-Fi downlink exposure in an indoor office environment: top figure a typical deployment, bottom figure an exposure-minimized topology.

Figure 21 shows a flow chart of the EI calculation module. For indoor populations, the user can draw a floor plan, upon which the WHIPP tool calculates the observed indoor uplink powers  $P_{Tx}$  and downlink power densities  $S_{inc}$  due to the indoor base stations. Other power (density) values  $P_{Tx}^*$  and downlink power densities  $S_{Rx}^*$  (e.g., for outdoor populations and/or base stations) are average values obtained from measurements or simulations and are stored in a database. The user defines a scenario (population fractions and exposure time durations (uplink and downlink)). This input scenario is then checked (sum of population fractions at any time instant corresponds to entire considered population). Reference SAR values for the defined



scenario are obtained from a database. Based on the population fractions, exposure time durations, UL powers, DL power densities, and reference SAR values, the El calculation module then calculates the El based on the El formula defined in WP2.

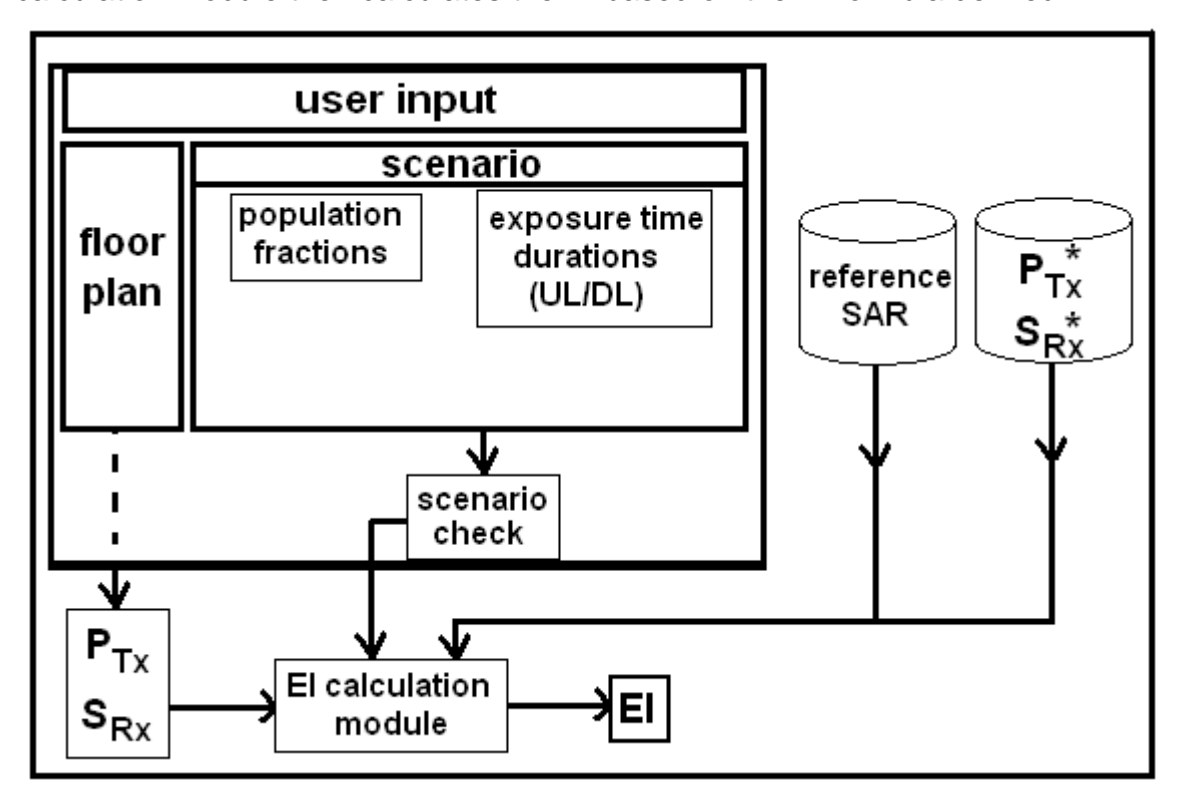


Figure 21: Flow chart of El calculation algorithm as implemented in WHIPP tool.

### 3.4 Life segmentation data

Life segmentation data was extracted from up-to-date life segmentation surveys performed in the countries involved in LEXNET.

In order to evaluate the EI we needed data for each of the considered population categories: children (under 15 y.o), young people (15-29 y.o), adults (30-59 y.o) and seniors (60 y.o and over).

How young people, adults and seniors spend their time in Europe was extracted from the HETUS survey [29], the French INSEE survey [30] and the time use survey in Republic of Serbia [31] (see Table 8).

Table 8: How young people, adults and seniors spend their time in Europe

	Adults	Young people	Seniors
Gainful work, study	5:00	4:40	0:05
Domestic work	3:00	1:15	4:00
Travel	1:30	1:20	00:50
Sleep	8:15	9:00	8:45
Meals, personal care	2:15	2:45	3:30



	Adults	Young people	Seniors
Free time indoor (TV, socializing, reading, internet surfing)	3:00	4:00	4:30
Free time outdoor (sports, gardening, hiking)	1:00	1:00	2:20
Total	24:00	24:00	24:00

How children spend their time in Europe was extracted from [32–35] (see Table 9). Average daily time spent at school or day care, for domestic work, sleeping, eating and personal care were deduced from [33] and [35]. Then it was difficult to extract the free time indoor and outdoor as categories in [33] do not details whether activities such as "other passive leisure" are outdoor or indoor activities. From [34] we could extract that American children spend in average 2h daily doing outdoor activities. From [32] we could deduce that UK children spend in average 45 min per day outdoor between 3.30 and 8.30 PM.

Table 9 How children spend their time in Europe

	Children
School-Day care	3:45
Domestic work	0:45
Travel	0:30
Sleep	10:40
Meals, personal care	2 :30
Free time indoor (TV, playing, reading, internet surfing)	4:35
Free time outdoor	1:30
Total	24:00

From Table 8 and Table 9 we extracted data we needed to input in the EI equation (see Table 10).



Table 10 Life segmentation inputs for evaluation of the Exposure Index

Population	Day (8 A	M-6 PM)		Night (6	Night (6 PM- 8AM)		
category	Indoor (office- school- home)	Outdoor	Transportation (bus, car, subway etc)	Indoor (home)	Outdoor	Transportation (bus, car, subway etc)	
Adults	8h15	1h10	35 min	13h05	20 min	35 min	
	(82.5%)	(11.5%)	(6%)	min (93.5%)	(2.5%)	(4%)	
Young	8h20	1h10	30 min	13h10	20 min	30 min	
people/students	(83%)	(11.5%)	(5.5%)	min (94%)	(2.5%)	(3.5%)	
Children	8h15	1h30	15 min	13h45	0 min	15 min	
	(82.5%)	(15 %)	(2.5%)	min (98.5%)	(0 %)	(1.5%)	
Seniors	7h35	2h10	15 min	13h05	40 min	15 min	
	(70%)	(27.5%)	(2.5%)	min (93.5%)	(5%)	(1.5%)	

### 3.5 ICT usage data

As described in Section 3.2 the network data are given by sensor installed on the operator's network which measure, among other values,

- the uplink and downlink data traffic volumes;
- the number of voice calls;
- the type of terminal (laptop, mobile or tablet);
- the duration of each voice call.

This group of data constitutes the ICT usage data.

In appendix are presented the results of a study done by TKS and in particular the dailies variations of voice traffic, total DL data traffic and total UL data traffic in various areas .

In the context of LEXNET project another study has been done in the Orange network by installing probes in three covered area representing three different environments: urban, suburban and rural. The data were registered during one week for each user (IMSI).

As an example and among all the measurements, we present in this section the extraction of the average volume of data exchanged by user and per day for each area types.



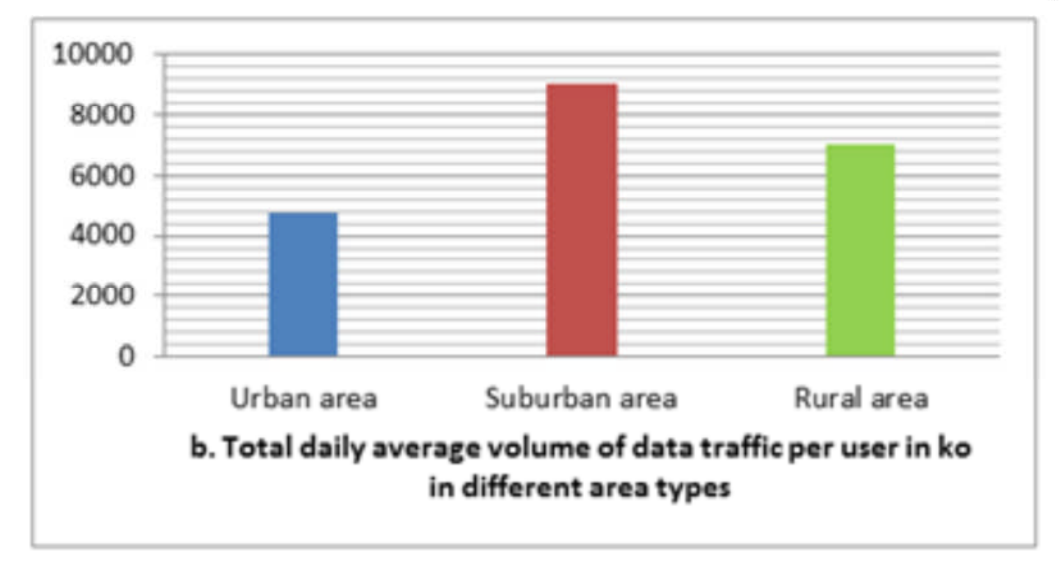


Figure 22: Analysis of ICT data usage

The ICT usage data, as other network data, are operator dependent because they are considered competitive and therefore can be difficult to obtain.

### 3.6 **SAR database**

As defined in D2.4 [1] and D2.6 [2], the mathematical formalization of the Exposure Index is described by Equation (1).

In this formulation the coefficients  $d_{t,p,l,e,r,c,u}^{UL}$  and  $d_{t,p,l,e,r,c,u}^{DL}$  are expressed as a dose induced by the UL and DL exposure. In Equation (1), dose appears as the normalized Specific Absorption Ratio (SAR) weighted by the time spent in the configuration.

 $\bar{P}_{TX}$  and  $\overline{S}_{inc}$  are respectively the mean Tx power and Rx power density given by the measurement data.

Considering the great number of situations (position, usage, frequency, device) that can be considered, it has been decided to create a SAR database which will give an exhaustive table of reference normalized SAR values (see [1], [2]).

### 3.6.1 Methodology and tools used to calculate the SAR database.

SAR values are calculated using numerical dosimetric simulations considering different usages and postures. Two numerical whole-body models, an 8 years old female (Eartha) and a 34 years old male (Duke) [36] were deformed to simulate the standing and sitting postures (see Figure 23). The exposure is estimated using numerical models of sources (mobile, laptop, tablet) considered as punctual emissions. The base stations are modeled by plane waves, small cells and Wi-Fi access points are modeled by spherical modes.

In order to have reference normalized SAR values, the simulations are performed with a power emitted by the source of 1 Watt in the case of punctual emissions and 1W/m2 in the case of DL exposure. The frequency bands of simulations are 400 MHz, 900MHz, 1940 MHz and 2.5 GHz.



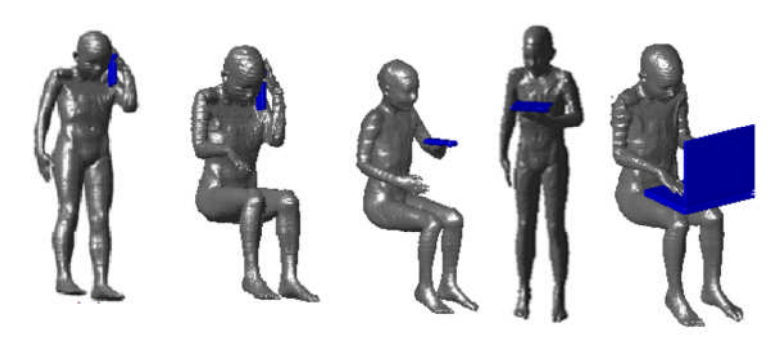


Figure 23: Eartha numerical models used for the simulation



### 4 EXTRAPOLATION MODELS

Considering the specific scenario of the simplified fixed dosimeter deployment in Santander. There are two main hurdles to be addressed.

- i. These dosimeters will be deployed at a certain height. We will obtain the DL E-field measurements over a given time period (one day, one week, or more). But this raw data will give us the E-field values from the base stations, small cells, and access points at a certain height (about 6m from ground level) depending on their deployment (either on walls or on the lamp posts). In order to obtain the DL E-field level at user height (about 1.5m), we need to have some extrapolation scheme.
- ii. The simplified dosimeter has a single axis probe. This means that it will underestimate the DL-EMF due to non-isotropic characteristics. Thus we need to study whether it is possible to have an extrapolation factor between data from single axis measurements and isotropic measurements, along with the associated uncertainty.

### 4.1 Estimation of EMF on ground level from lamp post dosimeters

The estimation of EMF on user height from dosimeter measurements at higher locations has been studied using simulations and measurements as explained in the following.

The extrapolation rules can be extracted from network simulations, based on the methodology described in section 3.3.1. For this purpose, DL field strength maps are predicted at both heights 1.5 m and 6 m above the ground. The difference between both predictions (field strength at height 6 m is the highest one) is calculated at each pixel of the maps and statistics on this difference are derived. A first study was realized based on a scenario in a dense urban area (Paris downtown) where three 3G macro-cell networks are deployed with an average inter-site distance of 450 m and operate in the frequency band 2.1 GHz. The mean and standard deviation of the difference obtained on this setup is respectively 1.5 dB and 1.4 dB. The Cumulative Distribution Function (CDF) of the difference is given in Figure 24.

This preliminary study will be completed in the framework of the Workpackage 6 (WP6) using the Santander scenario and the real cellular network deployment. The results of both the preliminary study in Paris and complementary study in Santander will be reported in the final WP6 deliverable.



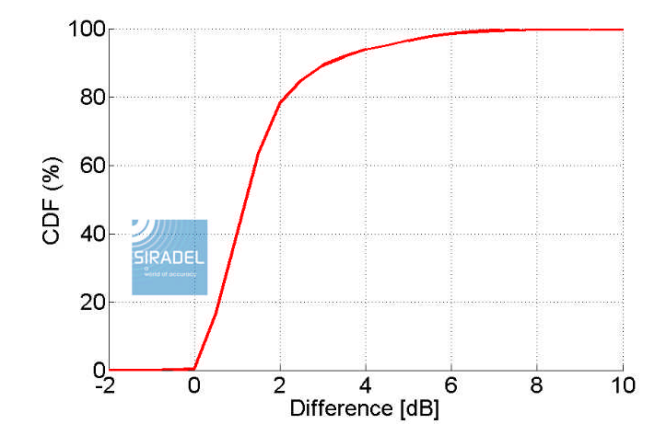


Figure 24: Difference between the DL field strengths predicted at 6m and 1.5m above the ground

A preliminary study using E-field measurements has been carried out in Brest, France. The objective was to observe the E-field levels at different heights (from 1.7m up to 6m) by placing a dosimeter (EME SPY 140) on an extendable tripod stand and recording DL E-fields over a 90 seconds time period for a given height. The measurement periodicity was 2 seconds. A second dosimeter was placed at a 1m horizontal distance on a fixed tripod at a height of 1.5m (user height) during the whole measurement cycle. The detailed measurement setup and results are shown in 7Appendix I.

The results from the measurement campaign showed no extrapolation factor that could be extracted. One reason is that the measurements were carried out at fixed points with no spatial averaging to eliminate the small scale fading. The second main reason is that the measurements were carried out at few points in different environments (dense urban, urban, and rural), so the data set was not large enough in order to obtain a statistical comparison with the simulation results.

To conclude, we will continue this study in the WP6 and carry out an extensive measurement campaign in Santander smart city using the fixed and portable dosimeters at different heights in order to generate enough data and extract some comparable results to the ones obtained from the network simulations. An enhanced measurement protocol will be used in order to cope the spatial small-scale or large-scale fading.

## 4.2 <u>Estimation of EMF from single-polarized measurements</u>

The objective of this study is to carry out measurements at different locations for a certain period of time and see whether we can extract an extrapolation factor to obtain isotropic measurements from single-axis measurements. This is a critical point as the fixed dosimeters designed for LEXNET measurements in a smart city scenario are capable of only mono-axial measurements.

For this purpose, an EME SPY 140 dosimeter has been used to carry out a comprehensive measurement campaign at different locations, which represent different scenarios (LOS, NLOS, single BS, several BS, urban, rural, campus area). Three frequency bands were monitored as shown in Table 11.



Table 11: Frequencies for the measurement campaign

Standard	Measurement frequency (MHz)
GSM-DL	925-960
DCS-DL	1805-1880
UMTS-DL	2110 - 2170

This study is complementary to the measurement campaign carried out in [23], where measurements using a wide band probe (no frequency selectivity) were carried out in order to see whether an extrapolation factor can be extracted between mono-axis and isotropic measurements. The measurements were carried out over a period of 2 hours with a sampling period of 2 seconds. Seven different scenarios were considered. It was concluded that an extrapolation factor of around 2 can be used to estimate the isotropic E-field from mono-axial measurements with an uncertainty (error) between 22% and 44%.

### 4.2.1 Measurement setup

The measurements were carried out an EME SPY 140 dosimeter fixed on a tripod at a height of 1.5 m. One measurement cycle was set to 2 seconds and the measurement period was around 13 minutes.

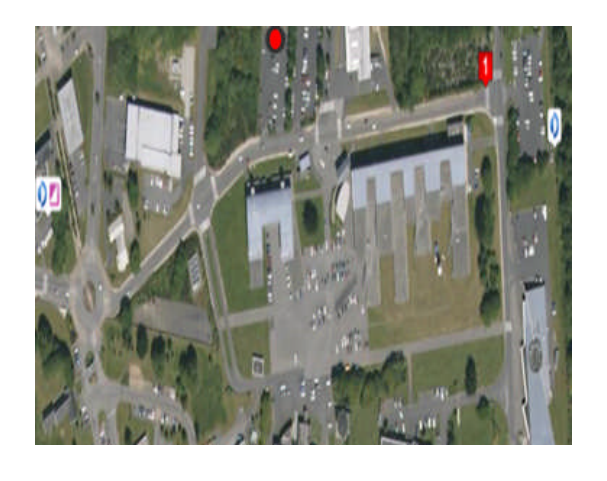
All measurements have been carried out in the city of Brest, France. Three measurement locations were selected representing three different scenarios.

- i- Location#1: Inside a playing ground representing line of sight (LOS) conditions with little or no reflecting objects around.
- ii- Location#2: In a parking area of a university campus with two BS (one on each side) with LOS and NLOS (no line of sight) conditions.
- iii- Location#3: In a dense urban area with LOS and NLOS conditions.

The measurement setup at the three locations is presented in the figure below.

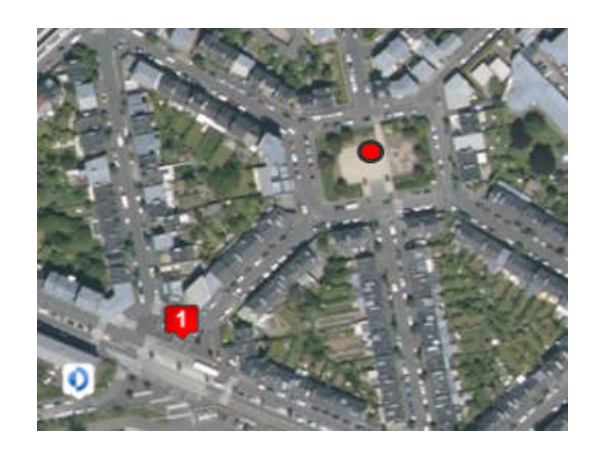


(a) Location#1



(b) Location#2







(c) Location#3

(d) Dosimeter on tripod

Figure 25: Measurement setup at different locations. The red circle represents the dosimeter location and the antenna icon represents the BS location on the map. The '1' represents the measurement location for ANFR

Two measurement runs were carried out at each location. The extrapolation factors for each of the three probes of the dosimeter are defined as:

$$\eta_{x} = \frac{E_{tot}}{E_{x}} \tag{2}$$

$$\eta_{y} = \frac{E_{tot}}{E_{y}} \tag{3}$$

$$\eta_z = \frac{E_{tot}}{E_z} \tag{4}$$

Where,  $\eta_i$  represents the extrapolation factor of axis i,  $E_{tot}$  represents the total E-field

$$E = \sqrt{E_x^2 + E_y^2 + E_z^2} (5)$$

The  $E_x$  and  $E_y$  represents the E-field with horizontal polarization and  $E_z$  the vertical polarization.

The mean values of  $\eta_x$ ,  $\eta_y$ , and  $\eta_z$  (calculated over the 13 minute measurement period), the standard deviation and uncertainty are calculated using the following formulas.

$$Mean = \frac{1}{N} \sum_{i=1}^{N} \eta_i \tag{6}$$



$$\sigma = \sqrt{\frac{1}{N} \sum_{i=1}^{N} (\eta_i - mean)^2}$$

$$Uncertainty = \frac{\sigma}{mean} \tag{8}$$

Where, N represents the total number of samples and i is the index. The value " $\eta$ " is calculated as the mean value of the three mono-axial values calculated above. The results for the different standards are presented in detail in 7Appendix C.

The variations of the extrapolation factor (around the mean value) and the uncertainties are summarized in the table below for the three standards.

Table 12: Summary of extrapolation factors and uncertainties for the three measured standards

	GSM-DL	DCS-DL	UMTS-DL
Min extrapolation factor	1.15	0.86	1.01
Mean extrapolation factor	1.83	1.76	1.93
Max extrapolation factor	3.31	2.83	3.41
Min uncertainty (%)	2.49	3.44	2.31
Mean uncertainty (%)	6.06	7.20	7.40
Max uncertainty (%)	10.24	15.91	20.03

We can see from the above table that the Extrapolation factor varies from 0.86 (for DCS-DL) up to 3.41 (for UMTS-DL) standard. The relative error if we carry out this extrapolation can vary between 2.5% (for GSM-DL) up to 20% (for UMTS-DL) depending upon the environment, and traffic load, etc.

To conclude, for the fixed dosimeters deployed in Santander which have a single measurement axis, one should take into account the errors induced when we want to estimate the isotropic E-field from a mono-axial measurements.



# 5 SIMULATION-GUIDED DESIGN AND EXPLOITATION OF THE WIRELESS SENSOR NETWORK

The Wireless Sensor Network (WSN) equipped with fixed and connected dosimeter is one solution promoted by LEXNET to capture live and continuous data on the EMF exposure. The simulation can help in the design of the WSN but also in the elaboration of rules to extrapolate the discrete measurements to a more representative data set.

The design of the WSN basically consists in the definition of the sensor density and selection of the probe locations. The design surely depends on the environment characteristics (suburban, urban, dense urban), wireless cellular network properties (density of base stations), number of sensors and installation constraints (access to energy, installation approval on private/public facilities, already-deployed sensors).

The simulation can help in taking into consideration the impact of the environment and wireless network characteristics. As soon it is able to predict the relative space variations of the outdoor DL EMF exposure in a realistic way, it provides valuable inputs for the determination of the sensor density, for characterization of the WSN measurement accuracy and possibly for the selection of sensor locations if installation constraints (i.e. location candidates) are known.

The methodology described below is viewed as an efficient way (simple and rapid) to optimize the WSN design according to a target on the DL EMF characterization accuracy. The basic concept is as follows:

- The simulation generates a realistic DL EMF exposure map that is used afterwards as a reference.
- The DL signal strength is predicted at discrete sensor locations, in order to compare the sensor measurement statistics to reference statistics extracted from the map.

The first step consists in making a simulation setup representative of the environment where the WSN will be deployed. This includes the high-resolution geographical map data and the design/setting of existing wireless cellular networks (location of sites, cell setting: antenna orientation, transmit power, etc.).

In a second step, reference statistics are computed from the DL field strength map predicted over the whole study area, with a fine resolution. An example is illustrated in Figure 26. Remark that those results already give interesting information regarding the DL field strength distribution in the WSN area. For instance, in Figure 26, peak values are observed as expected in the close vicinity of base stations while the variations over the remaining of the area are quite small, except the strong differences between confined/street areas (lower levels) and large open areas (higher levels).





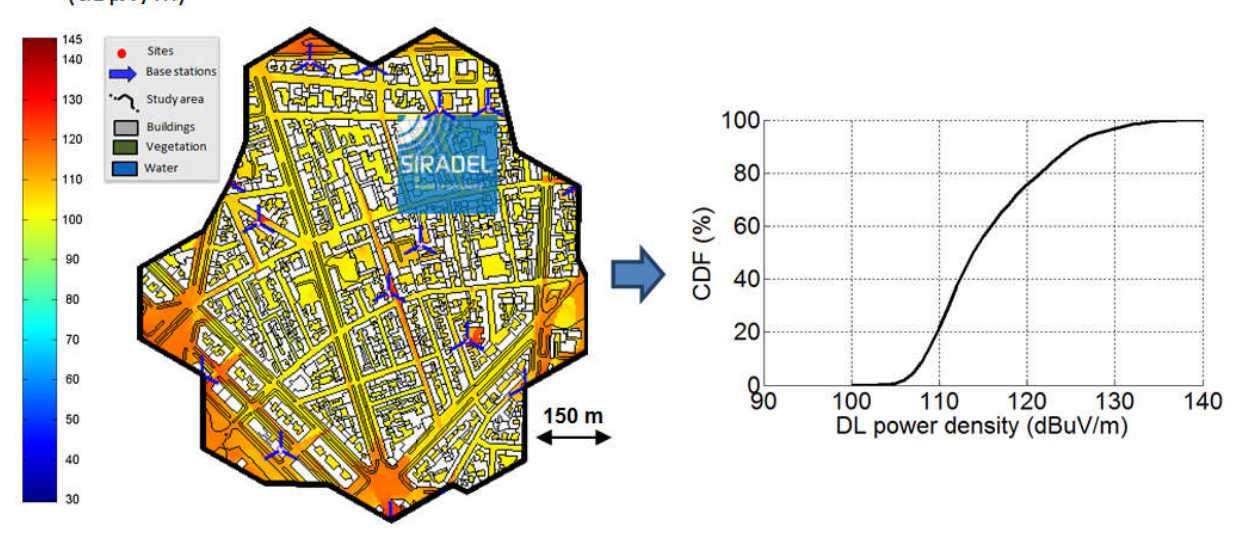


Figure 26: Example of reference DL EMF exposure statistics for WSN design.

Then the sensors are deployed, manually or automatically, in the simulation setup. Several deployment strategies can be evaluated, for instance uniform/non-uniform, different mean inter-sensor distances, specific sensor locations, etc. Figure 27 gives an example of an automatic sensor deployment from a uniform distribution along the streets, and a mean inter-sensor distance of 20 m. The prediction at the discrete sensor locations (considered here as the sensor measurements) is obtained by picking the sample values into the reference map.

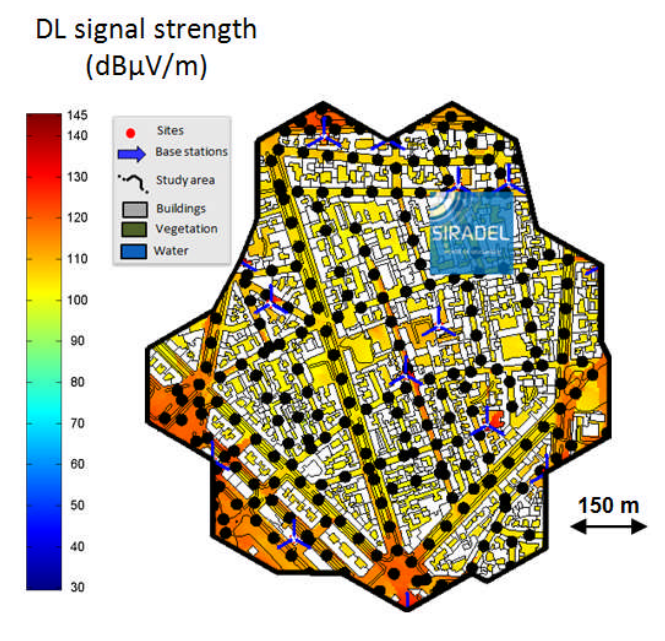


Figure 27: Sensors uniformly distributed along streets with a resolution of 50 m.

The performance of each sensor deployment is evaluated by a comparison between the EMF DL exposure statistics computed from the limited set of sensor measurements to the ones computed from the reference map (all pixels).

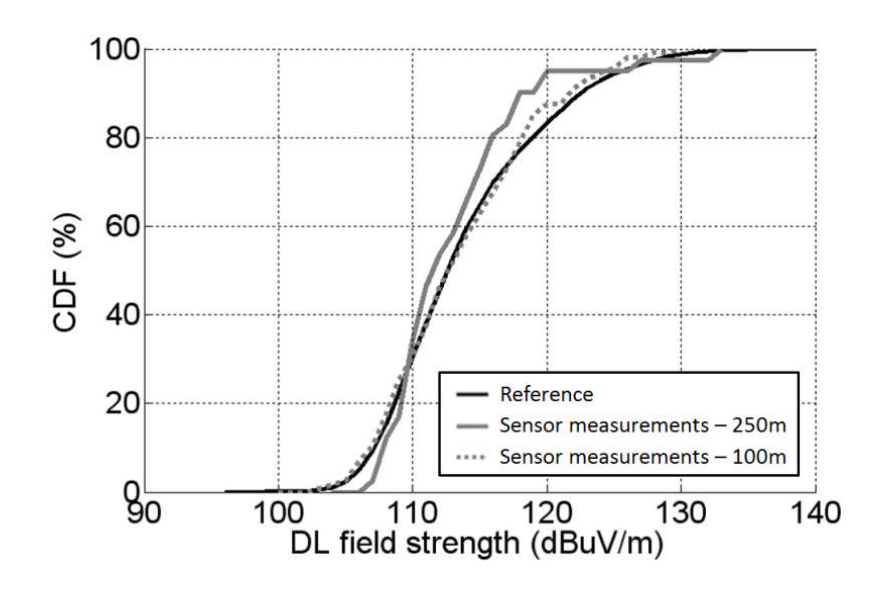


The statistical analysis can be enriched by the introduction of random elements to represent some variability in the setup or some uncertainty in the simulation. Then different random realizations of the reference map can be generated to either derive more representative statistics or observe the sensitivity of the result to some parameters.

- For instance, the propagation model predicts an average received-power that cannot reproduce all local signal variations. Then the introduction of a random shadowing component can lead to higher variability in the propagation data.
   We can determine from the several random realizations whether the WSN performance is sensible or not to the local propagation fading (and consequently to the precise sensor location).
- Another example is the variability in the base station loads. The WSN design
  will surely be done with a unique average cell load (or with a unique cell load
  per operator). Thus introducing some randomness in the individual cell loads
  allows us to observe the sensibility of the WSN performance to the real
  network load distribution.

The aforementioned methodology is currently employed in LEXNET for the design of the SmartSantander deployment. The results will be reported in the next WP6 public deliverable at the end of the project. Some of them are employed for illustration here below.

Different sensor densities and strategies (2D-uniform or only along the main streets) have been compared. Figure 28 shows a comparison of two 2D-uniform deployments with a mean inter-sensor distance of respectively 100 m and 250 m. The mean intersensor distance of 100 m leads to statistics very similar to the reference, while the mean inter-sensor distance of 250 m results in significant degradation of the statistical distribution, in particular a bias of 1.4 dB in the mean DL field strength estimation.





Sensor network with	resolution 100m	Sensor network with	resolution 250m	
Mean  bias  (dB)	RMSE (dB)	Mean   bias   (dB) RMSE (dB)		
0.49	1.71	1.38	4.00	

Figure 28: Comparison of two uniform deployments for respectively a mean inter-sensor distance of 100 m and 250 m

The simulation can also be used to extrapolate the statistics obtained from the WSN measurements (biased by installation constraints) to more representative statistics required for EI computation.

A first use case is reported in Section 4.2 for extrapolation from the sensor typical height (6m above ground) to the user typical height (1.5 m above ground).

A second use case is the indoor extrapolation. The population affected by DL EMF exposure is mainly located inside the buildings. However the WSN sensors are deployed on lampposts (or external building façades); and they only capture the outdoor EMF DL exposure levels. Here the simulation is helpful to build a transfer function from the measured outdoor levels to indoor statistics. A similar work could be done with on-field measurements, but this latter approach is obviously longer and more costly.

For this purpose, the DL field strength is simulated in both outdoor and indoor environments. Indoor and outdoor statistics are separately computed. The comparison between those statistics characterizes the differences between outdoor and indoor EMF DL exposures. Such indoor extrapolation study usually distinguishes "light" and "deep" indoor environments, where light indoor refers to locations less than 5 m away from the closest façade, and deep indoor refers to locations more than 5 meters away from the closest façade. As an illustration, the mean differences obtained on the SmartSantander-like setup from a mono-operator network for respectively light and deep indoor are 21.8 dB and 29.1 dB. Figure 29 shows the whole CDF for the three considered environments.

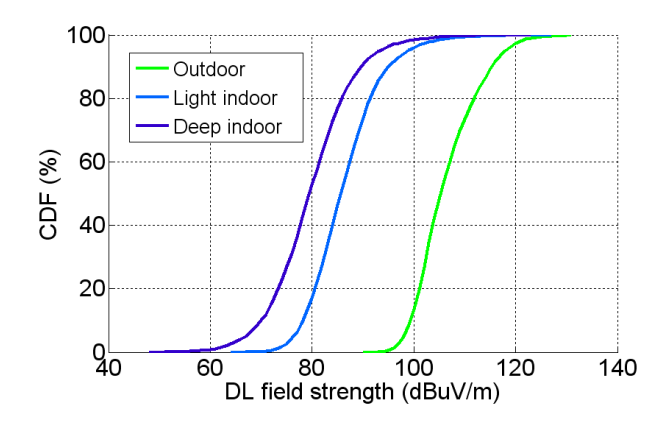


Figure 29: Comparison between outdoor and indoor DL field strength statistics.

It is interesting to notice that the mean differences obtained here (i.e. from DL field strength predicted with the SmartSantander-like setup considering a whole monoperator network) are greater than those commonly reported in the literature and that

## Document ID: D3.3 Exposure Index Assessment v2 FP7 Contract n°318273



assess the propagation loss predicted for a single cell, which are roughly equal to 15 dB and 20 dB for respectively light and deep indoor.

The different gap obtained between light and deep indoor (i.e. respectively +7 dB versus +9 dB) may be explained by the number of base stations that significantly contribute to DL field strength, which is greater at outdoor locations. Indoor locations more likely suffer from the exposure contributions that penetrate through the closest façade; thus the average number of significant contributions is reduced; the gap between outdoor and indoor increases when several base stations (thus potential contributors) are considered. A network with another site density will surely result to other figures. This result further highlights the interest to use precise simulation results for building transfer functions reliable and appropriated to each WSN.



### 6 DISCUSSION AND CONCLUSIONS

This deliverable updates D3.1, which was due in month 12 and provided an overview of the EMF data available for assessing (calculating) the EI and the concept to combine the heterogeneous sets of EMF data.

Deliverable D3.3 thoroughly describes the different steps to calculate the EI from the assessed numerical or experimental exposure metrics which includes interpolation, extrapolation, and combining data using co-kriging techniques. D3.3 also points out the different types of data sources (measurements, simulations, network data) and the associated tools available to assess the DL and UL exposure. The evaluation of the EI requires knowledge on both uplink and downlink exposure of the population in an area in the considered time frame.

Concerning the methodology to assess the exposure data from personal and fixed point dosimeters, the body shadowing effect was analysed for different on-body placements, considering realistic exposure scenarios and the human motion.

Based on the EI assessment methodology described in this deliverable, a web-based EI expert system is currently being implemented allowing the automatic calculation of the EI from assessed exposure metrics. The expert system will be demonstrated in WP6. It will then be proposed to the different stakeholders (operators, regulators, public agencies) as a methodology to assess the EI taking into account the tools and data that is available.

An important aspect in EI assessment is the uncertainty evaluation. The uncertainty of each of the assessed exposure metrics needs to be determined before the overall uncertainty can be determined. The uncertainty of a data set can serve as a metric to estimate the fidelity of the data in case of co-kriging.

The EI quantifies the realistic exposure in an area induced by wireless communication networks aiming at assessing and reducing the realistic exposure in an environment by combining data from exposure assessment, network data, and dosimetric data. Optimizing a communication network can be performed during the design stage of the network or can be integrated in the network management tools.



### 7 REFERENCES

- [1] E. Conil, N. Varsier, A. Hadjem, J. Wiart, G. Vermeeren, S. Aerts, W. Joseph, L. Martens, Y. Corre, C. Oliveira, M. Mackowiac, D. Sebastião, L. Correia, R. Agüero, L. Diez, M. Koprivica, A. Neškovic, M. Popovic, J. Milinkovic, S. Nikšic, and C. Roblin, "D2.4 Global wireless exposure metric definition v1," LexNet project, 2013.
- [2] N. Varsier, "D2.6 Global wireless exposure metric definition v2," LexNet project, 2013.
- [3] S. Aerts, D. Plets, L. Verloock, L. Martens, and W. Joseph, "Assessment and comparison of total RF-EMF exposure in femtocell and macrocell base station scenarios," *Radiation Protection Dosimetry*, Oct. 2013.
- [4] D. Krige, "A statistical approach to some basic mine valuation problems on the witwatersrand," *Journal of the chemical, metallurgical and mining society of South Africa*, vol. 52, pp. 119–39, 1951.
- [5] H. Chung and J. Alonso, "Using gradients to construct cokriging approximation models for high-dimensional design optimization problems," in *Problems, 40th AIAA Aerospace Sciences Meeting and Exhibit, AIAA, Reno, NV*, 2002, pp. 2002–317.
- [6] M. Kennedy and A. O'Hagan, "Predicting the output from a complex computer code when fast approximations are available," *Biometrika*, vol. 87, no. 1, pp. 1– 13, 2000.
- [7] J. Sacks, J. W, T. Welch, Mitchell, and H. Wynn, "Design and analysis of computer experiments," *Stat Sci*, vol. 4, pp. 409–23, 1989.
- [8] T. Simpson, J. Poplinski, P. Koch, and J. Allen, "Metamodels for computer-based engineering design: Survey and recommendations," *Eng Comput*, vol. 17, no. 2, pp. 129–50, 2001.
- [9] S. Aerts, D. Deschrijver, L. Verloock, T. Dhaene, L. Martens, and W. Joseph, "Assessment of outdoor radiofrequency electromagnetic field exposure through hotspot localization using kriging-based sequential sampling," *Environ Res*, vol. 126, pp. 184–91, 2013.
- [10] M. Azpurua and Dos Ramos, K, "A comparison of spatial interpolation methods for estimation of average electromagnetic field magnitude," *Prog Electromagn Res M*, vol. 14, pp. 135–45, 2010.
- [11] Y. Isselmou, H. Wackernagel, W. Tabbara, and J. Wiart, "Geostatistical estimation of electromagnetic exposure," *Quant Geo G*, vol. 15, pp. 59–70, 2008.
- [12] J. Paniagua, M. Rufo, A. Jimenez, and A. Antolin, "The spatial statistics formalism applied to mapping electromagnetic radiation in urban areas," *Environ Monit Assess*, vol. 185, pp. 311–22, 2013.
- [13] S. Koziel, S. Ogurtsov, I. Couckuyt, and T. Dhaene, "Variable-fidelity electromagnetic simulations and co-kriging for accurate modeling of antennas," *IEEE Transactions on Antennas and Propagation*, vol. 61, no. 3, pp. 1301–8, 2013.
- [14] S. Aerts, S. Ulaganathan, D. Deschrijver, L. Martens, T. Dhaene, and W. Joseph, "Combination of heterogeneous data in the spatial assessment of RF-EMF exposure." 2014.
- [15] Joint Committee for Guides in Metrology (BIPM, IEC, IFCC, ILAC, ISO, IUPAC, IUPAP and OIML), "Evaluation of measurement data Guide to the Expression of Uncertainty in Measurement," *JCGM*, vol. 100, 2008.



- [16] "http://www.ist-winner.org/." .
- [17] K. Kalliola, K. Sulonen, H. Laitinen, O. Kiveks, J. Krogerus, and P. Vainikainen, "Angular power distribution and mean effective gain of mobile antenna in different propagation environments," *IEEE Trans Veh Technol*, vol. 51, pp. 823–38, 2002.
- [18] T. Kientega, E. Conil, A. Gati, A. Hadjem, E. Richalot, M. Wong, O. Picon, and J. Wiart, "Analysis of the distribution of specific absorption rate induced by five plane waves with a fast and new method in Visible Human," in *URSI conference*, 2011.
- [19] X. Zhao, J. Kivinen, P. Vainikainen, and K. Skog, "Propagation characteristics for wideband outdoor mobile communications at 5.3 GHz," *IEEE J Sel Areas Commun*, vol. 20, pp. 507–14, 2002.
- [20] L. Diez, Rodríguez de Lope, L., R. Agüero, A. Clemente, S. Bories, G. Vermeeren, D. Plets, W. Joseph, L. Martens, B. Rocquelay, M. Lalam, S. M. Anwar, M. Le Henaff, Y. Toutain, Y. Corre, Y. Lostanten, M. Popovic, M. Koprivica, J. Milinkovic, S. Nikšic, Y. Fernández, A. Sánchez, P. Chambers, and M. Wilson, "D6.1: Validation platform framework and initial assessment," LEXNET project, Apr. 2014.
- [21] http://www.siradel.com/1/volcano-lab.aspx, "VOLCANO LAB." .
- [22] http://www.smartsantander.eu, "EU FP7 Project Smart Santander (ID 257992)."
- [23] S. Bories, S. M. Anwar, M. Le Henaff, Y. Toutain, Y. Fernandez, A. Sanchez, D. Dassonville, S. Bories, T. Sarrebourse, M. Koprivica, A. Neškovic, M. Popovic, J. Milinkovic, S. Nikšic, M. Mackowiak, L. Correia, and C. Roblin, "D3.2 Wideband dosimeter design study & performances characterization," LEXNET project, Jul. 2014.
- [24] M. Mackowiak, C. Oliveira, and L. M. Correia, "Radiation Pattern of Wearable Antennas: A Statistical Analysis of the Influence of the Human Body," *International Journal of Wireless Information Networks*, vol. 19, no. 3, pp. 209–18, Sep. 2012.
- [25] M. Mackowiak and L. M. Correia, "Statistical Model of the Influence of Body Dynamics on the Radiation Pattern of Wearable Antennas in Off-Body Radio Channels," *Wireless Personal Communications*, May 2013.
- [26] M. Popovic, M. Tešanovic, B. Radier, H. Sidi, Z. Altman, J. Penhoat, J. Milinkovic, S. Nikšic, M. Koprivica, A. Neškovic, L. Díez, Rodríguez de Lope, L., R. Agüero, F. Heliot, D. Sebastião, A. De Domenico, J. Stéphan, M. Brau, Y. Corre, V. Iancu, G. Popescu, E. Slusanschi, De Poorter, E., and M. Mehari, "D5.1 Smart low-EMF architectures: novel technologies overview," LEXNET project, 2014.
- [27] S. R. Saunders, Antennas and Propagation for Wireless Communication Systems, no. 2nd edition. NY: John Wiley & Sons, 2007.
- [28] D. Plets, K. Wand Vanhecke Joseph, E. Tanghe, and L. Martens, "Coverage prediction and optimization algorithms for indoor environments," *EURASIP Journal on Wireless Communications and Networking*, 2012.
- [29] C. Aliaga, "How is the time of women and men distributed in Europe," *Statistics in focus, population and social conditions*, 2006.
- [30] L. Ricroch and B. Roumier, "Enquête Emploi du temps 2009-2010, "Depuis 11 ans, moins de tâches ménagères, plus d'Internet," *Insee Premiere*, vol. 1377, 2011.
- [31] "Survey in Republic of Serbia.".



61

- [32] A. R. Cooper, A. S. Page, B. W. Wheeler, M. Hillsdon, P. Griew, and R. Jago, "Patterns of GPS measured time outdoors after school and objective physical activity in English children: the PEACH project," *International Journal of Behavioral Nutrition and Physical Activity*, vol. 7, no. 31, 2010.
- [33] S. L. Hofferth and J. F. Sandberg, "How american children spend their time," *Journal of Marriage and the Family*, vol. 63, 2001.
- [34] L. R. Larson, G. T. Green, and H. K. Cordell, "Children's Time Outdoors: Results and Implications of the National Kids Survey," *Journal of Park and Recreation Administratio*, vol. 29, no. 2, 2011.
- [35] R. Larson, "How U.S. Children and Adolescents Spend Time: What It Does (and Doesn't) Tell Us About Their Development," *Current Directions in Psychological Science*, vol. 10, no. 5, Oct. 2001.
- [36] I. I. Foundation, "Virtual Population, http://www.itis.ethz.ch.".
- [37] JCGM, "Evaluation of measurement data Supplement 1 to the 'Guide to the expression of uncertainty in measurement' Propagation of distributions using a Monte Carlo method," *JCGM*, vol. 101, 2008.
- [38] G. C. Casella and R. L. Berger, *Statistical Inference*. Pacific Grove: Duxbury Press, 2001.
- [39] C. F. Dietrich, *Uncertainty, Calibration and Probability: The Statistics of Scientific and Industrial Measurements*. Bristol, UK: Adam Hilger Series on Measurement Science and Technology, 1991.
- [40] "http://chemwiki.ucdavis.edu/Analytical\_Chemistry/Quantifying\_Nature/Signific ant\_Digits/Propagation\_of\_Error#Derivation\_of\_Exact\_Formula." .
- [41] Satimo, "Starmimo active measurement system.".
- [42] S. Dural, "Adaptive power control in 802.11 networks," Florida Atlantic University, 2009.
- [43] A. Sheth and R. Han, "An Implementation of Transmit Power Control in 802.11b Wireless Networks," *CU-CS-934-02*, Aug. 2002.
- [44] Cisco, "Adaptive Wireless LAN power management system.".
- [45] M. Mackowiak, "Modelling MIMO Systems in Body Area Networks in Outdoors," IST University of Lisbon, Lisbon, Portugal, 2013.
- [46] S. J. Orfanidis, *Optimum Signal Processing, An Introduction*. Prentice-Hall, Englewood Cliffs, NJ, USA, 1996.
- [47] G. Vermeeren, S. Aerts, D. Plets, W. Joseph, L. Martens, E. Conil, N. Varsier, J. Wiart, Y. Core, C. Oliveira, D. Sebastião, L. Correia, R. Agüero, L. Diez, L. Rodríguez, M. Koprivica, A. Neškovic, M. Popovic, J. Milinkovic, and S. Nikšic, "D2.3 Scenarios," LEXNET project, 2013.

Version 4.0



# Appendix A DEDICATED SIMPLIFIED LOW-COST UL/DL MEASUREMENT EQUIPMENT DEVELOPED BY SATIMO

To overcome the difficulty to acquire an expensive drive test equipment to carry out UL/DL measurements, a simple dedicated solution was sought. It was proposed that a single multi-standard modem can be used to carry out such measurements. This solution has been developed at Satimo industries, Brest, France. The initial introduction and evaluation has been presented in [20] (section 3.4.4). The measurement schematic diagram is shown below.

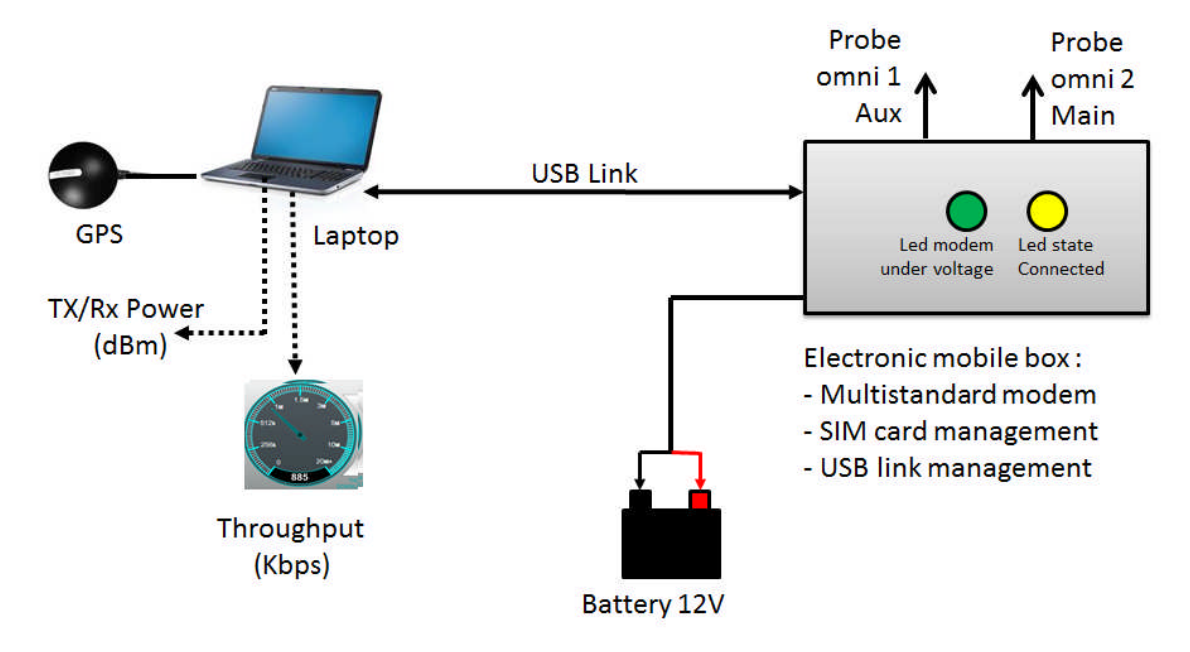


Figure A-1: Schematic showing the test setup for the low-cost UL/DL measurement equipment

This device is programmed using the IPERF software which is open source. We can get all the network parameters (RSSI, RSRP, RSRQ, SINR, Data rate, Tx power, cell-id, etc.) and the throughput using this software by interrogating the modem. A GPS is connected to the PC to have the coordinates of the measurements. The data from GPS, and the modem are then synchronized and stored with the time tag using an in-house software. The results of a measurement campaign for the LTE network carried out in the city of Brest, France are shown in the figure below.

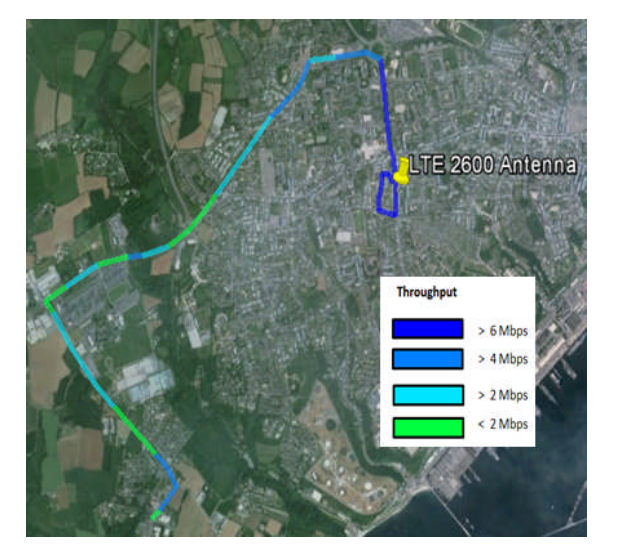
	RSSI	RSRP	RSRQ	CELL ID	SINR	TX Power
2G	yes	yes	yes	yes	no	no
3G	yes	yes	yes	yes	no	no
4G	yes	yes	yes	yes	yes	yes

(a) Summary of available data from the equipment

### PROPRIETARY RIGHTS STATEMENT

This document contains information, which is proprietary to the LEXNET Consortium. Neither this document nor the information contained herein shall be used, duplicated or communicated by any means to any third party, in whole or in parts, except with prior written consent of the LEXNET consortium.







(b) Results: LTE Tx and data rate throughput maps

Date	Time	Latitude	Longitude	RSSI (dBm)	RSCP (dBm)	Ec/No	CELLID	THROUGHPUT (Mb/sec)
07/11/2014	10:54:37	48°21.888N	04°32.921W	-51	-51	0	27129	0.511719
07/11/2014	10:55:27	48°21.888N	04°32.921W	-51	-51	0	27129	0.511719
07/11/2014	10:56:17	48°21 888N	04°32 921W	-51	-51	l n	27129	0.511719

2G measurements

Date	Time	Latitude	Longitude	RSSI (dBm)	RSCP (dBm)	Ec/No	CELLID	THROUGHPUT (Mb/sec)
07/11/2014	13:53:29	48°21.888N	04°32.921W	-77	-77	0	46084443	2.303711
07/11/2014	13:53:42	48°21.888N	04°32.921W	-71	-71	0	46084443	2.303711
07/11/2014	13:53:55	48°21.888N	04°32.921W	-73	-73	0	46084443	2.303711

### 3G measurements

	Date	Time	Latitude	Longitude	RSSI (dBm)	RSRP (dBm)	RSRQ (dB)	CELLID	SINR (dB)	TX (dBm)	THROUGHPUT (Mb/sec)
0	7/11/2014	14:17:53	48°21.888N	04°32.921W	-69	-97	-8	14238722	19	20	8.192383
0	7/11/2014	14:18:06	48°21.888N	04°32.921W	-69	-97	-8	14238722	20	20	8.192383
0	7/11/2014	14:18:18	48°21.888N	04°32.921W	-69	-97	-8	14238722	18	10	8.192383

### LTE measurements

(c) Tabular example of measured data in 2G, 3G and LTE

Figure A-2: Measurement results using the low-cost UL/DL measurement equipment

We can see from the above figure that we can have interesting results and network parameters with geo-localization using this simple UL/DL measurement equipment along with the throughput and other network parameters.

Version 4.0 63



### Appendix B Human Body Impact on UL measurements

In order to have an idea of the human body masking effect on dosimeter measurements, a simple measurement campaign was carried out.

A dosimeter was placed on the front end left pocket of a human subject. A mobile phone (Nokia) was used in voice communication at three different positions on the body.

- i- Mobile phone used to answer a voice call for minute using the left ear.
- ii- Mobile phone used to answer a voice call for minute using the right ear.
- iii- Mobile phone used to answer a voice call for minute using hands free in front of the person.

The dosimeter (EME SPY 200) was always placed on the left side jeans pocket in front of the person under test. The measurement setup schematic is shown in the figure below. Only GSM-UL measurements were carried out with a period of 2 seconds between two measurements over a 1 minute voice communication period. Each measured value represents an average value over a GSM-UL signal sampled over a 4.615 ms with a sampling frequency of 21 microseconds. After the one minute call duration, the call was interrupted, the mobile phone position was changed and the call was established again while the dosimeter measured continuously.

In the end the three scenarios were separated by post-processing. The measured average E-field value over the one minute voice call duration for the three scenarios is compared in the table below.

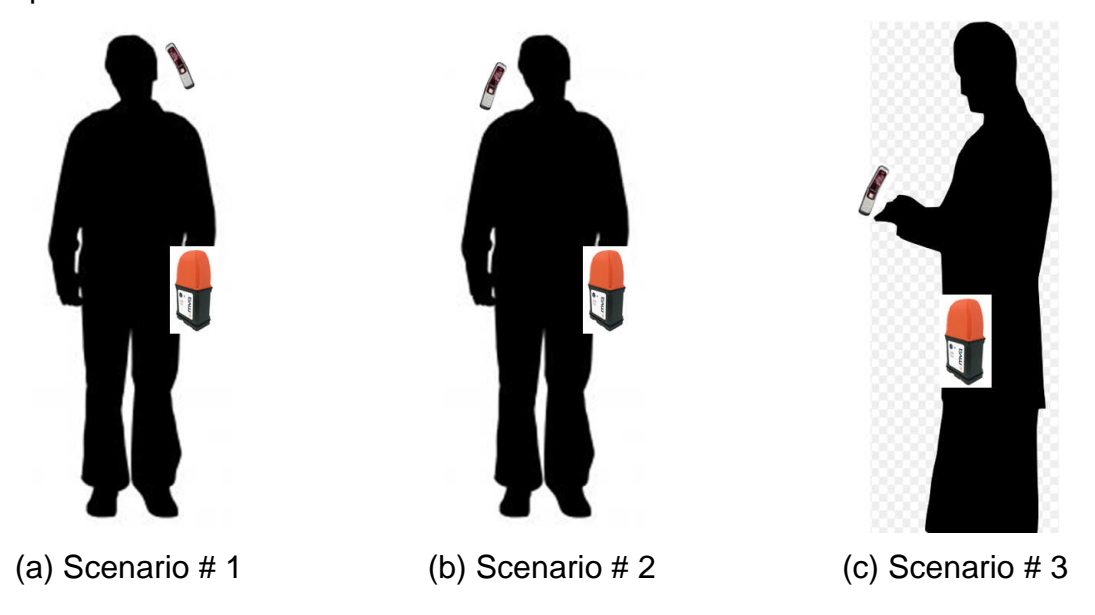


Figure B-1: Measurement schematic for the three scenarios.



Table B-1: Mean values for different scenarios for the total E-field and field measured by each probe of the dosimeter.

	Average value (mV/m) for horizontal probe 1	Average value (mV/m) for vertical probe	Average value (mV/m) for horizontal probe 2	Average value (mV/m) for total E-field
Scenario # 1	15,18	20,88	104,25	121,58
Scenario # 2	24,79	19,24	14,82	50,41
Scenario # 3	39,19	3,89	133,12	161,25

From the above table, comparing the total E-field values, one can see that when the mobile phone is on the same side as is the dosimeter (scenario # 1), the masking effect is significantly lower than the case when the mobile phone is on the opposite side (scenario # 2). Using the mobile phone in hands free mode (scenario # 3) shows the highest measurement reading as there is little impact of the body.

Taking the measurement from scenario 3 as a reference, a relative error of about 2 dB is observed in scenario#1 and about 10 dB in scenario 2. Of course these values would vary depending on the surrounding environment, the person morphology, and the type of mobile phone used. Thus no precise correction factor could be applied in order to estimate the real UL exposure.

To conclude, using a dosimeter attached to the human body has significant impact on the UL measurements due to the masking effect of the body, and the relative position of the dosimeter and the mobile device. Hence, the UL measurements in wearable topology are not reliable. To overcome this hurdle and to correctly estimate the UL-exposure, the information from the mobile device can be used as reliable source. The Tx-power from the mobile source can be recovered along with other useful data (RSSI, RSRP, cell-id, etc.). This gives us the real UL exposure due to the user device. But when the person is in a multi-user environment, the UL-exposure does no longer depend on one user and it is difficult to estimate the UL-exposure of a whole group of users, only if everyone is equipped with a measurement device recording the Tx-power.



# **Appendix C** Mono-axial vs. isotropic measurement results from a dosimeter study

### C.1 **GSM-DL results**

Table C-1: Measurement results for GSM-DL signal at the three locations

			GSM-DL			
			η×	ηz	<b>η</b> γ	η
Location#1	Mean	Run1	1,15	1,72	1,52	1,46
		Run2	1,72	1,50	2,22	1,81
	Median	Run1	1,15	1,71	1,50	1,45
		Run2	1,71	1,49	2,20	1,80
	Std. Deviation	Run1	0,05	0,15	0,09	0,09
		Run2	0,16	0,09	0,11	0,12
	Unvertainty (%)	Run1	4,07	8,52	5,90	6,17
		Run2	9,20	6,14	4,84	6,73
	Mean	Run1	1,46	2,03	1,93	1,81
		Run2	1,46	1,95	1,99	1,80
Location#2	Median	Run1	1,45	2,03	1,91	1,80
		Run2	1,45	1,93	1,96	1,78
	Std. Deviation	Run1	0,07	0,20	0,20	0,15
		Run2	0,08	0,15	0,17	0,13
	Unvertainty (%)	Run1	4,79	9,60	10,24	8,21
		Run2	5,47	7,88	8,33	7,23
Location#3	Mean	Run1	1,47	1,51	3,31	2,10
		Run2	1,49	1,50	3,10	2,03
	Median	Run1	1,46	1,50	3,32	2,09
		Run2	1,49	1,50	3,09	2,03
	Std. Deviation	Run1	0,04	0,05	0,21	0,10
		Run2	0,04	0,04	0,19	0,09
	Unvertainty (%)	Run1	3,05	3,19	6,42	4,22
		Run2	2,80	2,49	6,20	3,83

The E-field plots for each axis of the dosimeter and the total E-field along with the extrapolation factors are presented in the figure below. For the sake of brevity, only an example for location#1 is presented here.



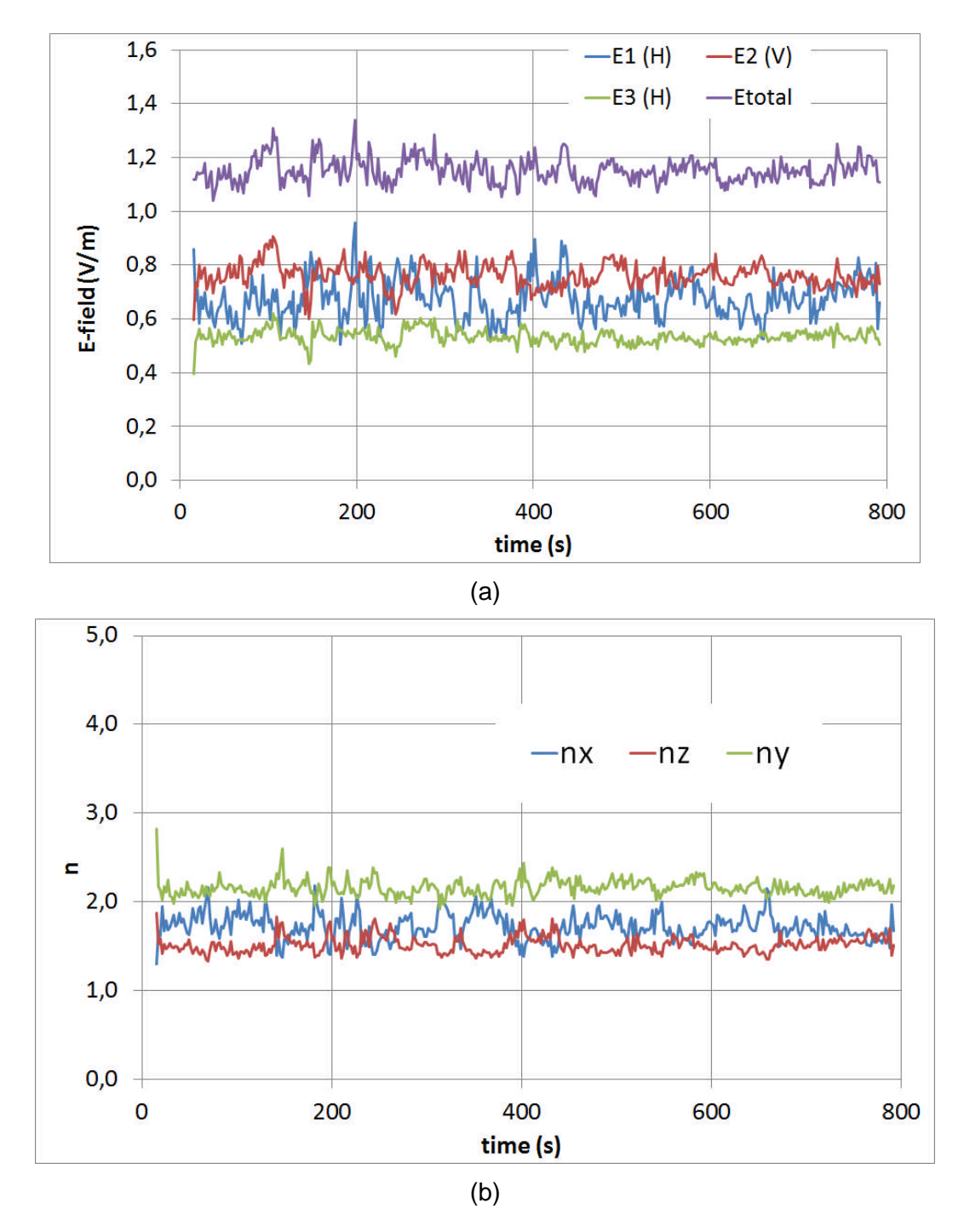


Figure C-1: (a) E-field plots, (b) Extrapolation factor plots for GSM-DL at location 1



## C.2 DCS-DL results

Table C-2: Measurement results for DCS-DL signal at the three locations

			DCS-DL				
			η×	ηz	$\eta_{\mathrm{Y}}$	η	
Location#1	Mean	Run1	0,86	1,71	1,81	1,46	
		Run2	<b>1,</b> 56	2,08	1,72	1,79	
	Median	Run1	0,86	1,70	1,81	1,45	
		Run2	<b>1,</b> 55	2,05	1,71	1,77	
Location#1	Std. Deviation	Run1	0,05	0,13	0,13	0,10	
-		Run2	0,11	0,22	0,14	0,16	
	Unvertainty (%)	Run1	6,27	7,42	7,06	6,92	
		Run2	7,05	10,75	8,31	8,71	
Location#2	Mean	Run1	1,81	1,91	1,58	1,77	
		Run2	1,64	2,83	1,45	1,97	
	Median	Run1	1,80	1,91	1,56	1,76	
		Run2	1,64	2,81	1,41	1,95	
	Std. Deviation	Run1	0,17	0,17	0,10	0,14	
		Run2	0,14	0,45	0,11	0,24	
	Unvertainty (%)	Run1	9,23	8,69	6,11	8,01	
		Run2	8,73	15,91	7,81	10,82	
Location#3	Mean	Run1	2,11	1,50	1,75	1,79	
		Run2	2,12	1,50	1,75	1,79	
	Median	Run1	2,11	1,50	1,75	1,79	
		Run2	2,12	<b>1,</b> 50	1,75	1,79	
	Std. Deviation	Run1	0,09	0,05	0,09	0,08	
		Run2	0,10	0,05	0,09	0,08	
	Unvertainty (%)	Run1	4,43	3,44	5,09	4,32	
		Run2	4,79	3,46	5,01	4,42	

The E-field plots for each axis of the dosimeter and the total E-field along with the extrapolation factors are presented in the figure below. For the sake of brevity, only an example for location#1 is presented here.



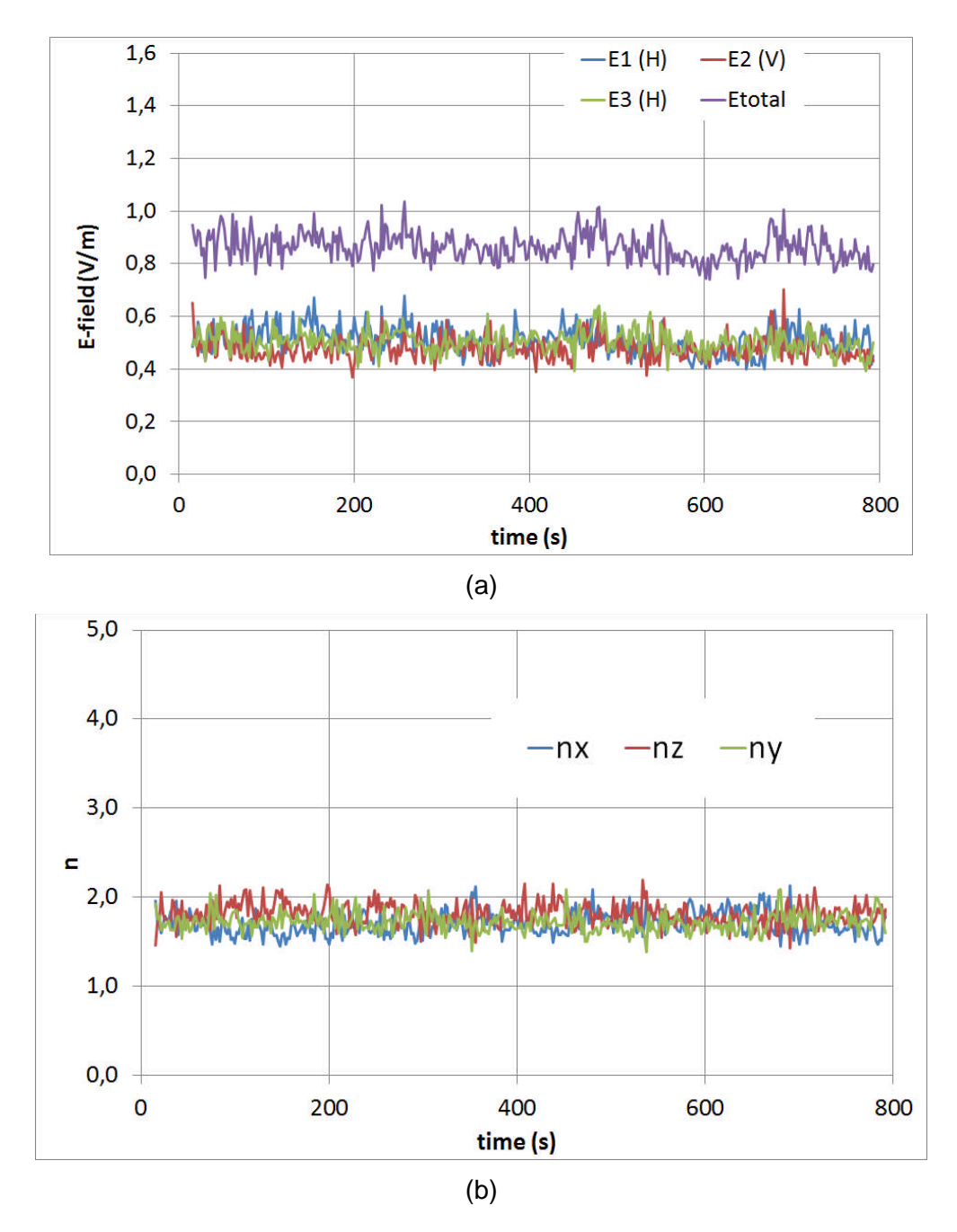


Figure C-2: (a) E-field plots, (b) Extrapolation factor plots for DCS-DL at location 1



## C.3 <u>UMTS-DL results</u>

Table C-3: Measurement results for UMTS-DL signal at the three locations

			UMTS-DL			
			η×	ηz	<b>η</b> γ	η
Location#1	Mean	Run1	1,01	2,00	1,32	1,45
		Run2	2,00	1,32	2,41	1,91
	Median	Run1	1,00	2,00	1,32	1,44
		Run2	2,00	1,32	2,40	1,91
Location#1	Std. Deviation	Run1	0,09	0,11	0,04	0,08
		Run2	0,09	0,03	0,11	0,08
	Unvertainty (%)	Run1	8,61	5,33	2,67	5,53
		Run2	4,61	2,31	4,46	3,79
Location#2	Mean	Run1	1,87	1,53	1,93	1,77
		Run2	2,00	1,46	1,92	1,80
	Median	Run1	1,85	1,52	1,92	1,76
		Run2	1,98	1,45	1,93	1,79
	Std. Deviation	Run1	0,15	0,09	0,16	0,13
		Run2	0,16	0,07	0,14	0,12
	Unvertainty (%)	Run1	7,79	6,18	8,13	7,37
		Run2	7,99	4,78	7,53	6,77
	Mean	Run1	3,20	1,19	2,40	2,26
Location#3		Run2	3,41	1,16	2,57	2,38
	Median	Run1	3,26	1,18	2,39	2,28
		Run2	3,39	1,15	2,58	2,37
	Std. Deviation	Run1	0,64	0,04	0,24	0,31
		Run2	0,53	0,03	0,27	0,28
	Unvertainty (%)	Run1	20,03	3,70	10,09	11,27
		Run2	15,46	2,94	10,51	9,64

The E-field plots for each axis of the dosimeter and the total E-field along with the extrapolation factors are presented in the figure below. For the sake of brevity, only an example for location#1 is presented here.



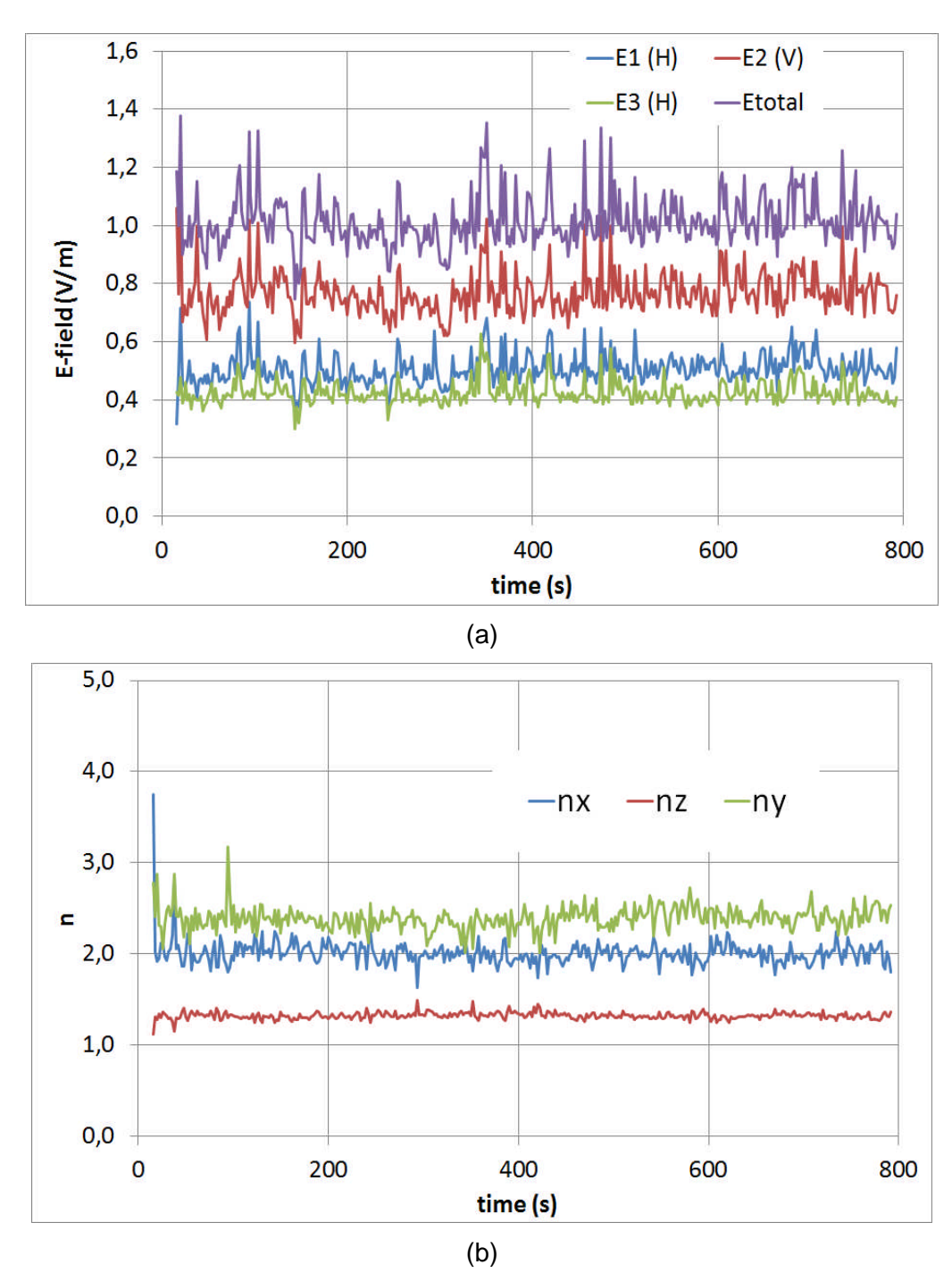


Figure C-3: (a) E-field plots, (b) Extrapolation factor plots for DCS-DL at location 1



# Appendix D EXAMPLES OF MEASUREMENT RESULTS OBTAINED FROM NETWORK MEASUREMENTS

In order to evaluate the properties of different types of areas defined in LEXNET EI, concerning traffic load and its fluctuations over time, for preliminary measurements sets of urban, suburban and rural cells had been chosen. Network statistics were gathered for these cells of interest. GSM900 and DCS1800 cells are analysed in GSM statistics section, while UMTS 2100 cells are analysed in UMTS section.

### D.1 **GSM** statistics

Urban area shows significant daily oscillations in overall traffic. Suburban area shows the oscillations to a somewhat lesser extent, but with much less visible difference between working days and weekend. Rural area, characterized with lowest traffic, has the smallest oscillations during the day and during the week.

### Sum of UsedNoOfTS 250 200 150 Area Rural Suburban Urban 100 03/12/2013 04/12/2013 05/12/2013 06/12/2013 07/12/2013 08/12/2013 09/12/2013 10/12/2013 11/12/2013 Date Hour

Number of used GSM time-slots over time per a type of area

Figure D-1: Number of used GSM time slots in DL for voice and data traffic. UsedNoOfTS represents an averaged number of Time Slots per cell and per hour used to carry BCCH, SDCCH, Half Rate TCH, Full Rate TCH and PDCH all together in down-link direction. Sum Of UsedNoOfTS represents an aggregated value for all cells of interest (for example cells belonging to the same type of area).

Packet traffic has a similar distribution over time and per type of area.



#### Number of used Down Link Packet Data Channel GSM time-slots over time per a type of area

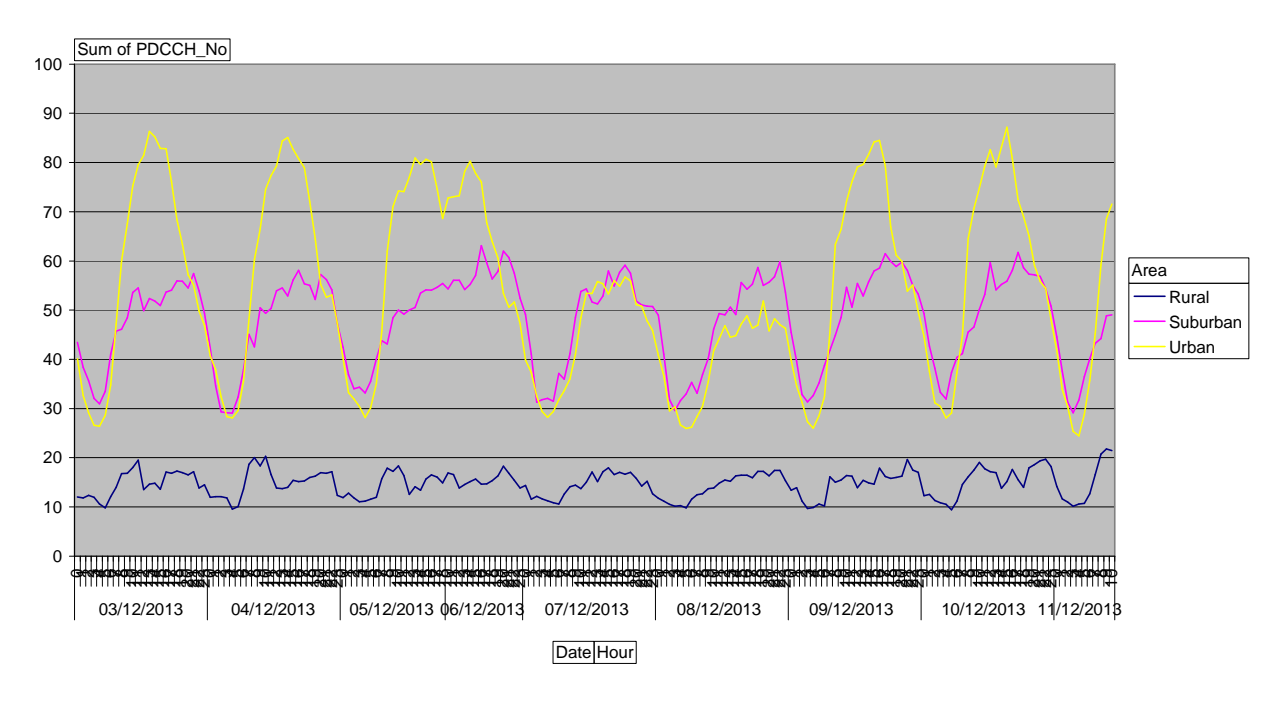


Figure D-2: Number of used DL Packet Data Channel GSM time slots. PDCCH\_No represents an averaged number of Time Slots per cell and per hour used to carry PDCH channels only in down-link direction. Sum Of PDCCH\_No represents an aggregated value for all cells of interest (for example cells belonging to the same type of area). This indicator shows us how much resources i.e. time slots are used for packet data transfer only.

Looking at single cells, significant differences in the overall traffic in cells are visible, Figure D-3:

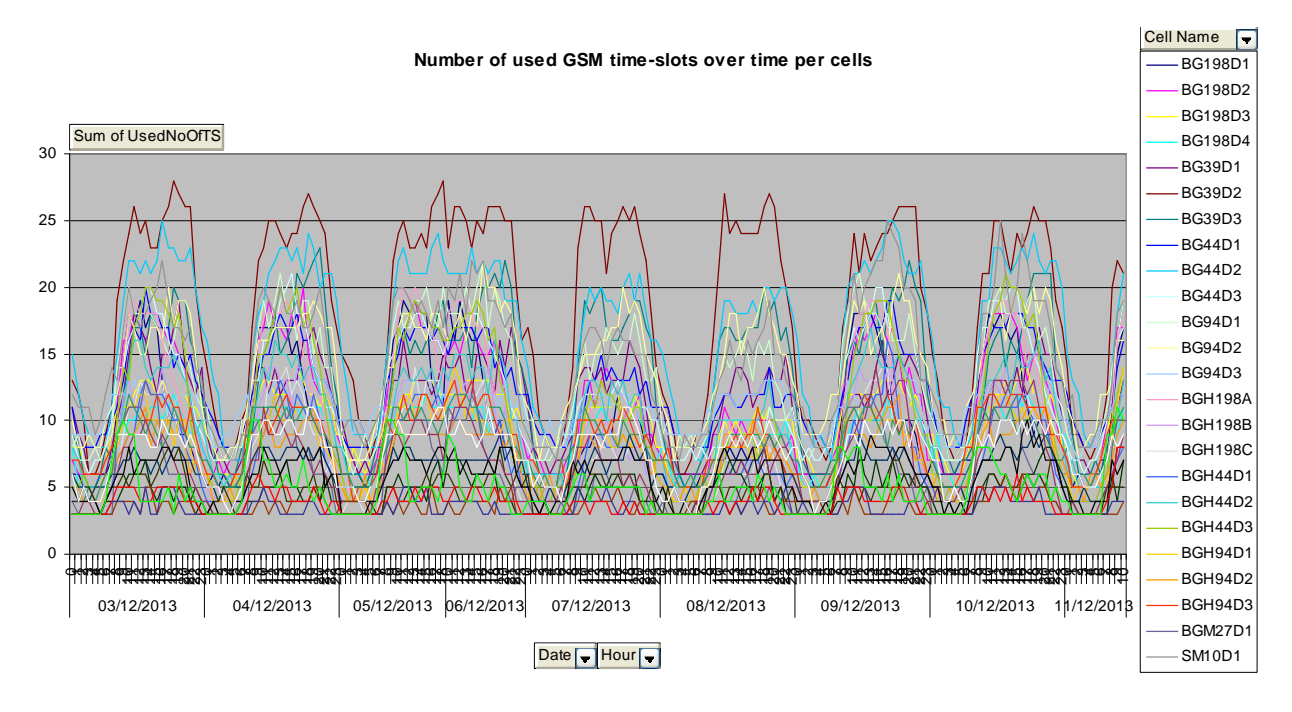


Figure D-3: Number of used GSM time slots in DL for voice and data traffic.

Version 4.0 Dissemination level: PUBLIC



The distribution of DL packet traffic in cells is similar to the distribution of the overall traffic, Figure D-4:

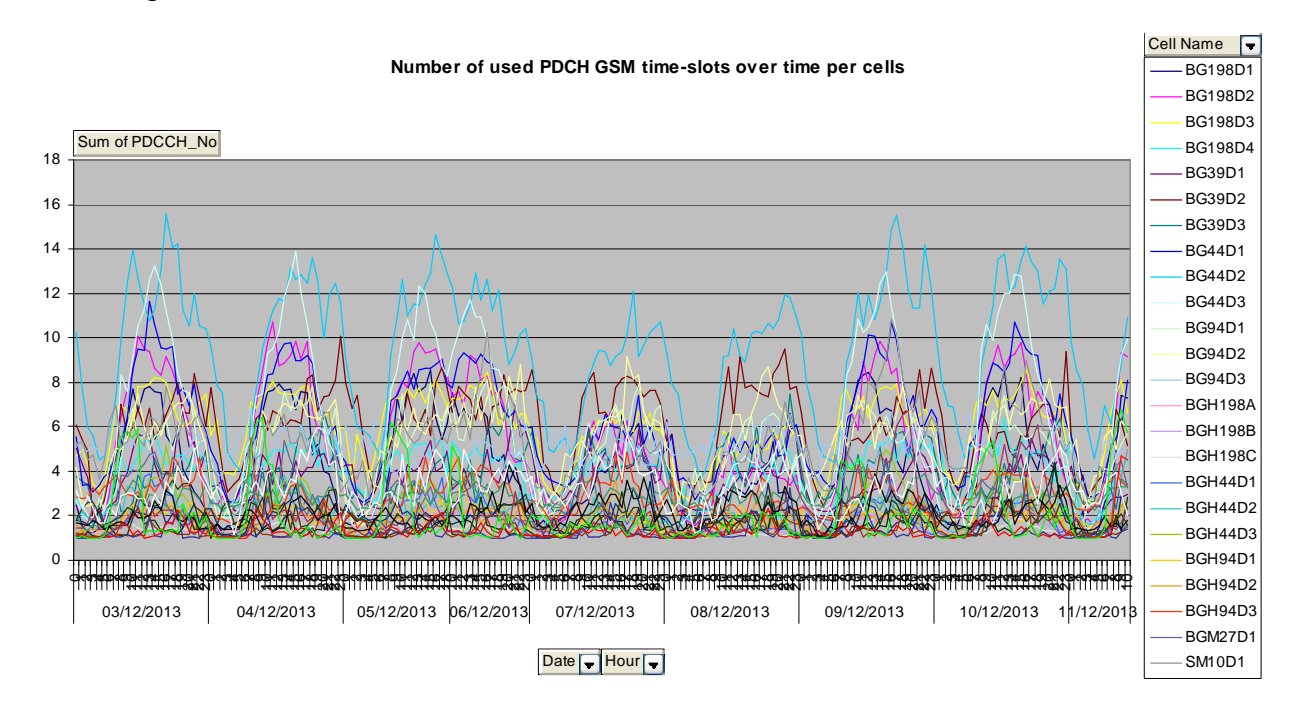


Figure D-4: Number of used DL Packet Data Channel GSM time slots.

#### Conclusions:

- Measurements with supposed small load of the GSM network may be performed in the period from 7 to 8 AM in the morning.
- Measurements with supposed high load of the GSM network may be performed in the period from 2 to 3 PM in the afternoon.

## D.2 UMTS statistics

Urban area shows significant daily oscillations in voice traffic. Suburban area does not show the difference in working days and weekend profiles. Rural area, characterized with the smallest traffic, has also the smallest traffic oscillations during the day and during the week (Figure D-5).



#### Speech traffic (Erl)

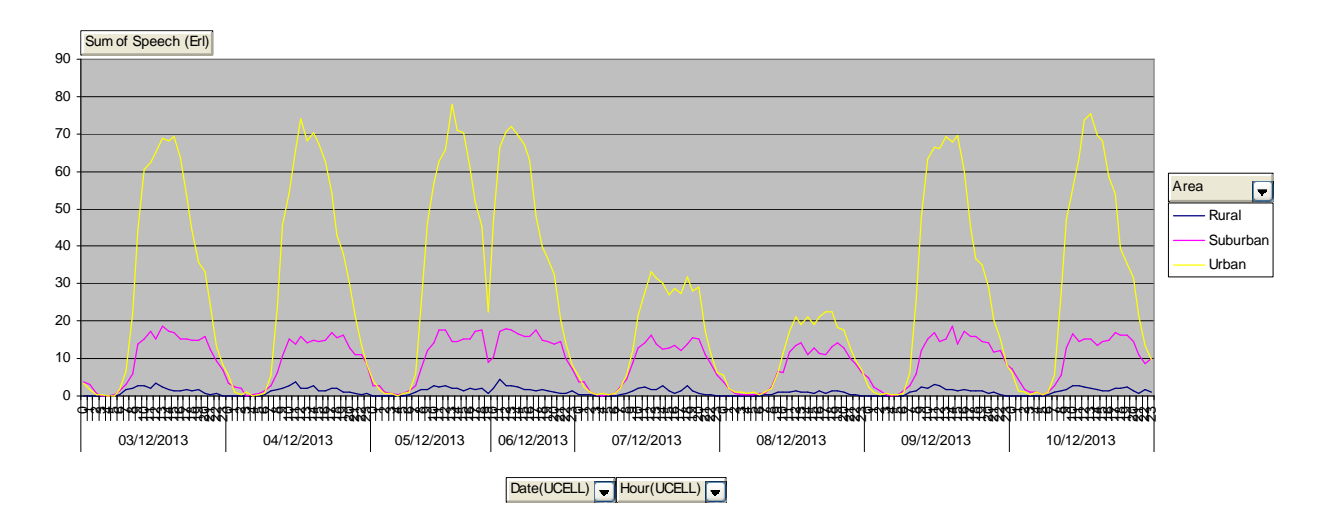


Figure D-5: Sum of Speech (Erl): represents an aggregated value for all cells of interest (for example cells belonging to the same type of area).

Concerning packet traffic, measured by the number of active users, it has a similar traffic distribution in time as the voice traffic, Figure D-6. In a suburban area, it is visible that the number of users is somewhat bigger in the evening hours.

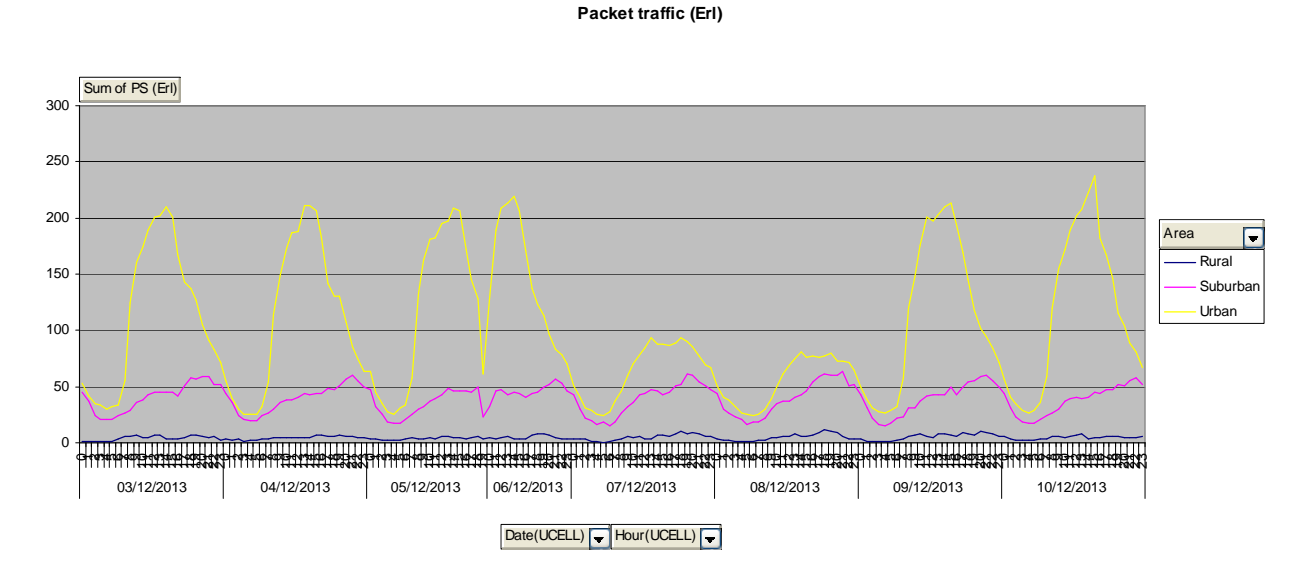


Figure D-6: Sum of PS (Erl): represents an aggregated value for all cells of interest (for example cells belonging to the same type of an area). Packet Service in Erlangs means total time that certain radio access bearer resource was kept whether it was Rel99 or HSDPA RAB counted for each connection. It is same as an average number of active Rel99 users plus an average number of active HSDPA users per a cell and per an hour.

Concerning packet traffic measured by the volume of transferred data in the DL, Figure D-7, the distribution does not show regularities (does not follow a pattern) to the extent it does when measured by the number of users.





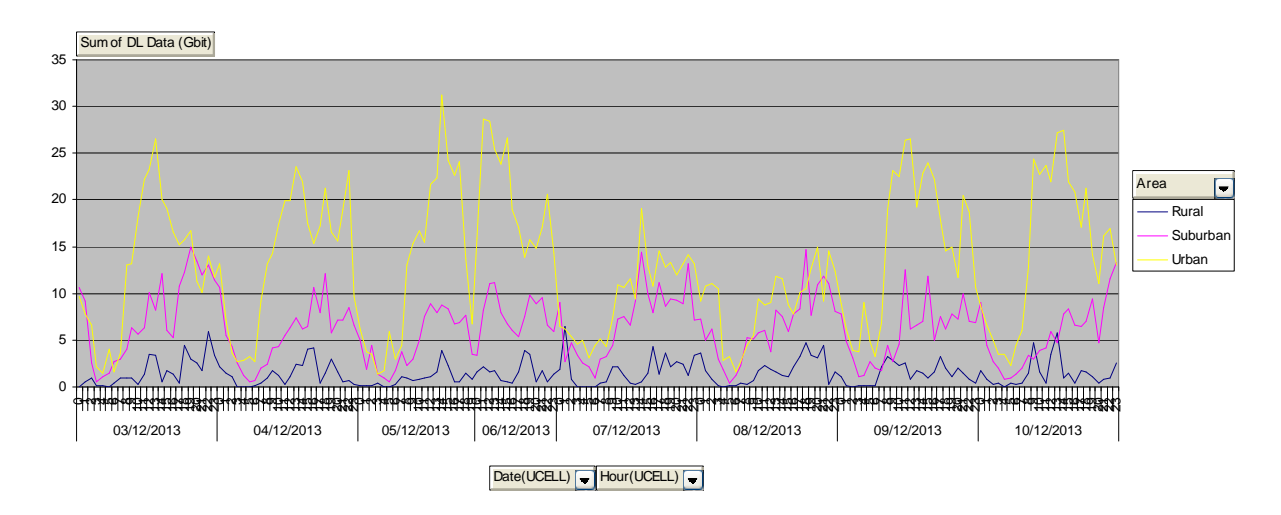


Figure D-7: Sum of DL data (Gbit)

Concerning packet traffic measured by the volume of transferred data in the UL, Figure D-8, the distribution does not show regularities (does not follow a pattern) to the extent it does when measured by the number of users.

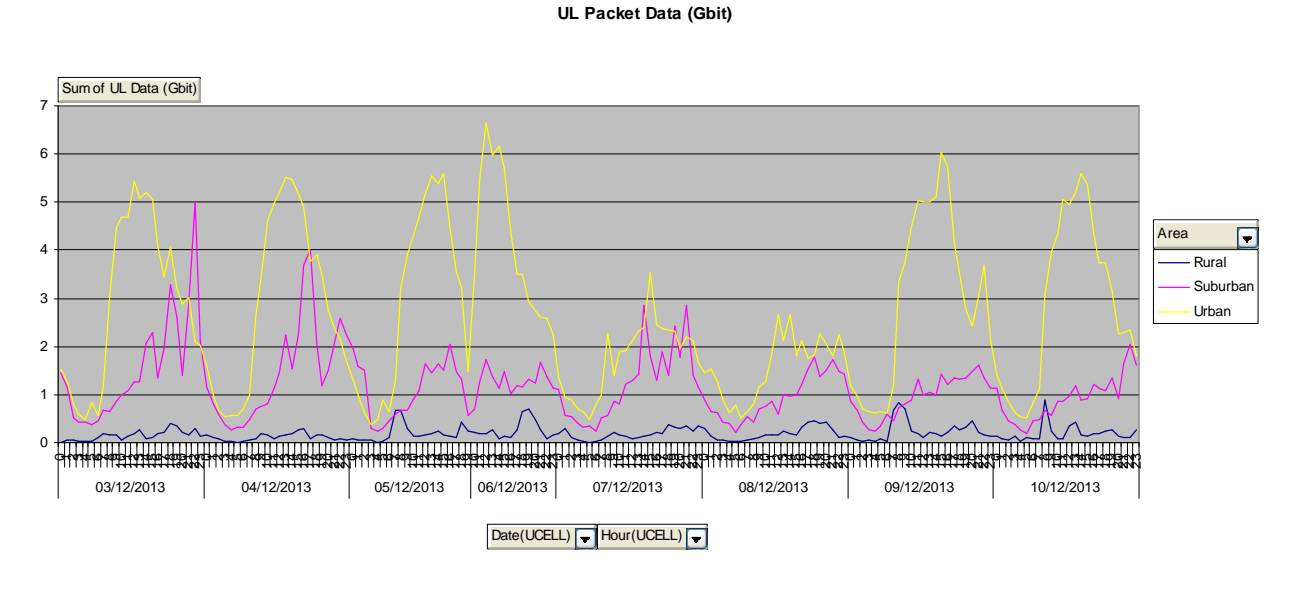
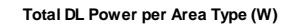


Figure D-8: Sum of UL data (Gbit)

The overall hourly-averaged power measured on antenna inputs of the UMTS base stations, given per type of area is shown in Figure D-9. The measurements are done in dBm, while the average power is calculated in W.





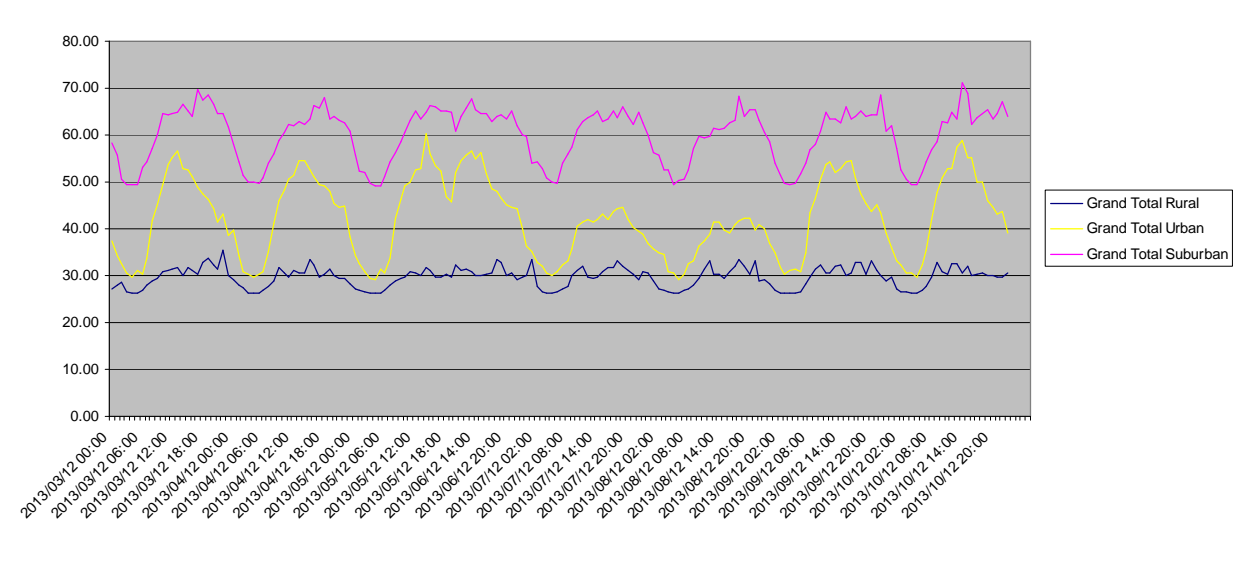


Figure D-9: Total DL Power per Area Type (W)

The overall hourly-averaged power measured on antenna inputs of the UMTS base stations, given per cells is shown in Figure D-10. The measurements are done in dBm, while the average power is calculated in W.

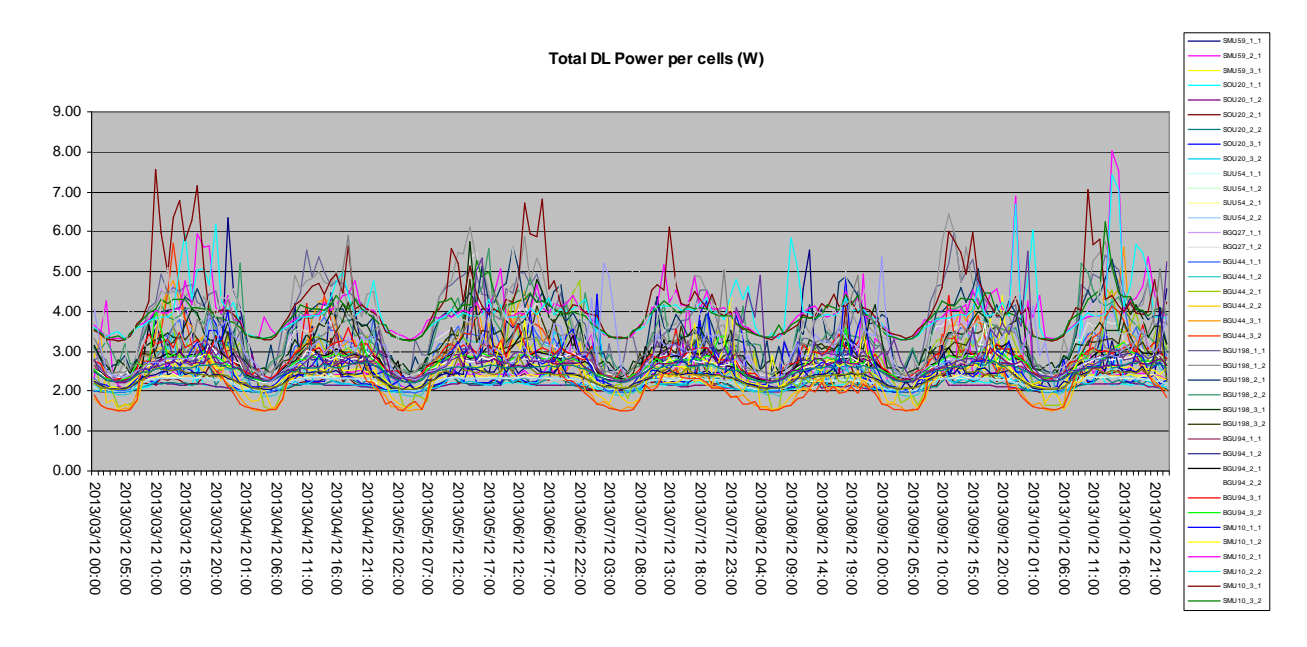


Figure D-10: Total DL Power per cells (W)



78

# **Appendix E** Example of analytical approach to EI Uncertainty Evaluation

## **E.1** Introduction

The process of uncertainty evaluation is referred to as the propagation of distributions [37]. The various approaches for the uncertainty evaluation are available:

- a) the GUM (*Guide to the expression of Uncertainty in Measurement*) uncertainty framework [15], constituting the application of the law of propagation of uncertainty, and the characterization of the output quantity Y by a Gaussian or a *t*-distribution [37],
- b) analytic methods, in which mathematical analysis is used to derive an algebraic form for the probability distribution for Y, and
- c) a Monte Carlo method (MCM).

For any particular uncertainty evaluation problem, approach a), b) or c) (or some other approach) can be used:

- a) being generally approximate,
- b) exact, and
- c) providing a solution with a numerical accuracy that can be controlled.

The GUM uncertainty framework [15] uses

- the best estimates  $x_i$  of the input quantities  $X_i$ ,
- the standard uncertainties  $u(x_i)$  associated with the  $x_i$ , and
- the sensitivity coefficients c<sub>i</sub>

to form an estimate y of the output quantity Y and the associated standard uncertainty u(y):

$$u(y) = \sqrt{\sum_{i=1}^{N} c_i^2 u^2(x_i)}$$
 (E-1)

Analytic methods by which an algebraic form for the probability distribution for the output quantity can be obtained do not introduce any approximation, but can be applied only in relatively simple cases. A treatment of such methods is available [38], [39]. Some cases that can be, for a general number N of input quantities, treated in such a way are linear functions, where the probability distributions for all input quantities are Gaussian, or all are rectangular with the same width.



Using Monte Carlo method (MCM) an approximation to the distribution function for Y is established numerically by making random draws from the probability distributions for the input quantities, and evaluating the model at the resulting values. MCM has fewer conditions associated with its use than the GUM uncertainty framework [37]. [37] provides an adaptive MCM procedure, in which the number of Monte Carlo trials is determined automatically by utilizing a measure of convergence of the overall process [37].

Considering the fact that the analytical expression of Exposure Index (EI) is known, to calculate the uncertainty of EI the analytical method is the most appropriate. Using the analytical method EI uncertainty can be determined, but this method cannot provide the information on the type of probability distribution function (pdf). Where the knowing of pdf is important, MCM can be used alternatively. However, MCM method is somewhat more complex and time consuming since it requires a simulation procedure to be implemented (and carried out for each individual value of EI).

## **E.2** Exposure Index definition

Exposure Index (EI) shall be calculated by crossing the database of raw SAR values with the set of configurations of exposure [1], [2]. Assume that we neglect the uplink exposure by mobile devices from other users – which can be regarded as a downlink exposure, then the EI becomes:

$$EI^{SAR} = \frac{1}{T} \sum_{t}^{N_{T}} \sum_{p}^{N_{P}} \sum_{e}^{N_{E}} \sum_{r}^{N_{E}} \sum_{c}^{N_{L}} \sum_{pos}^{N_{L}} f_{t,p,e,r,l,c,pos} \left[ \sum_{u}^{N_{U}} (d^{UL} \, \bar{P}_{TX}) + d^{DL} \, \bar{S}_{inc} \right] \quad \left[ \frac{W}{kg} \right]$$
 (E-2)

$$\begin{split} EI_{[J/kg]} &= \sum_{t}^{N_T} \sum_{p}^{N_P} \sum_{e}^{N_E} \sum_{r}^{N_R} \sum_{c}^{N_C} \sum_{u}^{N_U} \bigg[ \sum_{l}^{N_L} \bigg( d_{t,p,l,e,r,c,u[\frac{s}{kg}]}^{UL} \overline{P}_{TX[W]} \bigg) + \\ d_{t,p,e,r,c,u[\frac{s}{kg}]}^{DL} \overline{P}_{RX[W]} \bigg] \text{where:} \end{split}$$

- *EI*<sup>SAR</sup> is the Exposure Index value, the average exposure of the population of the considered geographical area over the considered time frame T. SAR refers to whole-body SAR, organ-specific SAR or localized SAR.
- $N_T$  is the number of considered periods within the considered time frame (e.g., single day);
- *N<sub>P</sub>* is the number of considered Population categories;
- $N_E$  is the number of considered Environments;
- $N_R$  is the number of considered Radio Access Technologies;
- $N_C$  is the number of considered Cell types;
- N<sub>L</sub> is the number of considered user Load profiles;
- $N_{\text{pos}}$  is the number of considered Postures



- N<sub>U</sub> is the number of considered Usages with devices;
- $\bar{P}_{TX}$  is the mean TX power transmitted by the users' devices during the period t, in usage mode u, connected to RAT r, in environment e. A TX power values map is given for the whole considered geographical area and the average value is taken into account for the EI evaluation.
- $\bar{S}_{\rm inc}$  is the mean incident power density on the human body during the period t, induced by RAT r, in environment e. A distribution of the incident power density for the whole considered geographical area is considered and the average value over this area is taken into account for the EI evaluation.
- $d^{UL}(\frac{Ws}{kg}/W)$  and  $d^{DL}(\frac{Ws}{kg}/\frac{W}{m^2})$  are the normalised raw dose values for UL and DL from base stations and access points, respectively, all multiplied by the time spent in the configuration.
- $f_{t,p,e,r,l,c,pos}$  is the fraction of the total population that corresponds to population category p, user load profile I, in posture pos, connected to RAT r, for a cell type c, in environment e, during the time period t.

## Coefficients $d^{UL}$ and $d^{DL}$

Coefficient  $d^{\mathit{UL}}$  is associated to the exposure induced by the uplink and expressed as an absorbed dose normalised to a transmitted power of 1 W :

$$d_{\left[\frac{S}{\text{kg}}\right]}^{UL} = \frac{TD_{t,p,l,e,r,c,u,pos[s]}^{UL}SAR_{p,r,u,pos[W/\text{kg}]}^{UL}}{P_{TX[W]}^{ref}} \left[\frac{\text{Ws}}{\text{kg}}/\text{W}\right]$$
 (E-3)

where:

- $TD^{UL}_{t,p,l,e,r,c,u,pos}$  is the time duration of usage u, and a user profile load I, when connected to the RAT r, operating in cell type c, in the environment e, for the population category p, in the posture pos, during the time period of the day t.
- $\frac{SAR_{p,r,u,pos}^{UL}}{P_{TX}^{ref}}$  can be the whole body or an organ-specific or tissue-specific SAR value for the usage u and the posture pos, in the frequency band of the RAT r, and the population category p, calculated for an incident emitted power of  $P_{TX}^{ref}$  and normalized to this power.

Coefficient  $d^{DL}$  is associated to the exposure induced by downlink and also expressed as an absorbed dose normalised to an incident power density of 1 W/m<sup>2</sup>:

$$d_{\left[\frac{S}{\log I}\right]}^{DL} = \frac{TD_{t,p,e,r,c,pos[s]}^{DL}SAR_{p,r,pos[W/\log I]}^{DL}}{S_{\mathsf{RX[W]inc}}^{ref}} \quad \left[\frac{Ws}{kg} / \frac{W}{m^2}\right] \tag{E-4}$$



#### where:

- TD<sup>DL</sup><sub>t,p,e,r,c,pos</sub> is the time duration of posture pos, when connected to the RAT r, operating in cell type c, in the environment e, for the population p, during the time period of the day t.
- $\frac{SAR_{p,r,pos}^{DL}}{S_{RXinc}^{ref}}$  can be the whole body or an organ-specific or tissue-specific SAR value induced by the base station or access points of the RAT r, in the population p, for the posture pos, normalized to the received power density  $S_{ing}^{ref}$ .

## **E.3** Propagation of Error

**Propagation of Error** (or **Propagation of Uncertainty**) is defined as the effect on a function by a variable's uncertainty [40]. It is a calculus derived statistical calculation designed to combine uncertainties from multiple variables, in order to provide an accurate measurement of uncertainty.

#### E.3.1 Introduction

Every measurement has an air of uncertainty about it, and not all uncertainties are equal. Therefore, the ability to properly combine uncertainties from different measurements is crucial. Uncertainty in measurement comes about in a variety of ways: instrument variability, different observers, sample differences, time of day, etc. Typically, error is given by the standard deviation ( $\sigma_x$ ) of a measurement.

Anytime a calculation requires more than one variable to solve, propagation of error is necessary to properly determine the uncertainty.

#### E.3.2 Derivation of Exact Formula

Suppose a certain experiment requires multiple instruments to carry out. These instruments each have different uncertainties in their measurements. The results of each instrument are given as: a, b, c, d... (For simplification purposes, only the variables a, b, and c will be used throughout this derivation). The end result desired is x, so that x is dependent on a, b, and c. It can be written that x is a function of these variables:

$$x = f(a, b, c) \tag{E-5}$$

Because each measurement has an uncertainty about its mean, it can be written that the increment  $\Delta x_i$  of the *i*-th measurement of x depends on the uncertainties of the *i*-th measurements of a, b, and c. The total deviation of x can be derived from the partial derivative of x with respect to each of the variables:

Version 4.0 81



$$\Delta x_i = \left(\frac{\partial x}{\partial a}\right)_{h,c} \Delta a_i + \left(\frac{\partial x}{\partial b}\right)_{a,c} \Delta b_i + \left(\frac{\partial x}{\partial c}\right)_{a,h} \Delta c_i \tag{E-6}$$

A relationship between the standard deviations of *x* and *a, b, c, etc...* is formed in two steps:

- by squaring Equation ((E-6), and
- taking the total sum from i = 1 to i = N, where N is the total number of measurements (by assumption N is sufficiently large).

$$\sum_{i=1}^{N} (\Delta x_i)^2 = \sum_{i=1}^{N} \left[ \left( \frac{\partial x}{\partial a} \right)^2 (\Delta a_i)^2 + \left( \frac{\partial x}{\partial b} \right)^2 (\Delta b_i)^2 + \left( \frac{\partial x}{\partial c} \right)^2 (\Delta c_i)^2 \right]$$

$$+ 2 \left( \frac{\partial x}{\partial a} \right) \left( \frac{\partial x}{\partial b} \right) \Delta a_i \Delta b_i + 2 \left( \frac{\partial x}{\partial a} \right) \left( \frac{\partial x}{\partial c} \right) \Delta a_i \Delta c_i$$

$$+ 2 \left( \frac{\partial x}{\partial b} \right) \left( \frac{\partial x}{\partial c} \right) \Delta b_i \Delta c_i$$

$$\left[ (E-7) \right]$$

Two unique terms appear on the right hand side of the equation (square terms and cross terms):

Square terms: 
$$\left(\frac{\partial x}{\partial a}\right)^2 (\Delta a_i)^2$$
,  $\left(\frac{\partial x}{\partial b}\right)^2 (\Delta b_i)^2$ ,  $\left(\frac{\partial x}{\partial c}\right)^2 (\Delta c_i)^2$  (E-8)

Cross terms: 
$$\left(\frac{\partial x}{\partial a}\right) \left(\frac{\partial x}{\partial b}\right) \Delta a_i \Delta b_i$$
,  $\left(\frac{\partial x}{\partial a}\right) \left(\frac{\partial x}{\partial c}\right) \Delta a_i \Delta c_i$ ,  $\left(\frac{\partial x}{\partial b}\right) \left(\frac{\partial x}{\partial c}\right) \Delta b_i \Delta c_i$  (E-9)

Square terms, due to the nature of squaring, are always positive, and therefore never cancel each other out. By contrast, cross terms may cancel each other out, due to the possibility that each term may be positive or negative. If  $\Delta a$ ,  $\Delta b$ , and  $\Delta c$  represent random and independent uncertainty variables, about half of the cross terms will be negative and half positive (this is primarily due to the fact that the variables represent uncertainty about a mean). In effect, the sum of the cross terms should approach zero, especially as N increases. However, if the variables are correlated rather than independent, the cross term may not cancel out.

Assuming the cross terms do cancel out, then the equation (E-7) can be simplified:

$$\sum_{i=1}^{N} (\Delta x_i)^2 = \left(\frac{\partial x}{\partial a}\right)^2 \sum_{i=1}^{N} (\Delta a_i)^2 + \left(\frac{\partial x}{\partial b}\right)^2 \sum_{i=1}^{N} (\Delta b_i)^2 + \left(\frac{\partial x}{\partial c}\right)^2 \sum_{i=1}^{N} (\Delta c_i)^2$$
 (E-10)

Let's divide both sides of the previous equation by N-1:



$$\frac{\sum_{i=1}^{N}(\Delta x_i)^2}{N-1} = \left(\frac{\partial x}{\partial a}\right)^2 \frac{\sum_{i=1}^{N}(\Delta a_i)^2}{N-1} + \left(\frac{\partial x}{\partial b}\right)^2 \frac{\sum_{i=1}^{N}(\Delta b_i)^2}{N-1} + \left(\frac{\partial x}{\partial c}\right)^2 \frac{\sum_{i=1}^{N}(\Delta c_i)^2}{N-1}$$
(E-11)

Now, the left hand side of the equation (E-11) represents variance ( $\sigma_x^2$ ) of x:

$$\frac{\sum_{i=1}^{N} (\Delta x_i)^2}{N-1} = \frac{\sum_{i=1}^{N} (x_i - \bar{x})^2}{N-1} = \sigma_x^2$$
 (E-12)

The similar stands for the terms on the right hand side of the equation, but for the variables *a*, *b* and *c*. Rewriting equation (E-11) using the statistical relationship created yields the exact formula for propagation of error:

$$\sigma_x^2 = \left(\frac{\partial x}{\partial a}\right)^2 \sigma_a^2 + \left(\frac{\partial x}{\partial b}\right)^2 \sigma_b^2 + \left(\frac{\partial x}{\partial c}\right)^2 \sigma_c^2 \tag{E-13}$$

Thus, the end result is achieved. Equation (E-13) shows a direct statistical relationship between multiple variables and their standard deviations. In the next section, derivations for common calculations are given.

### **E.3.3** Arithmetic Error Propagation

Derivations for common calculations for direct statistical relationship between multiple variables and their standard deviations are given in Table E-1.

Table E-1: Arithmetic Calculations of Error Propagation

Туре	Example*	Standard Deviation ( $\sigma_x$ )
Addition or Subtraction	x = a + b - c	$\sigma_x = \sqrt{{\sigma_a}^2 + {\sigma_b}^2 + {\sigma_c}^2}$
Multiplication or Division	$x = a \times b/c$	$\frac{\sigma_x}{x} = \sqrt{\left(\frac{\sigma_a}{a}\right)^2 + \left(\frac{\sigma_b}{b}\right)^2 + \left(\frac{\sigma_c}{c}\right)^2}$
Exponential	$x = a^y$	$\frac{\sigma_x}{x} = y\left(\frac{\sigma_a}{a}\right)$
Logarithmic	$x = \log(a)$	$\sigma_{x} = 0.434 \left(\frac{\sigma_{a}}{a}\right)$
Anti-logarithmic	$x = \operatorname{antilog}(a)$	$\frac{\sigma_x}{x} = 2.303(\sigma_a)$

<sup>\*</sup> a, b, and c are measured variables from an experiment; and  $\sigma_a$ ,  $\sigma_b$ , and  $\sigma_c$  are the standard deviations of those variables.



**Note** that addition, subtraction, and logarithmic equations leads to an absolute standard deviation, while multiplication, division, exponential, and anti-logarithmic equations lead to relative standard deviations (uncertainties).

## E.4 Evaluation of Exposure Index Uncertainty - analytic method

The expression for El calculation, Equation (E-1), can be written in an alternative form:

$$EI^{SAR} = \frac{1}{T} \sum_{t}^{N_{T}} \sum_{p}^{N_{E}} \sum_{e}^{N_{E}} \sum_{r}^{N_{E}} \sum_{c}^{N_{C}} \sum_{l}^{N_{L}} \sum_{pos}^{N_{pos}} \left[ \sum_{u}^{N_{U}} (A) + B \right] \left[ \frac{W}{kg} \right]$$
 (E-14)

where:

$$A = f_{t,p,e,r,l,c,pos} \frac{TD_{t,p,l,e,r,c,u,pos[s]}^{UL} SAR_{p,r,u,pos[W/kg]}^{UL}}{P_{TX[W]}^{ref}} \bar{P}_{TX[W]}$$
(E-15)

$$B = f_{t,p,e,r,l,c,pos} \frac{TD_{t,p,e,r,c,pos[s]}^{DL} SAR_{p,r,pos[W/kg]}^{DL}}{S_{RX[W]inc}^{ref}} \bar{S}_{RX[W]}$$
(E-16)

Let denote the uncertainties of terms A and B with u(A) and u(B), respectively.

Having in mind that  $P_{TX[W]}^{ref}$  and  $S_{RX[W]}^{ref}$  are constants and according to Table E-1, the uncertainties u(A) and u(B) can be determined in the following way:

$$u(A)$$
 (E-17)

$$= \sqrt{u^2(f_{t,p,e,r,l,c,pos}) + u^2(t_{t,p,l,e,r,c,u[s]}^{UL}) + u^2(SAR_{p,r,u[W/kg]}^{UL}) + u^2(\bar{P}_{TX[W]})}$$

$$u(B) = \sqrt{u^2 (f_{t,p,e,r,l,c,pos}) + u^2 (t_{t,p,e,r,c,u[s]}^{DL}) + u^2 (SAR_{p,r,u[W/kg]}^{DL}) + u^2 (\bar{S}_{RX[W]})}$$
 (E-18)

Now, exposure index uncertainty u(EI) can be determined in the following way:

$$u(EI) = \frac{\sqrt{\sum_{t}^{N_{T}} \sum_{p}^{N_{P}} \sum_{e}^{N_{E}} \sum_{r}^{N_{R}} \sum_{c}^{N_{C}} \sum_{l}^{N_{L}} \sum_{pos}^{N_{pos}} \left[ \sum_{u}^{N_{U}} \left( A^{2} * u^{2}(A) \right) + B^{2} * u^{2}(B) \right]}}{\sum_{t}^{N_{T}} \sum_{p}^{N_{P}} \sum_{e}^{N_{E}} \sum_{r}^{N_{R}} \sum_{c}^{N_{C}} \sum_{l}^{N_{L}} \sum_{pos}^{N_{pos}} \left[ \sum_{u}^{N_{U}} (A) + B \right]}$$
(E-19)



## E.4.1 Probability distribution function assessment

The product of *N* mutually independent log-normal random variables is log normal. This is itself a special case of a more general case where the logarithm of the product can be written as the sum of the logarithms. It should be noted that for random variables with relatively large mean values and small standard deviations (i.e., small uncertainties) a log-normal distribution seems like (converges to) normal distribution.

#### Proof:

The probability density function of a log-normal distribution is:

$$f(x) = \frac{1}{x\sigma\sqrt{2\pi}}e^{-\frac{(\ln x - \mu)^2}{2\sigma^2}}, \quad x > 0$$
 (E-20)

For log-normal distribution, the mean  $\bar{x}$  and variance  $\sigma_x^2$  are:

$$\overline{x} = e^{\mu + \sigma^2/2} \tag{E-21}$$

$$\sigma_r^2 = (e^{\sigma^2} - 1)e^{2\mu + \sigma^2}$$
 (E-22)

Let's divide  $\sigma_x$  by  $\overline{x}$ :

$$\frac{\sigma_{\chi}}{\bar{\chi}} = \sqrt{e^{\sigma^2} - 1} \tag{E-23}$$

By assumption of small uncertainty:  $\frac{\sigma_x}{\bar{x}} = \sqrt{e^{\sigma^2} - 1} \ll 1$ . Further, it means that  $1 < e^{\sigma^2} \ll 2$ . Applying Taylor series expansion, expression (E-23) becomes:

$$\frac{\sigma_x}{\overline{r}} \approx \sigma$$
 (E-24)

On the other side, substituting  $\mu$  with  $\mu = \ln e^{\mu}$  in Equation (E-20):

$$f(x) = \frac{1}{x\sigma\sqrt{2\pi}}e^{-\frac{(\ln x - \ln e^{\mu})^2}{2\sigma^2}}$$
 (E-25)

$$f(x) = \frac{1}{r\sigma\sqrt{2\pi}}e^{-\frac{(\ln\frac{x}{e^{\mu}})^2}{2\sigma^2}}$$
 (E-26)

Knowing that  $\frac{x}{e^{\mu}} \approx 1$ :



$$f(x) = \frac{1}{x\sigma\sqrt{2\pi}}e^{-\frac{(\ln[1+(\frac{x}{e^{\mu}}-1)])^2}{2\sigma^2}}$$
 (E-27)

 $\left|\frac{x}{e^{\mu}}-1\right|\ll 1$  and applying Taylor series expansion:

$$f(x) = \frac{1}{x\sigma\sqrt{2\pi}}e^{-\frac{(\frac{x}{e^{\mu}}-1)^2}{2\sigma^2}}$$
 (E-28)

$$f(x) = \frac{1}{x\sigma\sqrt{2\pi}}e^{-\frac{(x-e^{\mu})^2}{2\sigma^2e^{2\mu}}}$$
 (E-29)

$$f(x) = \frac{1}{\frac{x}{e^{\mu}} \sigma e^{\mu} \sqrt{2\pi}} e^{-\frac{(x - e^{\mu})^2}{2\sigma^2 e^{2\mu}}}$$
 (E-30)

Finally,

$$f(x) = \frac{1}{\frac{x}{\overline{x}} \sigma_x \sqrt{2\pi}} e^{-\frac{(x-\overline{x})^2}{2\sigma_x^2}}$$
 (E-31)

And finally,

$$f(x) = \frac{1}{\sigma_x \sqrt{2\pi}} e^{-\frac{(x-\bar{x})^2}{2\sigma_x^2}}$$
 (E-32)

What represents normal distribution.

This means that for the mean value much larger than standard deviation (small uncertainty) a log-normal distribution seems like (converges to) normal distribution.

Therefore, the product of random variables with relatively large mean values and small standard deviations (small uncertainties) could be considered to have normal distribution also. By assuming that all variables in Equation (E-2) are positive, mutually independent, and with small uncertainties, the probability distribution function of the Exposure Index is approximately normal.



## **Appendix F** CALIBRATION OF THE JDSU DRIVE TEST.

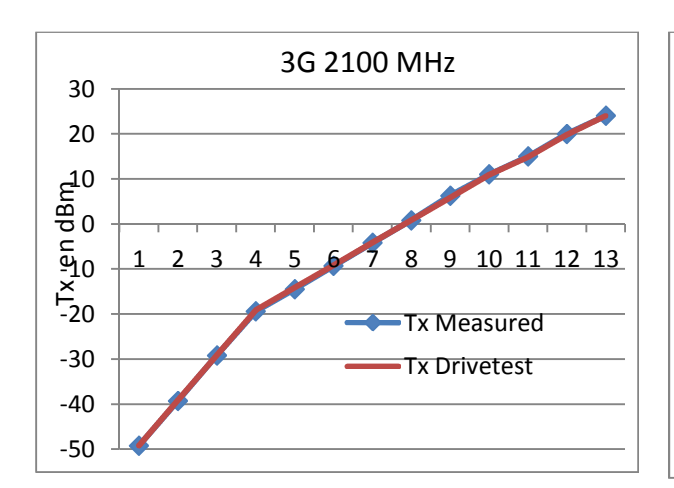
In order to know the uncertainty due to the JDSU drive test measurement tool installed on a Samsun Galaxy S4 smartphone a calibration campaign has been achieved.

This smartphone have an external connector that allows connecting a measurement cable before the mobile phone antenna.

This capability has been used to connect the drive test to a Wireless Communication Tester Rhode & Schwarz CMW 500 in order to establish a communication between the tester and the Galaxy S4.

During this communication we can vary the power emitted by the mobile phone, measure it with the CMW500 and verify the value given by the JDSU drive test tool.

Below are the Tx results for 3G 2100 MHz and LTE 2600 MHz.



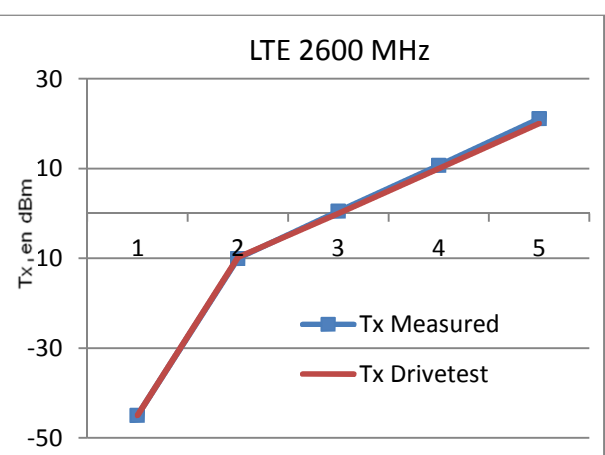


Figure F-1: Comparison Tx measured, Tx given by the Drive test

The conclusion is that the values given by the drive test are very close to the measured values (less than 0.7 dB).



## Appendix G SMARTPHONE VS A DOSIMETER FOR DL POWER MEASUREMENTS.

The isotropy of a smartphone (Samsung galaxy S4) and an EME SPY 200 dosimeter were measured in the Starmimo [41] plaftorm at Satimo, Paris. The measurement system is presented in the figure below.

It consists of horizontal and vertical arcs with dual-polarized probes to simulate a multi-patch MIMO environment. An external emulator (radiocom tester) can be connected to generate a real signal environment and to carry out several types of measurements on mobile devices, such as device throughput measurements, Bit Error Rate, RSSI plots, channel capacity, etc.

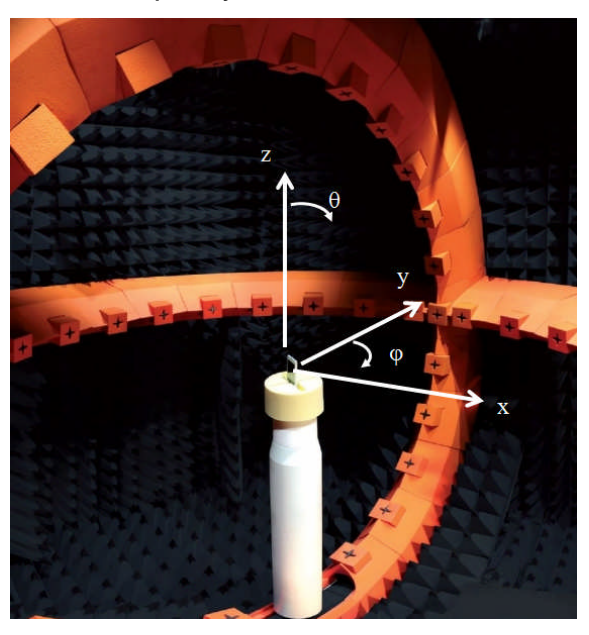


Figure G-1: Starmimo measurement platform at satimo industries, microwavevision, Paris, France.

This platform was used to carry out RSSI measurements for a smartphone (model S4). For this purpose a radiocommunication tester was connected to the Starmimo arc. Only the vertical arc was connected for RSSI measurements. The radiocom tester and the arc was programmed using a software developed by Satimo industries. The type of signal required for the measurement was chosen with corresponding channels and modulation type. The mobile phone was rotated in the azimuth plane and a 3D RSSI plot was obtained.

The following standards have been measured.

Table G-1: Frequencies for the measurement campaign.

Standard	Measurement frequency (MHz)
LTE XX - DL	942.6
GSM 900 - DL	806



DCS-DL	1842.6
UMTS-DL	2140
(WCDMA band I)	2140
LTE VII -DL	2655

Only a single frequency channel was measured at the central frequency shown in the above table. The plots were extracted for three observation planes for horizontal and vertical polarizations:

- i. 90° in the elevation plane corresponding to the XoY plane
- ii. 75° in the elevation plane corresponding the the +15° angle of observation from the XoY plane
- iii. 105° in the elevation plane corresponding the -15° angle of observation from the XoY plane.

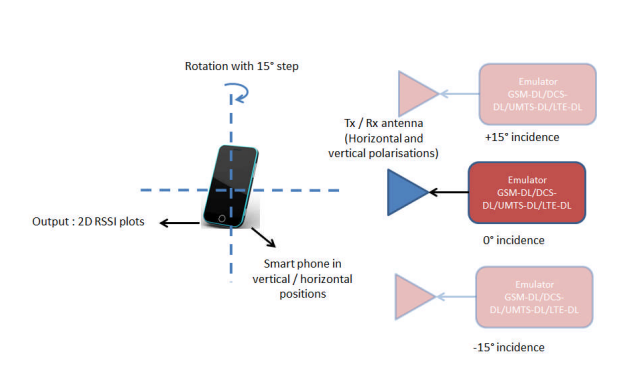
The above three observation planes correspond approximately to the direction of arrival of the DL exposure.

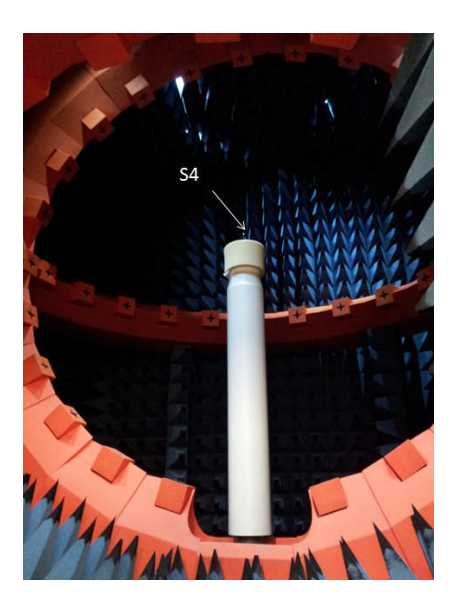
The same study was carried out for the EME SPY. The measurement setup schematic is shown in the figure below for both configurations along with measurement setup pictures.

The measurements for the EME SPY dosimeters were carried out by illuminating one polarization at a time (horizontal or vertical) for a single probe (at 90°, 75° or 105°) and the dosimeter was rotated to generate the isotropy plot. The dosimeter was programmed to carry out measurements for a given frequency standard, with a cycle of 4 seconds over a period of 6 minutes. The power plots were generated by converting the measured E-field to the power (in dBm) using the following formula:  $P_{dBm} = 20*log10~(E_{V/m}) + 13 - AF_{dB/m}$ . Where AF is the mean antenna factor for the three probes of the dosimeter.

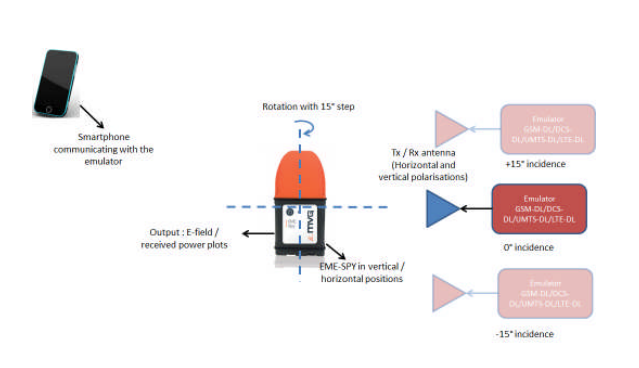
To have a better comparison between the smartphone and the dosimeter, the plots were normalized to the maximum value obtained from the given device because the RSSI value obtained from the smartphone and the power measured by the dosimeter depends on the antenna factor and thus cannot be the same.

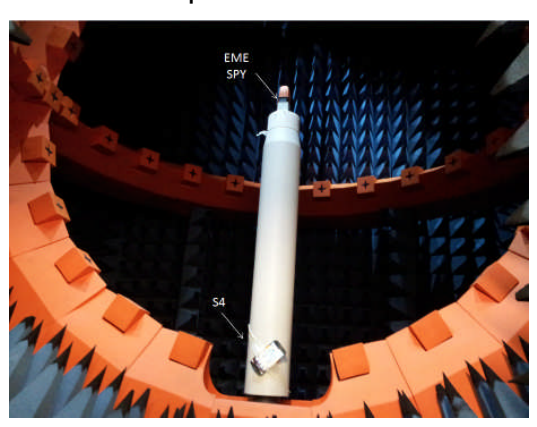






## (a) Measurement setup with the smart phone





## (b) Measurement setup with the EMESPY 200 dosimeter

Figure G-2: Measurement setup for active isotropy measurements.

The results for each frequency band are presented in the following.



#### LTE XX-DL results

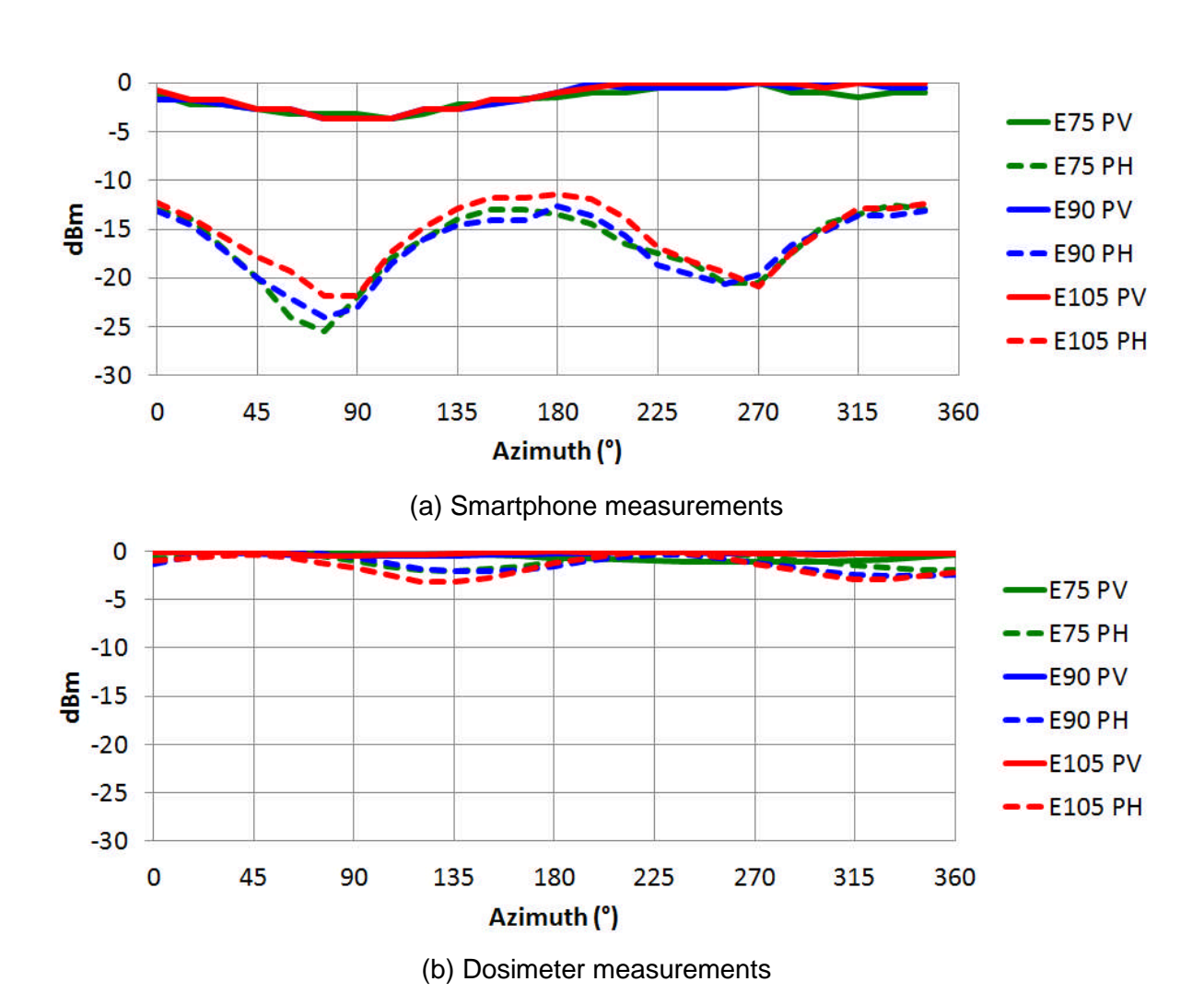
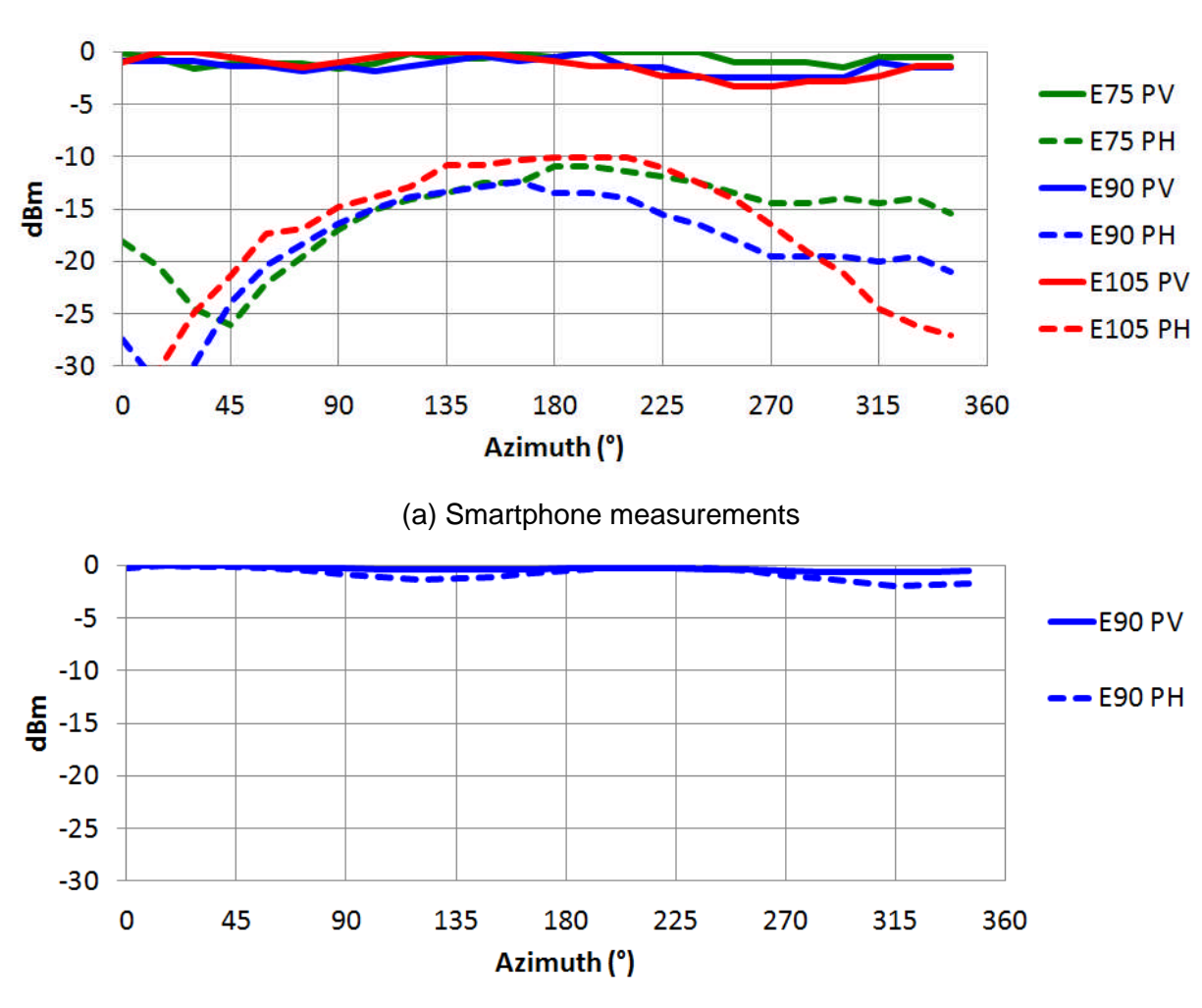


Figure G-3: Isotropy comparison for the smartphone and the EME SPY 200 dosimeter for the LTE-XX DL frequency band.



## **GSM900- DL results**

For the GSM900 standard, the EME SPY isotropy was measured at 90° only.

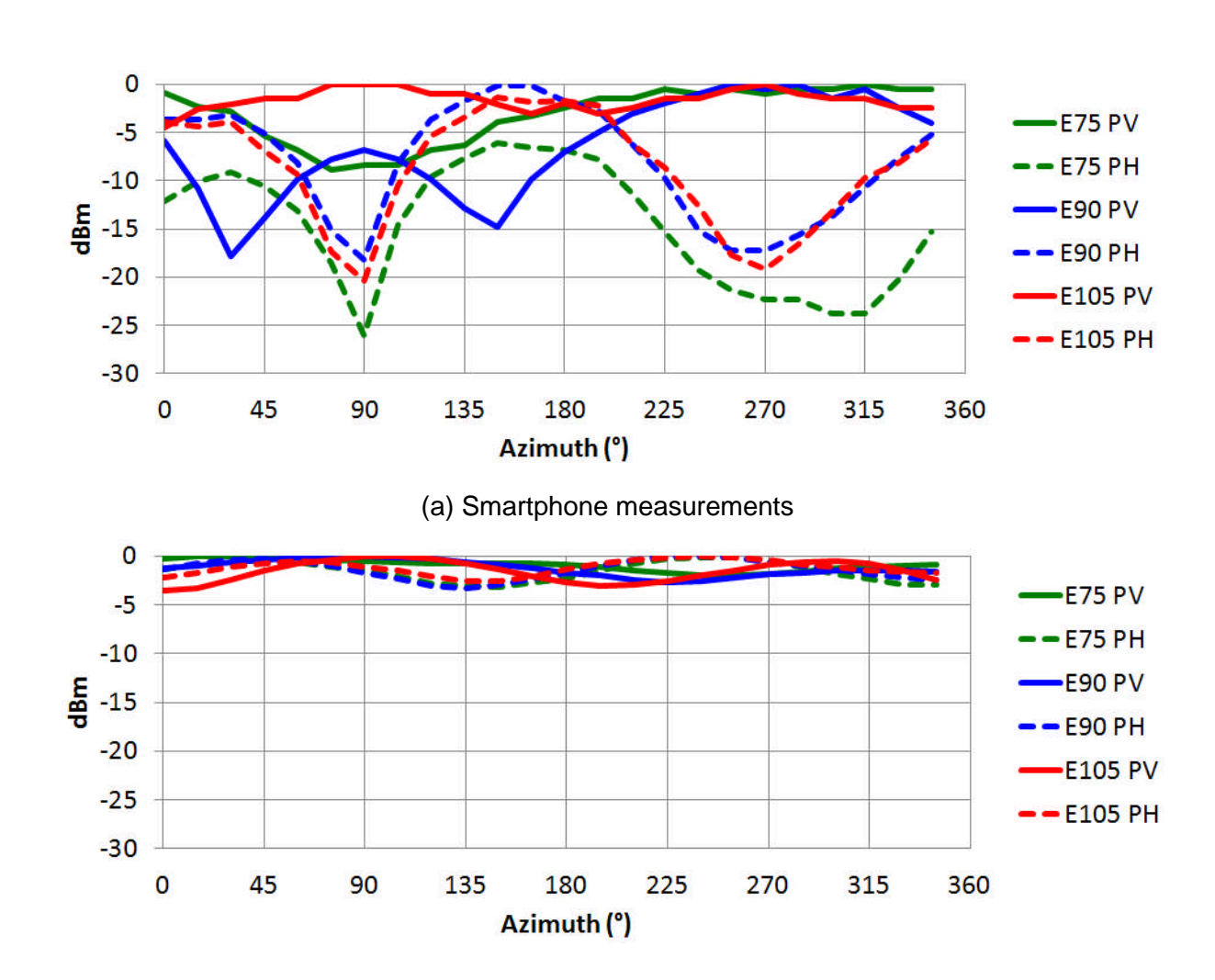


(b) Dosimeter measurements

Figure G-4: Isotropy comparison for the smartphone and the EME SPY 200 dosimeter for the GSM 900 DL frequency band.



## **GSM-1800** results



(b) Dosimeter measurements

Figure G-5: Isotropy comparison for the smartphone and the EME SPY 200 dosimeter for the GSM 1800 DL frequency band.



## **UMTS-2100** results

For the UMTS standard, the EME SPY isotropy was measured at 90° only.

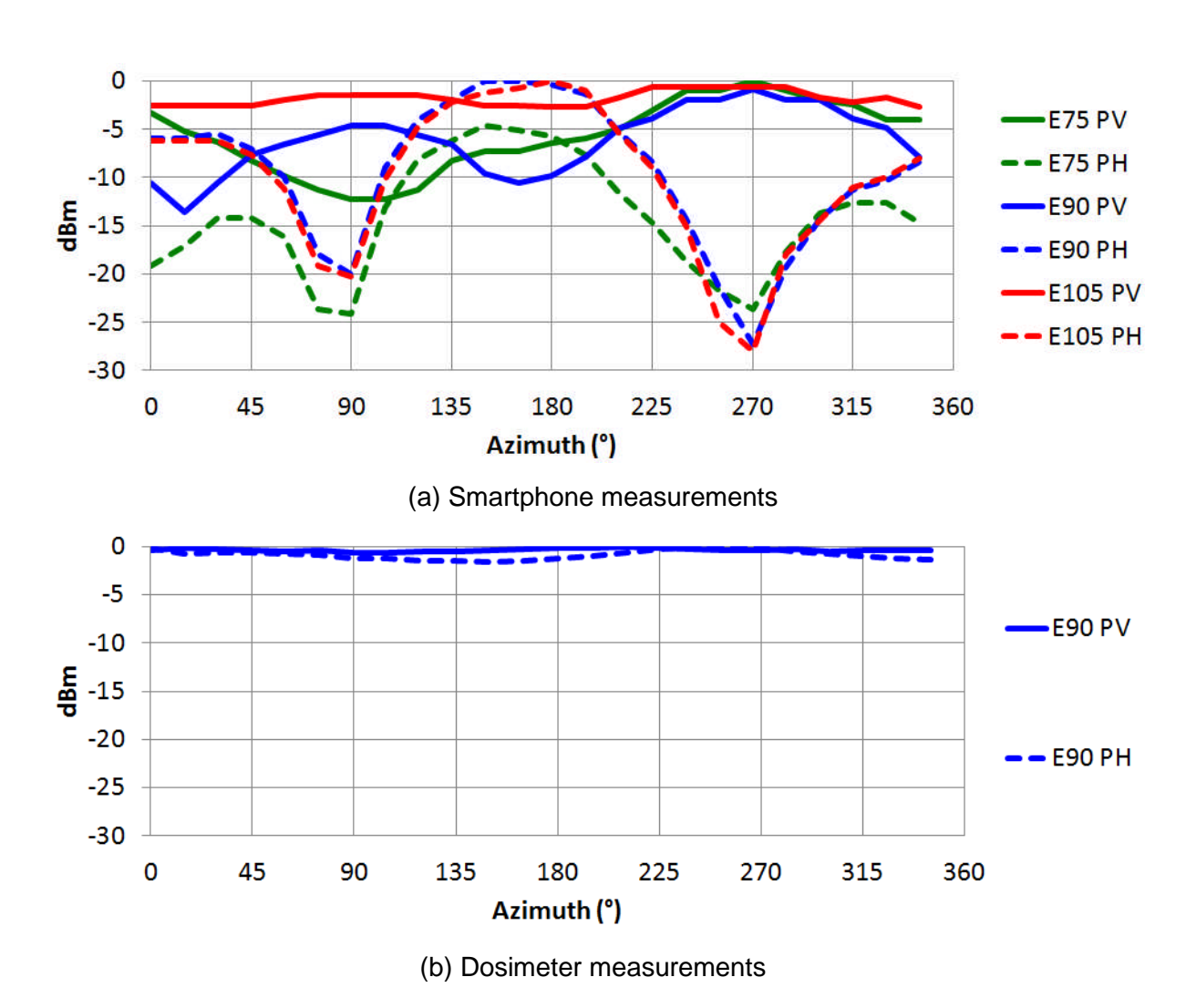


Figure G-6: Isotropy comparison for the smartphone and the EME SPY 200 dosimeter for the UMTS DL frequency band.



## LTE band VII results

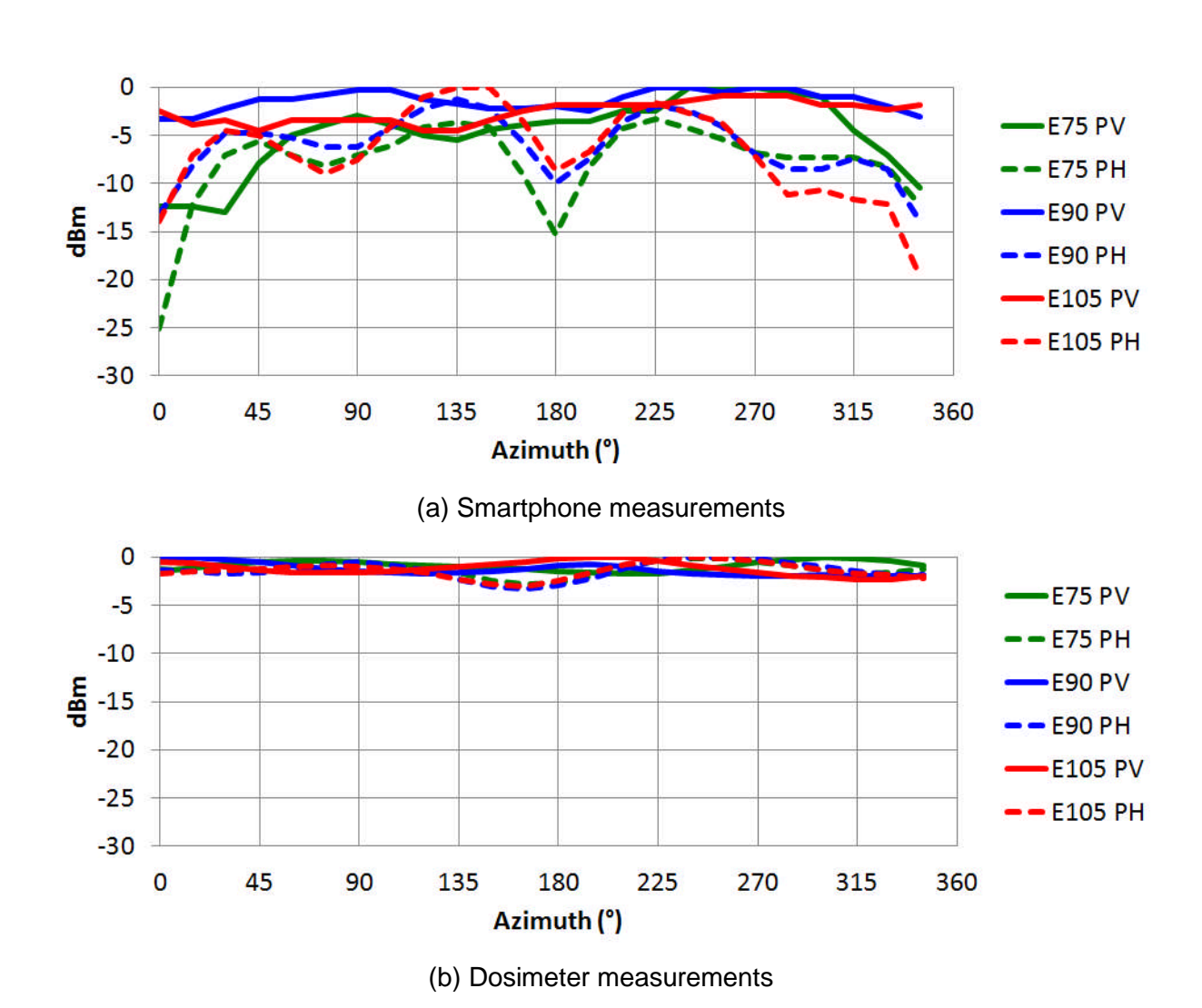


Figure G-7: : Isotropy comparison for the smartphone and the EME SPY 200 dosimeter for the LTE VII DL frequency band.



#### **Conclusions**

The isotropy of a smart phone (Samsung Galaxy S4) and a dosimeter has been compared in this report over an angular aperture of ±15° around the XoY plane using active measurements in the Starmimo setup at Satimo Microwavevision Paris. A tabular comparison is presented below. The isotropy at GSM900-DL and UMTS-DL for the dosimeter was measured at 90° incidence only due to limited time.

Table G-1: Isotropy comparison between a smartphone and an EME SPY 200 dosimeter

	Isotropy (±) dB						
	Dosir	neter	Smartphone (S4)				
Standard	PV	PH	PV	PH			
LTEXX-DL	0.55	1.58	1.85	7.05			
GSM900-DL	0.32 (@90° only)	0.95 (@90° only)	1.66	10.91			
GSM1800-DL	1.79	1.62	8.91	12.98			
UMTS-DL	0.26 (@90° only)	0.77 (@90° only)	6.80	14.00			
LTEVII-DL	1.13	1.62	6.47	12.55			

We can see that the isotropy of the smartphone for vertical polarization incidence not too bad in the lower frequency bands of LTEXX and GSM900 ( $< \pm 2$  dB). A part from that, the isotropy for the smartphone is at best  $\pm 6.5$  dB for the vertical polarization. For the horizontal polarization, the isotropy degrades with frequency and varies between  $\pm 7$  dB at lower frequencies up to  $\pm 14$  dB at higher frequencies. For the dosimeter it remains below  $\pm 1.79$  dB over the entire frequency band.

Hence, we can conclude that if we use a smart device to carry out E-field measurements, the error would be quite considerable and thus the measurements would not be reliable.



# Appendix H UL DUTY CYCLE MEASUREMENTS USING A DOSIMETER.

The objective of this study is to carry out measurements using a customized EME SPY dosimeter and to see whether we can separate the UL and DL signals for the Wi-Fi 2GHz standard which use the same frequency band for both UL and DL signals by using time division duplexing.

For this purpose, an EME SPY 140 dosimeter has been customized so that it can carry out measurements continuously for a single standard on only one probe (vertical probe chosen). This was done in order to see the time domain signal for a given standard (Wi-Fi) during several data cycles (trams). The frequency band for the Wifi standard is from 2400 MHz up to 2483.5 MHz.

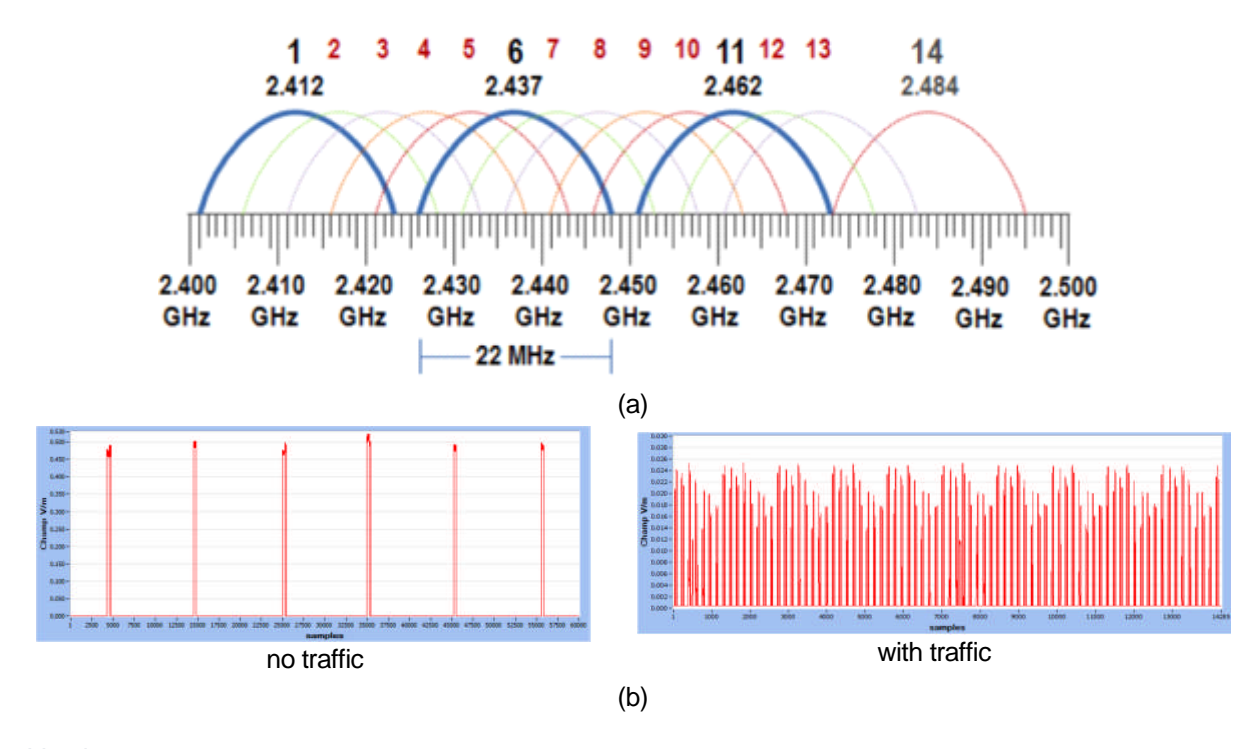
The different parameters for the dosimeter are summarized in the table below.

Table H-1: Dosimeter configuration.

Standard	Sampling period	Tram period	Number of consecutive data trams measured	Total number of samples per tram	Total number of trams measured	Measurement duration
Wi-Fi 2G	62,5 μs	100 msec	3	1600 samples	51	6 minutes

## H.1 Wi-Fi signal characteristics

The Wi-Fi signal is widely deployed for indoor communications. It operates around a central frequency of 2.4GHz and is divided into 14 channels (Figure H-1a below). Each channel has a bandwidth of 22 MHz. By default, the non-overlapping channels (1, 6, and 11) are used. The frequency band extends from 2400 MHz up to 2483.5 MHz. Channel 14 is only used in Japan.



Version 4.0 Dissemination level: PUBLIC



Figure H-1: Wi-Fi characteristics, (a) frequency domain, (b) time domain.

The time domain characteristics of the Wi-Fi signal are shown in Figure H-1 (measured signal). It consists of reference signals emitted by the access points, known as beacons, which are spaced at 100 ms apart (default value which can be modified). These signals carry information regarding the presence of a particular access point and all information regarding the network. The traffic signals (both UL and DL) are distributed between these beacon signals. Another parameter for the Wi-Fi is the duty cycle, it is the ratio of the number of time slots filled between two beacons to the beacon period (100ms by default).

As the same frequency channel is used for both UL and DL transmission, the separation between the two is done in the time domain. Hence, using a frequency domain based measurement device (spectrum analyzer, drive test), we cannot differentiate between the UL and DL signals of a Wi-Fi network. A customized dosimeter can be used to overcome this problem and estimate the two signals.

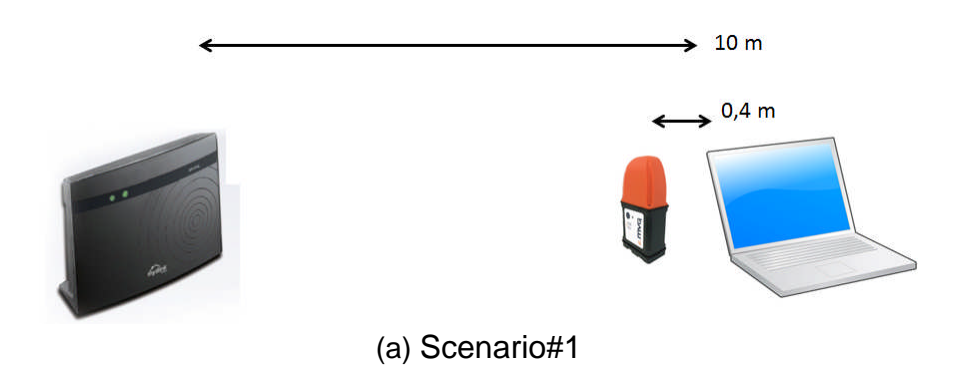
Regarding the transmit power control for a Wi-Fi standard in order to avoid interference in a dense network, no standardization exist. Manual change of transmit power can be applied by the user but no automatic power control scheme exists in the standard for now although several studies have been done [42], [43]. Some devices are starting to appear in the market offering adaptive power management techniques [44].

### H.2 Wi-Fi measurements

Three scenarios were considered in the Wi-Fi measurements.

- i. Scenario#1: Dosimeter placed at 40 cm from the PC on a table and the access point is at about 10m from the PC.
- ii. Scenario#2: Dosimeter placed at 40 cm from the access point and the PC is at about 10m from the access point
- iii. Scenario#3: Dosimeter placed at 3m from the PC on a table and the access point is at about 10m from the PC and about 7m from the dosimeter.

In all the above mentioned scenarios, there is no data traffic. The access point is a dual-band DLINK DIR800L router. The schematic for the three scenarios is shown in Figure H-2.



Version 4.0 Dissemination level: PUBLIC



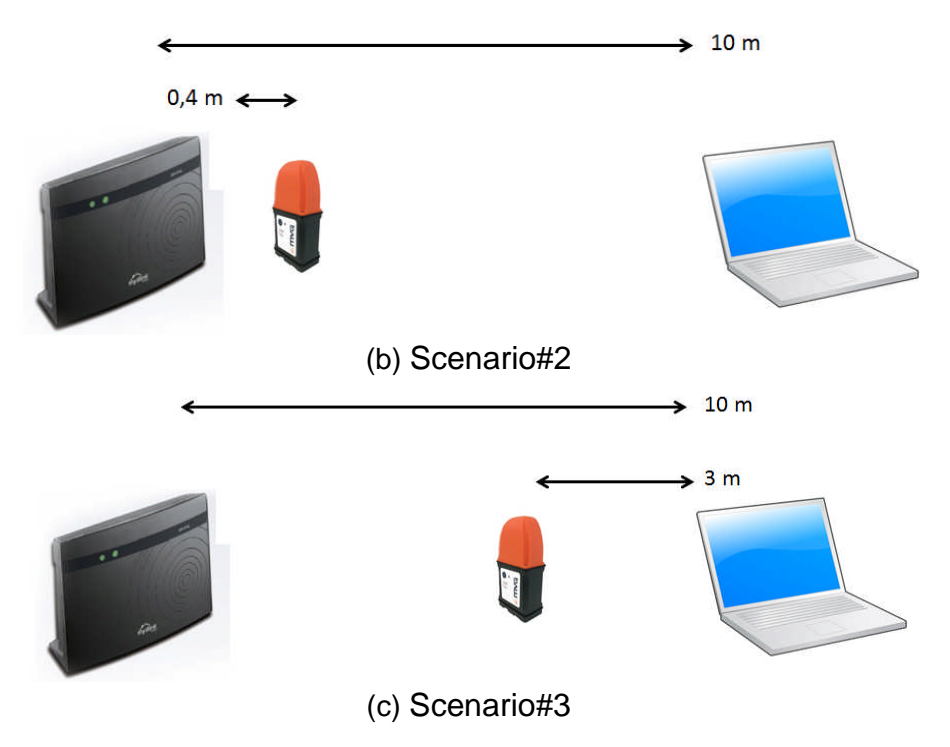
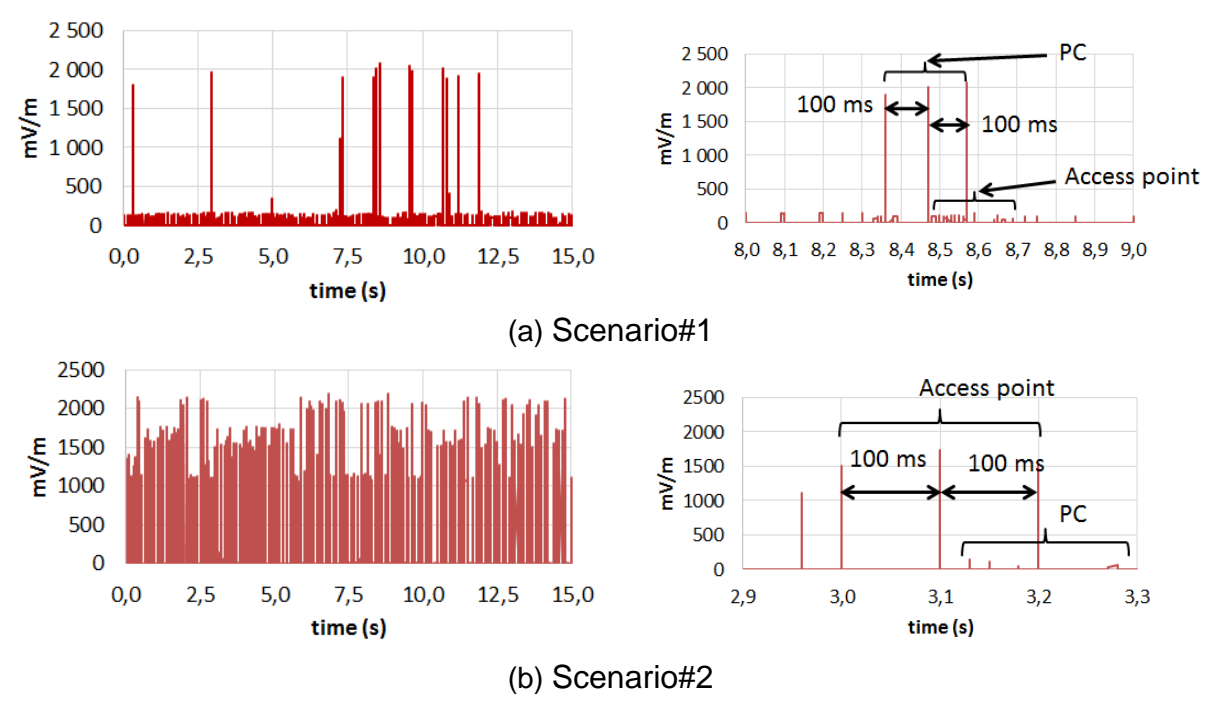


Figure H-2: Wi-Fi measurement setup with different scenarios.

The measurement results for the three scenarios are shown in the figure below. The total measurements presents only 15 seconds out of the 6 minutes measurement cycle. The rest of the time is used for data acquisition, processing, calculations, and storage.





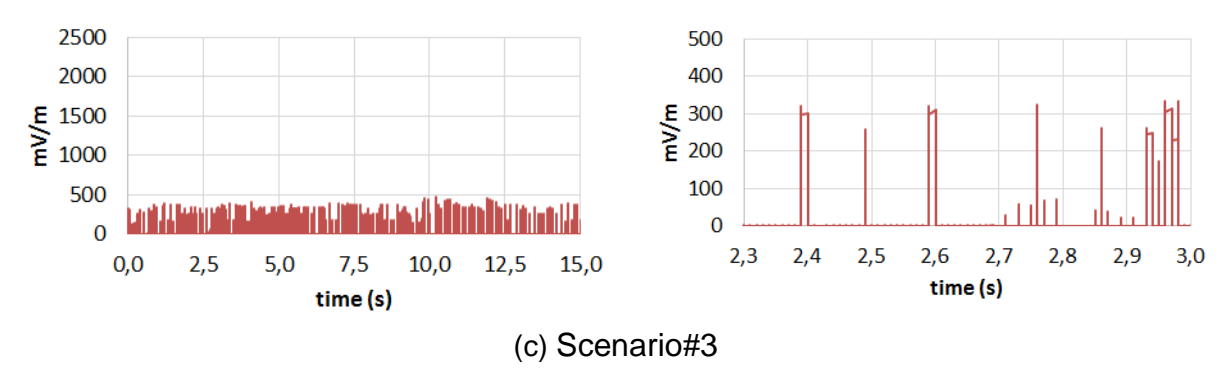


Figure H-3: Wi-Fi measurement results with different scenarios.

The left column in the above figure shows the complete measurements and the right column shows a zoom in the measurement cycle.

The above results show us clearly that if we want to evaluate the UL exposure from a mobile device (PC in this example), we can place the dosimeter close to the device and away from the access point (scenario#1). And by selecting a suitable threshold level we can eliminate all the exposure from the other devices and access points. Thus one can easily obtain the UL power and the duty cycle from dosimeter measurements for Wifi standards.

If the dosimeter is in between the access point and the mobile device (scenario#3), it will not be possible to differentiate between the contribution of the power received from the access point and the mobile device.

## **H.3** Conclusions

The Wi-Fi signals were measured in different scenarios using a customized EMESPY 140 dosimeter. The results show that we can distinguish the UL and DL signals for both standards looking at the raw data by placing the dosimeter close to the device (UL measurements) or the access point (DL measurements).

Version 4.0
Dissemination level: PUBLIC



# Appendix I EXTRAPOLATION OF E-FIELD MEASUREMENTS FROM 6M TO 1.5M.

## I.1 Introduction

The objective of this study is to carry out measurements at different heights using a dosimeter and to evaluate if it is possible to extract an extrapolation factor between these measurements.

For this purpose, an EME SPY 200 dosimeter has been used to carry out a comprehensive measurement campaign at different locations, which represent different scenarios (LOS, NLOS, single BTS, several BTS, urban, rural, campus area). Three frequency bands were monitored as shown in the table below.

Table I-1: Frequencies for the measurement campaign

Standard	Measurement frequency (MHz)
GSM-DL	925-960
DCS-DL	1805-1880
UMTS-DL	2110 - 2170

## I.2 <u>Measurement setup</u>

The measurements were carried out using two dosimeters. One was fixed on a tripod at a height of 1.5m. The other dosimeter was fixed on another mast whose height could vary between 1.7m up to 6m. We fixed the dosimeter on the extendable mast in two different ways; either along the mast or on the top of the mast. The distance between the two measurement locations was 1m.

All measurements have been carried out in the city of Brest, France. Three measurement locations were selected representing three different scenarios.

- i. Location#1: Inside a playing ground representing line of sight (LOS) conditions with little or no reflecting objects around.
- ii. Location#2: In a parking area of a university campus with two BTS (one on each side) with LOS and NLOS (no line of sight) conditions.
- iii. Location#3: In a dense urban area with LOS and NLOS conditions.

The measurement setup at the three locations is presented in the figure below.

Version 4.0
Dissemination level: PUBLIC





(a) Location#1



(b) Location#2



(c) Location#3

Figure I-1: Measurement setup at different locations. The red circle represents the dosimeter location and the antenna icon represents the BTS location on the map. The '1' represents the measurement location for ANFR.

Both dosimeters were synchronized in time. That means that the measurement started at the same time for both dosimeters. The dosimeter on the extendable mast was placed at heights from 6m down to 1m70 passing through 5m, 4m, 3m and 2m measurement heights.

At each height, the average value of 45 points was taken which represented a measurement period of 1min 30 seconds with a measurement cycle of 2seconds.



The diameter of the extendable mast is 6cm and the dosimeter was placed either on the top of the mast or alongside it using a fixation support system (Figure I-2). Several runs were made at the same location (at different times of a day and different days) to see the repeatability of the results.

The results for each frequency band are shown below. The difference in dB is calculated between the measurement location at a given height and the measurement from the dosimeter fixed at 1.5m (shown by the light blue line for each location).

Another difference in dB is also calculated between the measurements at 6m and 1.7m for the same dosimeter on the extendable mast (shown in the column marked by "difference 6m/1m70"). This difference also includes the time variation of the E-field because the measurements were done successively at these two points with a difference of about 13 minutes between the two measurements. The last column shows the variation of the measurements at the between the fixed (1.5m) and the extendable dosimeter (at 1.7m) height who are 1m apart to show the spatial variation of the E-field.





Figure I-2: (a) Dosimeter placed on top of the mast, (b) along-side the mast.



## I.3 **GSM-DL results**

The measurements for location#2 (day1) were erroneous and were discarded.

Table I-2: Measurement results for GSM-DL signal at the three locations

						22	E-field (	V/m)	0.	0)	difference	variation				
meas location	date	Test	ID	Dosimeter	6m	5m	4m	3m	2m	1m70	6m / 1m70	1m70 /				
				Mark	0.20	0.44	0,44	0.50	0.57	0.40		1m50				
17	17/06/2014	Run#1	L1-J1-R1	Mast	0,29	0,44	20000000	0,53	0,57	0,48	-4,23	-0,32				
	17/00/2014	Kulimi	LITTINI	fixed @ 1m50	0,51	0,52	0,50	0,51	0,46	0,49	-4,23	-0,32				
				Difference (dB)	-4,86	-1,32	-1,25	0,28	1,86	-0,32						
	17/06/2014	D#2	14 14 00	Mast	0,22	0,42	0,40	0,42	0,50	0,53	7.00	5,41				
location #1	17/06/2014	Run#2	L1-J1-R2	fixed @ 1m50 Difference (dB)	0,27 -1,67	0,27 3,74	0,28 3,11	0,27 3,75	4,74	0,28 5,41	-7,60	5,41				
(petite kerzu)	7			Mast Mast	0,27	0,31	0,38	0,53	0,32	0,36						
LOS conditions	17/06/2014	Run#3	L1-J1-R3	fixed @ 1m50	0,38	0,31	0,36	0,37	0,32	0,30	-2,72	-1,01				
playing ground with little	17/00/2014	, nams		Difference (dB)	-3,01	-1,88	0,41	3,13	-1,36	-1,01	2,72	1,01				
reflecting objects				Mast	0,58	0,27	0,37	0,33	0,26	0,18						
renecting objects	23/06/2014	Run#1 : dosimeter	L1-J2-R4-top	fixed @ 1m50	0,81	0,80	0,79	0,77	0,78	0,78	10,17	-12,68				
		on top of mast	5.0	Difference (dB)	-2,85	-9,31	-6,46	-7,41	-9,39	-12,68	S 00	161				
		Run#2: dosimeter		Mast	0,51	0,36	0,39	0,25	0,22	0,20						
	23/06/2014	attached along	L1-J2-R5-	fixed @ 1m50	0,82	0,78	0,79	0,80	0,80	0,76	8,25	-11,75				
		the mast	side	Difference (dB)	-4,17	-6,81	-6,07	-9,99	-11,28	-11,75						
		Duntti e de simetar		Mast												
	19/06/2014	Run#1 : dosimeter on top of mast	L2-J1-R1-top	fixed @ 1m50												
		on top or mast		Difference (dB)	#DIV/0!	#DIV/0!	#DIV/0!	#DIV/0!	#DIV/0!	#DIV/0!						
		Run#2: dosimeter	L2-J1-R2-	Mast												
	19/06/2014	attached along	side	fixed @ 1m50												
AUTO-POPULATION AND DESCRIPTION AND DESCRIPTIO		the mast	side	Difference (dB)	#DIV/0!	#DIV/0!	#DIV/0!	#DIV/0!	#DIV/0!	#DIV/0!						
location #2		Run#1 : dosimeter		Mast	0,22	0,15	0,14	0,12	0,08	0,16	8					
(parking ENIB)	25/06/2014	on top of mast	L2-J2-R3-top	fixed @ 1m50	0,81	0,79	0,88	0,86	0,87	0,84	2,90	-14,40				
LOS / NLOS		A. O. O. A.		Difference (dB)	-11,13	-14,65	-15,93	-17,41	-20,54	-14,40						
conditions		Run#2: dosimeter	L2-J1-R4- side	Mast	1,85	1,17	1,10	0,95	0,92	1,64	/ secondary	1000000000				
University	25/06/2014	attached along		fixed @ 1m50	0,15	0,16	0,14	0,14	0,13	0,14	1,06	21,26				
campus area		the mast	1	Difference (dB)	22,09	17,40	18,11	16,58	17,05	21,26						
	25/06/2014	Run#3 : dosimeter	L2-J2-R5-top	Mast	1,35	0,98	0,90	0,72	0,55	0,98	2,79	10.76				
		on top of mast		fixed @ 1m50	0,12 21,24	0,11	0,12	0,13 15,19	0,11	0,11		18,76				
		Run#4: dosimeter		Difference (dB) Mast	0,30	18,82 0,19	17,56 0,19	0,15	14,03 0,16	18,76 0,29						
	25/06/2014	attached along L2-J1-	L2-J1-R6-	fixed @ 1m50	0,84	0,13	0,13	0,13	0,76	0,73	0,43	-8,01				
	25/00/2014	the mast	side	Difference (dB)	-8,88	-12,21	-12,18	-14,31	-13,56	-8,01	0,43	-0,01				
				Mast	0,34	0,23	0,19	0,14	0,13	0,12						
	19/06/2014	Run#1 : dosimeter on top of mast		Run#1 : dosimeter on top of mast		L3-J1-R1-top	fixed @ 1m50	0,07	0,07	0,07	0,07	0,07	0,07	8,93	5,25	
						on top of mast	25 52 112 100	Difference (dB)	13,70	9,99	8,38	5,99				
		Run#2: dosimeter		Mast	0,46	0,34	0,21	0,20	0,17	0,11						
	19/06/2014	attached along	L3-J1-R2-	fixed @ 1m50	0,07	0,07	0,07	0,07	0,07	0,07	12,73	3,67				
		the mast	side	Difference (dB)	16,56	13,32	9,18	8,89	7,67	3,67		•				
				Mast	0,33	0,22	0,16	0,14	0,12	0,12						
	19/06/2014	Run#3 : dosimeter	L3-J1-R3-top	fixed @ 1m50	0,07	0,07	0,07	0,07	0,07	0,07	9,04	4,37				
		on top of mast		Difference (dB)	13,41	9,80	7,32	5,83	4,79	4,37	1					
location #3 (franc		Run#4: dosimeter	L3-J1-R4-	Mast	0,37	0,25	0,16	0,15	0,15	0,12						
tireurs)	19/06/2014	attached along	side	fixed @ 1m50	0,07	0,07	0,07	0,07	0,07	0,07	9,74	5,29				
LOS / NLOS		the mast	Side	Difference (dB)	14,38	10,66	6,64	6,29	6,41	5,29						
conditions		Run#5 : dosimeter		Mast	0,22	0,17	0,13	0,10	0,10	0,11						
dense urban area	25/06/2014	on top of mast	L3-J1-R5-top	fixed @ 1m50	0,36	0,34	0,35	0,32	0,34	0,34	6,29	-10,01				
				Difference (dB)	-4,16	-5,93	-8,54	-10,35	-11,03	-10,01						
		Run#6 : dosimeter	L3-J1-R6-	Mast	0,24	0,17	0,13	0,08	0,09	0,11						
	25/06/2014	on top of mast	side	fixed @ 1m50	0,35	0,34	0,34	0,35	0,35	0,35	7,04	-10,33				
				Difference (dB)	-3,22	-5,94	-8,73	-12,20	-11,82	-10,33						
	05/05/55	Run#7 : dosimeter		Mast	1,24	0,95	0,71	0,49	0,54	0,59						
	25/06/2014	on top of mast	L3-J1-R7-top	fixed @ 1m50	0,06	0,06	0,06	0,05	0,06	0,05	6,47	20,97				
		·		Difference (dB)	26,81	24,52	22,21	19,09	19,73	20,97						
	05/05/00	Run#8: dosimeter	L3-J1-R8-	Mast	1,91	1,37	0,93	0,76	0,88	1,00						
	25/06/2014	attached along	side	fixed @ 1m50	0,06	0,05	0,06	0,06	0,06	0,06	5,58	25,11				
		the mast		Difference (dB)	30,47	27,93	24,41	22,25	23,84	25,11						



## **DCS-DL** results

Table I-3: Measurement results for DCS-DL signal at the three locations.

						E-field (	V/m)		. 1	difference	variation
meas location	date	Test	Dosimeter	6m	5m	4m	3m	2m	1m70	6m / 1m70	1m70 / 1m50
			Mast	0,33	0,32	0,31	0,26	0,26	0,24		(fixed)
17/06/2	17/06/2014	Run#1	10000000						1780000	2,96	-1,21
			fixed @ 1m50	0,27	0,28	0,27	0,28	0,28	0,27		
	2		Difference (dB) Mast	1,79 0,34	1,19 0,29	1,23 0,34	-0,48 0,25	-0,68 0,27	-1,21 0,24		×
location #1	17/06/2014	Run#2	fixed @ 1m50	0,34	0,25	0,34	0,29	0,27	0,24	3,30	-0,61
(petite kerzu)	17/00/2014	Nullifiz	Difference (dB)	2,75	1,06	1,51	-1,55	-0,73	-0,61	3,30	-0,01
LOS conditions		-	Mast	0,22	0,24	0,27	0,26	0,22	0,24		
playing ground	17/06/2014	Run#3	fixed @ 1m50	0,31	0,29	0,30	0,29	0,31	0,29	-0,78	-1,51
with little	27/00/2021	, manua	Difference (dB)	-2,77	-1,67	-0,78	-0,92	-3,25	-1,51		
reflecting		Run#1:	Mast	0,27	0,24	0,23	0,22	0,26	0,21		8
objects	23/06/2014	dosimeter on	fixed @ 1m50	0,87	0,86	0,84	0,87	0,81	0,84	1,99	-11,97
	EV 35	top of mast	Difference (dB)	-10,25	-11,29	-11,23	-11,94	-9,96	-11,97	(2)	98
		Run#2:	Mast	0,25	0,24	0,21	0,23	0,26	0,22		(5
	23/06/2014	dosimeter	fixed @ 1m50	0,89	0,80	0,89	0,84	0,84	0,90	1,28	-12,35
		attached along	Difference (dB)	-11,05	-10,62	-12,42	-11,35	-10,20	-12,35		
		Run#1:	Mast	0,11	0,09	0,09	0,17	0,12	0,15		
	19/06/2014	dosimeter on	fixed @ 1m50	0,38	0,38	0,38	0,42	0,42	0,41	-2,66	-8,63
	58530.87238550.0	top of mast	Difference (dB)	-10,62	-12,88	-12,68	-8,10	-11,16	-8,63		575(MRT=3
		Run#2:	Mast	0,22	0,24	0,15	0,18	0,10	0,12	5,26	-7,57
	19/06/2014	dosimeter	fixed @ 1m50	0,31	0,33	0,31	0,31	0,32	0,29		
	5	attached along	Difference (dB)	-2,86	-2,58	-6,49	-4,68	-10,56	-7,57		
location #2	200 200	Run#1:	Mast	0,29	0,21	0,14	0,16	0,19	0,24		
(parking ENIB)	25/06/2014	dosimeter on	fixed @ 1m50	1,80	1,87	1,82	1,93	1,97	1,89	1,51	-17,83
LOS / NLOS		top of mast	Difference (dB)	-15,88	-18,89	-22,09	-21,48	-20,26	-17,83		
conditions	25/06/2014	Run#2:	Mast	1,73	1,87	2,07	1,56	0,68	2,36		
University		dosimeter	fixed @ 1m50	0,32	0,31	0,34	0,39	0,41	0,37	-2,67	16,11
campus area		attached along	Difference (dB)	14,64	15,69	15,60	12,07	4,25	16,11		
	25/06/2014	Run#3:	Mast	2,22	1,36	1,40	1,14	1,16	1,86	1,55	
		dosimeter on	fixed @ 1m50	0,44	0,37	0,36	0,37	0,39	0,38		13,78
		top of mast	Difference (dB)	14,12	11,22	11,70	9,84	9,50	13,78		
	/ /	Run#4:	Mast	0,21	0,40	0,33	0,24	0,13	0,41	-5,69	
	25/06/2014	dosimeter	fixed @ 1m50	2,71	2,73	2,66	2,42	2,48	2,60		-15,98
		attached along	Difference (dB)	-22,03	-16,62	-18,02	-20,23	-25,37	-15,98		
	10/05/2014	Run#1:	Mast	0,50	0,44	0,32	0,19	0,15	0,13		0.07
	19/06/2014	dosimeter on	fixed @ 1m50	0,14	0,13	0,14	0,14	0,14	0,13	11,69	0,07
		top of mast	Difference (dB)	11,40	10,38	7,38	2,68	0,65	0,07		
	10/05/2014	Run#2:	Mast	0,35	0,30	0,21	0,15	0,11	0,12	0.03	0.22
	19/06/2014	dosimeter	fixed @ 1m50	0,12	0,12	0,12	0,12	0,13	0,13	8,93	-0,23
		attached along Run#3:	Difference (dB) Mast	8,92	7,73	4,76	1,72	-0,95 0.15	-0,23		
	19/06/2014	dosimeter on	fixed @ 1m50	0,53 0,13	0,50 0,14	0,30 0,13	0,20	0,15 0,13	0,13 0,13	12,05	-0,03
	13/00/2014	top of mast	Difference (dB)	12,05	11,32	7,62	4,26	1,16	-0,03	12,00	0,03
location #3		Run#4:	Mast	0,37	0,33	0,23	0,17	0,14	0,15		
(franc tireurs)	19/06/2014	dosimeter	fixed @ 1m50	0,37	0,33	0,23	0,17	0,14	0,13	7,69	2,08
LOS / NLOS	15/00/2014	attached along	Difference (dB)	9,95	8,66	5,94	3,35	1,39	2,08	,,03	2,00
conditions		Run#5:	Mast	0,47	0,43	0,31	0,25	0,15	0,13		
dense urban	25/06/2014	dosimeter on	fixed @ 1m50	0,62	0,43	0,64	0,63	0,63	0,62	11,38	-13,76
area	,,	top of mast	Difference (dB)	-2,32	-2,91	-6,37	-8,02	-12,56	-13,76	,_,	
		Run#6:	Mast	0,48	0,41	0,30	0,23	0,13	0,13		
	25/06/2014	dosimeter on	fixed @ 1m50	0,61	0,60	0,59	0,60	0,61	0,60	11,71	-13,58
		top of mast	Difference (dB)	-1,94	-3,33	-5,98	-8,27	-13,53	-13,58	1 '	
		Run#7:	Mast	2,91	2,74	1,82	1,47	0,91	0,81		
	25/06/2014	dosimeter on	fixed @ 1m50	0,10	0,10	0,09	0,10	0,10	0,09	11,16	18,66
		top of mast	Difference (dB)	29,57	29,17	25,80	23,67	19,63	18,66	1	-,
		Run#8:	Mast	2,39	1,81	1,68	1,05	0,82	0,77		
	25/06/2014	dosimeter	fixed @ 1m50	0,10	0,10	0,10	0,10	0,10	0,09	9,88	18,16
	.,,	attached along	Difference (dB)	27,60	25,53	24,80	20,04	18,56	18,16	1 -,	



## I.4 <u>UMTS-DL results</u>

Table I-4: Measurement results for UMTS-DL signal at the three locations

						E-field (	V/m)			difference	variation 1m70 /
meas location	date	Test	Dosimeter	6m	5m	4m	3m	2m	1m70	6m / 1m70	1m50 (fixed)
			Mast	0,23	0,22	0,23	0,21	0,19	0,16		
	17/06/2014	Run#1	fixed @ 1m50	0,17	0,17	0,17	0,16	0,16	0,18	3,00	-0,80
			Difference (dB)	2,65	2,26	2,97	2,01	1,54	-0,80		
			Mast	0,23	0,26	0,27	0,25	0,19	0,13		
location #1 (petite	17/06/2014	Run#2	fixed @ 1m50	0,16	0,19	0,18	0,16	0,16	0,16	4,89	-1,55
kerzu)	2003 1000		Difference (dB)	3,15	2,95	3,61	3,71	1,71	-1,55	22	22
LOS conditions			Mast	0,17	0,17	0,18	0,20	0,21	0,16		
playing ground	17/06/2014	Run#3	fixed @ 1m50	0,16	0,16	0,16	0,15	0,16	0,16	0,50	0,26
with little			Difference (dB)	0,45	0,36	1,02	2,41	2,47	0,26		
reflecting objects		Run#1: dosimeter	Mast	0,30	0,24	0,22	0,21	0,20	0,16	200000	
WALLES CAN DE SAN BUSINESS	23/06/2014	on top of mast	fixed @ 1m50	1,01	0,96	1,03	1,02	1,02	1,03	5,55	-16,13
			Difference (dB)	-10,41	-12,18	-13,25	-13,74	-14,06	-16,13		
		Run#2: dosimeter	Mast	0,28	0,26	0,21	0,19	0,17	0,15		
	23/06/2014	attached along	fixed @ 1m50	1,00	0,99	0,97	0,99	0,99	0,97	5,21	-16,09
		the mast	Difference (dB)	-11,16	-11,62	-13,40	-14,32	-15,34	-16,09		
	2. 2	Run#1: dosimeter	Mast	0,11	0,09	0,10	0,06	0,08	0,07	.	
	19/06/2014	on top of mast	fixed @ 1m50	0,12	0,12	0,12	0,11	0,12	0,12	4,23	-4,48
			Difference (dB)	-0,73	-3,08	-1,12	-4,92	-3,75	-4,48		
		Run#2: dosimeter	Mast	0,15	0,09	0,08	0,08	0,11	0,10	**********	
	19/06/2014	attached along	fixed @ 1m50	0,08	0,09	0,08	0,09	0,09	0,08	3,68	1,14
		the mast	Difference (dB)	4,80	0,70	-0,18	-1,02	2,44	1,14		
location #2		Run#1: dosimeter	Mast	0,17	0,21	0,13	0,12	0,12	0,14		
(parking ENIB)	25/06/2014	5/06/2014 on top of mast	fixed @ 1m50	0,73	0,74	0,80	0,83	0,76	0,79	1,33	-14,68
LOS / NLOS			Difference (dB)	-12,67	-11,06	-16,00	-16,95	-15,65	-14,68		
area		Run#2: dosimeter	Mast	1,58	1,72	0,85	0,78	1,29	1,39		
	25/06/2014	attached along	fixed @ 1m50	0,14	0,14	0,14	0,14	0,15	0,15		19,39
		the mast	Difference (dB)	20,89	21,48	15,42	14,73	18,85	19,39		
		Run#3 : dosimeter on top of mast	Mast	0,96	1,02	0,81	0,81	0,70	0,88	0,73	15,55
	25/06/2014		fixed @ 1m50	0,14	0,15	0,14	0,14	0,14	0,15		
			Difference (dB)	16,45	16,52	15,05	15,17	14,09	15,55		
		Run#4: dosimeter	Mast	0,34	0,37	0,14	0,13	0,24	0,26		
		attached along	fixed @ 1m50	0,80	0,80	0,79	0,78	0,77	0,86	2,40	-10,50
		the mast	Difference (dB)	-7,51	-6,68	-15,22	-15,28	-10,26	-10,50		
		Run#1: dosimeter	Mast	0,24	0,22	0,15	0,10	0,14	0,09		
	19/06/2014	on top of mast	fixed @ 1m50	0,09	0,08	0,08	0,08	0,09	0,09	8,29	0,34
			Difference (dB)	8,82	9,02	6,15	2,57	3,94	0,34		
		Run#2: dosimeter	Mast	0,21	0,18	0,13	0,10	0,10	0,06		
	19/06/2014	attached along	fixed @ 1m50	0,08	0,08	0,08	0,07	0,07	0,07	10,58	-0,68
		the mast	Difference (dB)	8,08	7,63	4,48	2,46	2,40	-0,68		
	40/05/0044	Run#3: dosimeter	Mast	0,21	0,21	0,16	0,10	0,10	0,07		
	19/06/2014	on top of mast	fixed @ 1m50	0,07	0,08	0,07	0,07	0,07	0,08	9,28	-0,58
			Difference (dB)	9,33	8,38	6,81	2,86	2,74	-0,58		
location #3 (franc		Run#4: dosimeter	Mast	0,25	0,25	0,17	0,11	0,12	0,10		
tireurs)	19/06/2014	attached along	fixed @ 1m50	0,07	0,07	0,07	0,07	0,07	0,08	8,01	2,26
LOS / NLOS		the mast	Difference (dB)	10,83	11,04	7,50	3,69	4,78	2,26		
conditions	25 /06 /2011	Run#5 : dosimeter	Mast	0,39	0,30	0,22	0,12	0,09	0,09	12.40	16.00
dense urban area	25/06/2014	on top of mast	fixed @ 1m50	0,66	0,58	0,63	0,55	0,58	0,61	12,40	-16,38
and a ca			Difference (dB)	-4,73	-5,72	-8,92	-13,61	-15,90	-16,38		
	25 /05 /2011	Run#6: dosimeter	Mast	0,31	0,29	0,19	0,11	0,09	0,09	10.54	17.40
	25/06/2014	on top of mast	fixed @ 1m50	0,57	0,57	0,60	0,57	0,56	0,68	10,61	-17,40
			Difference (dB)	-5,25	-5,68	-10,11	-13,91	-15,68	-17,40		
	25/25/224	Run#7 : dosimeter	Mast	1,61	1,47	0,92	0,59	0,43	0,43	,, .,	40.00
	25/06/2014	on top of mast	fixed @ 1m50	0,11	0,11	0,11	0,12	0,11	0,10	11,46	12,29
			Difference (dB)	23,28	22,31	18,19	13,95	12,08	12,29		
		Run#8: dosimeter	Mast	1,32	1,16	0,84	0,54	0,39	0,45		
	25/06/2014	attached along	fixed @ 1m50	0,14	0,12	0,13	0,12	0,11	0,12	9,32	11,62
		the mast	Difference (dB)	19,76	19,71	16,40	13,32	10,72	11,62		



## I.5 Conclusions

We can see from the above results that there is no clear extrapolation factor observed from the measurements at 6m height and 1.7m or 1.5m height. The results provide a wide dispersion for each frequency band.

To conclude we have observed no co-relation between measurements at different heights. The principal reason is that the fixed point measurements suffer from fading and no spatial averaging was done to eliminate this fading. This is a preliminary study and it will be extended to a more comprehensive measurement campaign concentrating on the Smart Santander test bench. The work will be carried out in WP6.

Version 4.0



# **Appendix J** ESTIMATION OF EMF FROM PERSONAL AND FIXED POINT DOSIMETERS.

## J.1 Introduction

An important task is to develop a methodology to assess the exposure data obtained from personal and fixed point dosimeters. Obviously, due to body shadowing, the exposure data obtained from personal dosimeter will be different depending on the on-body placement. Moreover, the temporal variation and correlation between exposure data obtained from personal and fixed point dosimeters should be analysed. Accordingly, this section presents a study aiming to assess the impact of the body shadowing on the wearable dosimeter EMF measurements.

When modelling the radio link between the dosimeter located on the body and the base station, one considers the influence of the body (*i.e.*, body coupling, [24], and body movements, [25]), and accounts for the propagation environment using a geometrically based statistical channel (GBSC) model (*i.e.*, multipath propagation). Therefore, the modelling of the radio channel has been separated into several steps, as described in [45], Figure J-1.

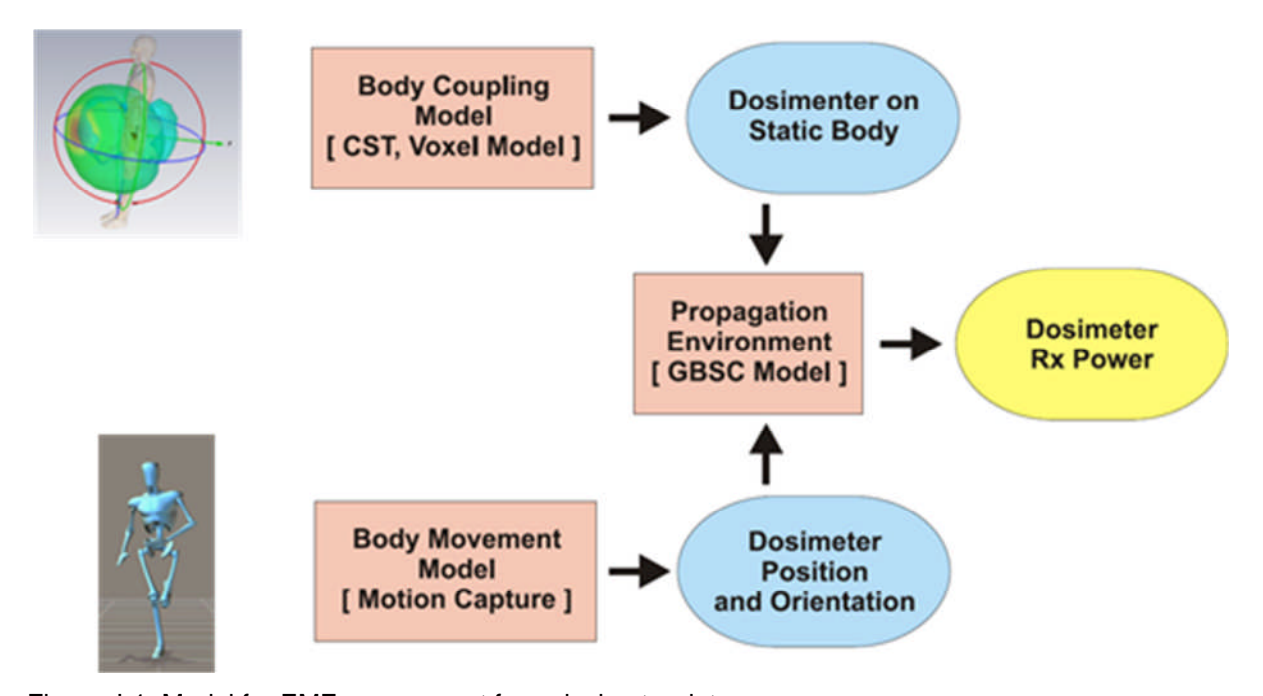


Figure J-1: Model for EMF assessment from dosimeter data.

For the downlink, the received (Rx) power,  $P_{Rx}$ , at the mobile terminal (or dosimeter) is calculated from:

$$P_{Rx_{[dBm]}} = P_{BS_{[dBm]}} - L_{total_{[dB]}}$$
 (J-1)

where:

- *P<sub>BS</sub>*: base station (BS) transmitted (Tx) power,
- L<sub>total</sub>L<sub>total</sub>: total path loss including gains of mobile terminal (or dosimeter) and BS.

Version 4.0 Dissemination level: PUBLIC



The received power density,  $S_{Rx}$ , at the mobile terminal (or dosimeter) is calculated from:

$$S_{Rx[W/m^2]} = \frac{P_{Rx[W]}}{A_{eff_{[m^2]}}}$$
 (J-2)

where  $A_{eff}$  is the mobile terminal antenna effective area:

$$A_{eff[m^2]} = \frac{\lambda^2_{[m]}}{4\pi} \overline{G_{Rx_{[dB_1]}}}$$
 (J-3)

where:

- λ: wavelength,
- $\overline{G_{Rx}}$ : average gain of the receiving antenna (*i.e.*, dosimeter probe) in off body direction (*e.g.*, half-hemisphere of the gain pattern, *i.e.*,  $\theta \in [-90,90]^{\circ}$  and  $\varphi \in [-90,90]^{\circ}$ ):

$$\overline{G_{Rx_{[dBi]}}} = \frac{1}{N_{\theta}N_{\varphi}} \sum_{n=1}^{N_{\theta}} \sum_{m=1}^{N_{\varphi}} G_{Rx_{[dBi]}}(\theta_n, \varphi_m)$$
(J-1)

where:

•  $N_{\theta}$  and  $N_{\varphi}N_{\varphi}$ : number of elevation ( $\theta$ ) and azimuth ( $\varphi$ ) directions.

The correlation,  $\rho$ , of the Rx power densities obtained from two dosimeters is the envelope correlation. To calculate  $\rho$ , the signals are initially aligned (shifted) in time, through the cross-correlation function [46], so that the maximum value is obtained. For the case of the case of the on-body dosimeters and the reference isotropic probe, one has:

$$\left(S_{Rx}^{dosim} * S_{Rx}^{isotr}\right)(\tau) = \int_{-\infty}^{\infty} S_{Rx}^{dosim}(t) S_{Rx}^{isotr}(\tau + t) dt \tag{J-1}$$

then,  $\rho$  is computed by:

$$\rho = \max(\left(S_{Rx}^{dosim} * S_{Rx}^{isotr}\right)(\tau)) \tag{J-1}$$

The ratio, R, between the Rx power densities obtained from different on-body dosimeters is calculated as:

$$R = \frac{S_{Rx[W/m^2]}^{dosim A}}{S_{Rx[W/m^2]}^{dosim B}}$$
(J-1)

The simulated scenarios consider a reference isotropic dosimeter on the head of the user (simulating the real body exposure), together with five wearable dosimeters, as depicted in Figure J-2.

A macro cell outdoor street scenario has been considered, including a set of 10 clusters, of 3 scatterers each, with a Uniform Distribution in the half space of an ellipsoid. A 3-sector base station antenna is located in the middle of the street, at x=100 m. In Figure J-3(a), the user is moving on a straight line, in the middle of the



street (i.e., y=10 m,  $x \in [50, 150]$  m), while in Figure J-3(b), a loop movement is considered.

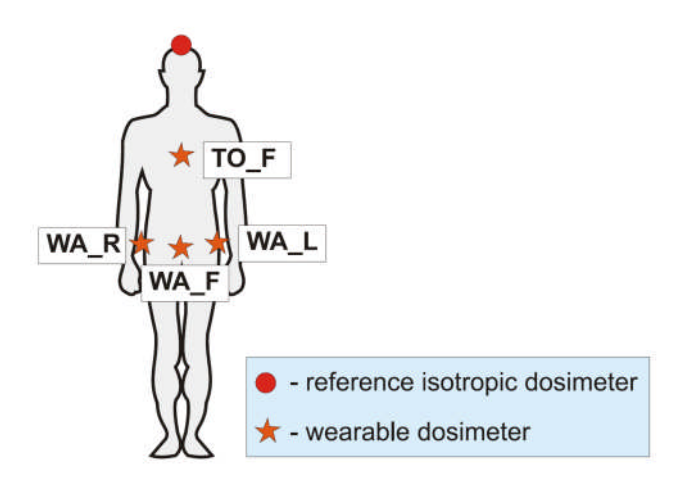


Figure J-2: Placement of wearable dosimeters on the body.

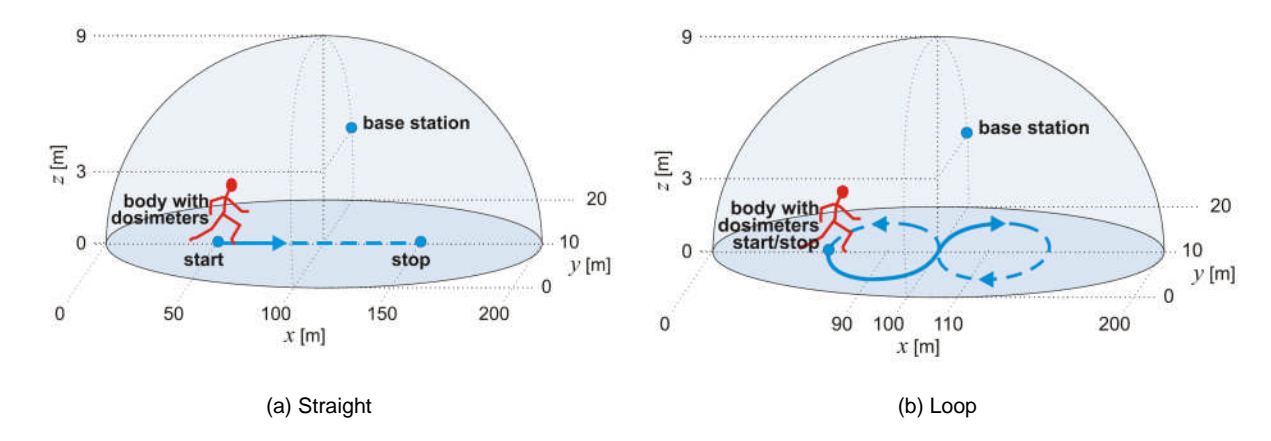


Figure J-3: Scenarios.

Figure J-4 illustrates the considered macro cell base station antenna and the dosimeter realised gain patterns.

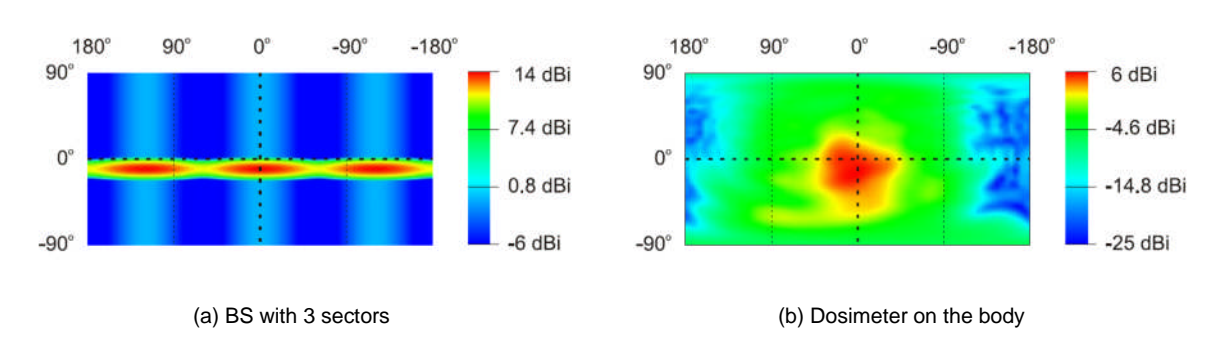


Figure J-4: Realised gain pattern.

The parameters of the scenario are presented in Table J-1.



Table J-1: Scenario overview.

System	Frequency [MHz]	2600	Reference
	EIRP [dBm]	46	[47]
BS	Number of sectors	3	
	Tilt [ º]	10	
Dosimeter	$\overline{G}_{\mathrm{Rx}}\overline{G_{Rx}}$ [dBi]	1.22	[23]

## J.2 Results for scenario "Straight"

The average Rx power density obtained from the isotropic reference probe and the dosimeters located at WA L and WA R is presented in Figure J-5.

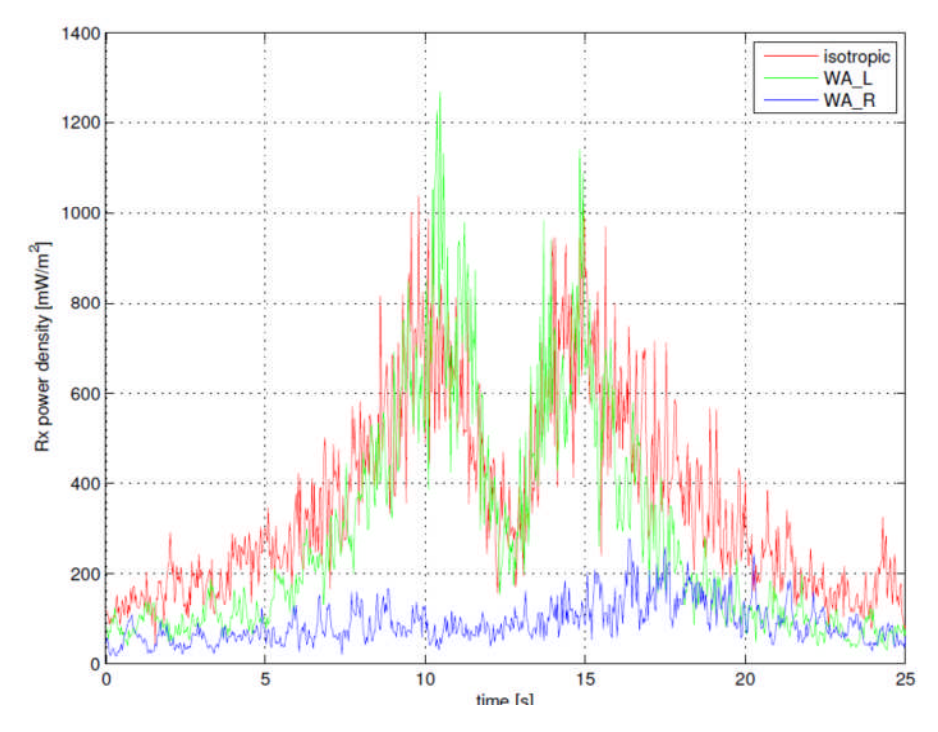


Figure J-5: Rx power density for straight scenario at 2600 MHz.

The received power density at WA\_L dosimeter is very similar to the one gathered at the isotropic probe, which mainly comes from the similar Line-Of-Sight (LOS) propagation conditions. As expected, the power received in WA\_R dosimeter is much lower, due to the body shadowing.

The distribution of the Rx power density is presented in Figure J-6.



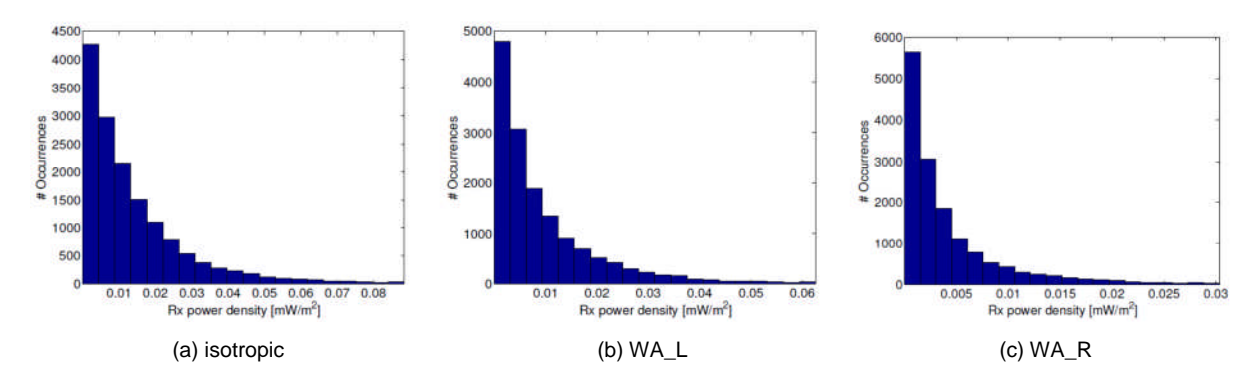


Figure J-6: Rx power density histograms.

In spite of the body shadowing, the distribution of the Rx power density at the WA\_R dosimeter is much similar to the ones for the reference and the WA\_L dosimeters. All of them follow an exponential decay, which should be subject to further investigation.

The correlation of the envelope of the Rx power density obtained from on-body dosimeters and the reference one (*i.e.*, isotropic probe) is presented in Table J-2. The ratio between the Rx power densities is also indicated in Table J-2.

Table J-2: Correlation between Rx power densities obtained from on-body dosimeters.
---

	ρ	R
WA_L and isotropic	0.81	0.79
WA_R and isotropic	0.33	0.25
WA_F and isotropic	0.42	0.51
WA_B and isotropic	0.41	0.82
TO_F and isotropic	0.37	0.51
WA_L and WA_R	0.13	3.15
WA_F and WA_B	-0.45	0.62
WA_L and WA_F	0.46	1.55

As expected, the correlation between the WA\_L dosimeter and the isotropic probe is the highest (0.81), because of the LOS propagation conditions. For the other dosimeters, correlation is much lower, ranging in [0.33, 0.42]. Note that front and back dosimeters (WA\_F and WA\_B) have a negative correlation value, meaning an opposite trend of the measured received power densities.

The ratio of the Rx power densities gathered by the different dosimeters to the reference dosimeter ranges in [0.25, 0.82]. These ratios can be used as a measure of the body shadowing effect, which is really severe is non LOS conditions. In this scenario, the use of a wearable dosimeter in the right side of the body displays a Rx power density reading about 4 times lower than the real one.



## J.3 Results for scenario "Loop"

The average Rx power density obtained from the isotropic reference probe and the dosimeters located at WA\_L and WA\_R is presented in Figure J-7.

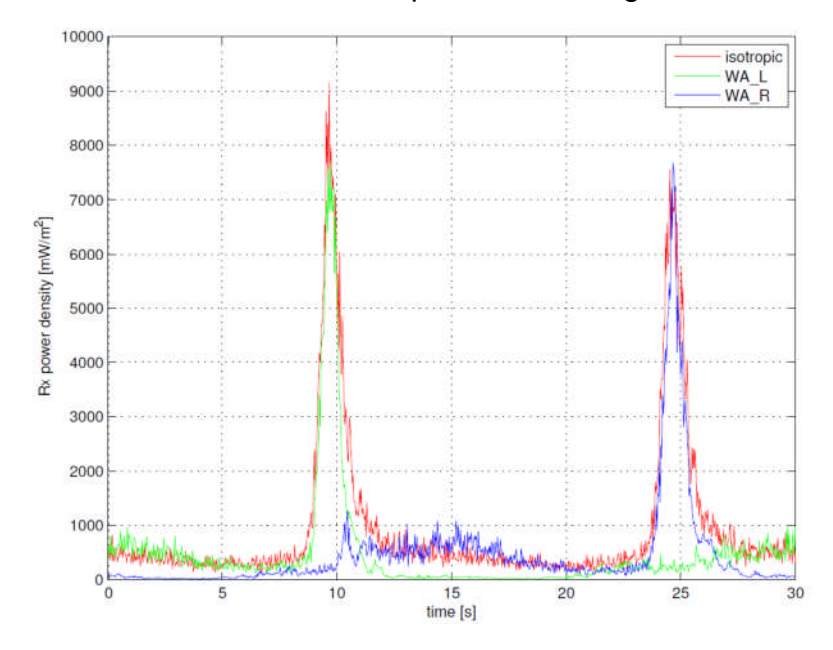


Figure J-7: Rx power density for loop scenario at 2600 MHz.

In this case, when there are LOS conditions, the Rx power densities at WA\_L and WA\_R are very similar to the one gathered at the isotropic probe. The WA\_L and WA\_R power densities have a symmetric trend, due to the loop movement.

The distribution of the Rx power density is presented in Figure J-8.

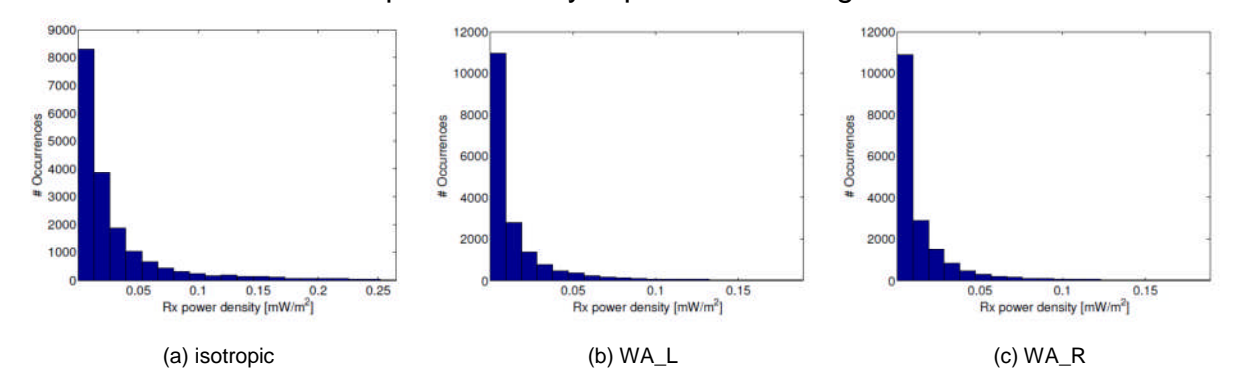


Figure J-8: Rx power density histograms.

As expected, the distribution of the Rx power densities of WA\_L and WA\_R dosimeters is very similar. They are also similar to the one gathered at the isotropic dosimeter.

The correlation of the envelope of the Rx power density obtained from on-body dosimeters and the reference one (*i.e.*, isotropic probe) is presented in Table J-3. Table J-3 also presents the ratio between the Rx power densities.

A similar correlation value around 0.6 is found at all the dosimeter locations, which was expected due to the loop movement of the user. Note that left and right

Version 4.0
Dissemination level: PUBLIC



dosimeters (WA\_L and WA\_R) have a negative correlation value, meaning an opposite trend of the measured Rx power densities.

In this case of loop movement, the ratio of the Rx power densities gathered by the different dosimeters to the reference dosimeter is more balanced. Two dosimeters worn in the right and left sides of the body will display a similar Rx power density reading. Concerning front and back locations, the readings can be much different, because there is not the same symmetry (*i.e.*, the user is inclined to the front, and the back dosimeter always displays higher Rx power densities).

Table J-3: Correlation between Rx power densities obtained from on-body dosimeters.

	ρ	R
WA_L and isotropic	0.69	0.49
WA_R and isotropic	0.63	0.49
WA_F and isotropic	0.61	0.25
WA_B and isotropic	0.69	0.80
TO_F and isotropic	0.68	0.27
WA_L and WA_R	-0.07	1.01
WA_F and WA_B	0.09	3.15
WA_L and WA_F	0.19	0.52

Version 4.0 Dissemination level: PUBLIC



## Appendix K INTERNAL REVIEW

		Reviewer 1: Nadège Varsier			Reviewer 2: Ramon Aguero					
		Answer	Comments	Type*	Answer	Comments	Type*			
Is the deliverable in accordance with										
(i)	the Description of Work?	⊠Yes □ No		□ M □ m □ a	⊠Yes □ No		□ M □ m □ a			
(ii)	the international State of the Art?	⊠Yes □ No		M   m   a	⊠Yes □ No		□ M □ m □ a			
2. Is the quality of the deliverable in a status										
(i)	that allows to send it to EC?	☐ Yes ⊠ No		□ М □ m □ a	☐ Yes ⊠ No	Comments provided in a track change version	□ M □ m □ a			
(ii)	that needs improvement of the writing by the editor of the deliverable?	⊠Yes □ No	D3.3 needs to be aligned with D2.6, especially concerning the used terminology for EI input data.		⊠Yes □ No		□ M ⊠ m □ a			
(iii)	that needs further work by the partners responsible for the deliverable?	⊠Yes □ No	The EI formula in Appendix E has not been updated, it should be in line with the formula in D2.6		⊠ Yes □ No		□ M ⊠ m □ a			

#### PROPRIETARY RIGHTS STATEMENT

This document contains information, which is proprietary to the LEXNET Consortium. Neither this document nor the information contained herein shall be used, duplicated or communicated by any means to any third party, in whole or in parts, except with prior written consent of the LEXNET consortium.

<sup>\*</sup> Type of comments: M = Major comment; m = minor comment; a = advice